Universidad de Málaga

Escuela Técnica Superior de Ingeniería de Telecomunicación

Programa de Doctorado en Ingeniería de Telecomunicación

TESIS DOCTORAL

Cost-Effective and Energy-Efficient Techniques for Underwater
Acoustic Communication Modems

Autor:

Muhammad Yousuf Irfan Zia

Directores:

Pablo Otero Roth

Miguel Ángel Luque Nieto

Málaga 2020

UNIVERSIDAD
DE MÁLAGA

AUTOR: Muhammad Yousuf Irfan Zia

https://orcid.org/0000-0003-4181-5997

EDITA: Publicaciones y Divulgación Científica. Universidad de Málaga

DECLARACIÓN DE AUTORÍA Y ORIGINALIDAD DE LA TESIS PRESENTADA PARA OBTENER EL TÍTULO DE DOCTOR

D./Dña MUHAMMAD YOUSUF IRFAN ZIA

Estudiante del programa de doctorado INGENIERÍA DE TELECOMUNICACIÓN de la Universidad de Málaga, autor/a de la tesis, presentada para la obtención del título de doctor por la Universidad de Málaga, titulada: COST-EFFECTIVE AND ENERGY-EFFICIENT TECHNIQUES FOR UNDERWATER ACOUSTIC COMMUNICATION MODEMS

Realizada bajo la tutorización de PABLO OTERO ROTH y dirección de PABLO OTERO ROTH y MIGUEL ÁNGEL LUQUE NIETO,

DECLARO QUE:

La tesis presentada es una obra original que no infringe los derechos de propiedad intelectual ni los derechos de propiedad industrial u otros, conforme al ordenamiento jurídico vigente (Real Decreto Legislativo 1/1996, de 12 de abril, por el que se aprueba el texto refundido de la Ley de Propiedad Intelectual, regularizando, aclarando y armonizando las disposiciones legales vigentes sobre la materia), modificado por la Ley 2/2019, de 1 de marzo.

Igualmente asumo, ante a la Universidad de Málaga y ante cualquier otra instancia, la responsabilidad que pudiera derivarse en caso de plagio de contenidos en la tesis presentada, conforme al ordenamiento jurídico vigente.

En Málaga, a 26 de septiembre de 2020

Fdo.: MUHAMMAD YOUSUF IRFAN ZIA

Edificio Pabellón de Gobierno. Campus El Ejido. 29071

Tel.: 952 13 10 28 / 952 13 14 61 / 952 13 71 10

E-mail: doctorado@uma.es

This page intentionally left blank

This page intentionally left blank

Abstract

Underwater wireless sensor networks (UWSNs) are widely used in many applications related to ecosystem monitoring, search for wrecks, infrastructures maintenance, security and defense, among others. Due to the absorption of electromagnetic waves in water and line-of-sight communication of optical waves, acoustic waves are the most suitable medium of communication in underwater environments. Underwater acoustic modem (UAM) is an essential component of a UWSN which is responsible for the transmission and reception of acoustic signals in an aquatic channel. Many commercial and research modems have been designed for different applications. Commercial modems may communicate at longer distances with reliability but they are expensive and less power efficient. On the other hand, the research modems have diverse characteristics and are designed by using a digital-signal-processor (DSP) and field-programmable-gate-array (FPGA). In addition to the employment of a DSP (which is expensive) and FPGA (which is a high power consuming device), the use of a microcontroller is also a common practice (which is less expensive) but provides limited computational power. Hence, there is a need for a cost-effective and energy-efficient UAM to be used in budget limited applications.

In this thesis different objectives are proposed, which have been reflected in the corresponding technical contributions. First, to identify the limitations of state-of-the-art commercial and research UAMs through a comprehensive survey. The outcome of the conducted survey is a thorough analysis/comparison in terms of various performance attributes (such as operating range, data rate, center frequency, bandwidth, bit-error-rate, power consumption etc.).

Based on the outcomes of the conducted survey, the second contribution of the research has been the design of a low-cost acoustic modem for short-range underwater communications using a modular approach that can be configured for various applications. The proposed modem is based on a single board computer (Raspberry-Pi) while the low level functionality is controlled using a microcontroller (Atmega328P). Furthermore, the modulator, demodulator and amplifiers are designed with discrete components to make the design economical. Moreover, the transducers in the proposed modem are made by piezo ceramic elements to reduce the overall cost.

In addition to the reduction in design cost, the verification/testing cost is equally important. In order to reduce the testing cost, the third contribution of this thesis is to design a web based underwater acoustic communication testbed along with a simulation platform. The testbed works as an emulator to test different types of modems in a controlled laboratory setup and simulates the underwater channel as well as sound propagation models. Remote accessibility of the testbed using a web browser further reduces the overall testing cost.

Besides low-cost, the energy-efficiency plays an important role in difficult-to-access areas like underwater communication as these systems are operated by an electric accumulator (battery), and therefore, preserving the accumulator's energy is of paramount importance. Power amplifier is the most energy demanding module and usually consists of a Class-D amplifier (which is the most energy efficient in terms of power). Conventionally, two different modules are used, for modulation (such as phase shift keying or frequency shift keying etc.) and amplification (such as Class-D amplifier) in an

underwater acoustics modem. Consequently, two modulations are found: once in the modulator (phase shift keying) and then in a Class-D amplifier (pulse width modulation).

The fourth contribution of this thesis is based on the idea of using the side effect of phase modulation found in a PWM modulator to integrate the both the PSK modulator and the power amplifier in a single module. The final transmitter is simpler and, which is more important, shows a higher power efficiency. Furthermore, the replacement of two modules with a single module also reduces the cost of the overall system.

In order to validate the proposed low-cost modem, component level as well as system level testing have been performed. For component level testing, each module such as analogue module (modulator, demodulator and amplifier), digital controller (Raspberry-Pi and microcontroller) and underwater transducers have been tested individually in a controlled laboratory setup. The individual modules are then integrated to perform system level testing in an aquatic environment at different data rates with a fixed range of 1 meter and a center frequency of $31.5\ kHz$. The ultrasonic frequency band is used to mitigate the issues of audible frequency range (such as noise). The data rates used for system level testing are $100, 300, 600$ and 1200 bits per second (bps). The achieved results show that the proposed modem can communicate at higher data rates with better accuracy as compared to state-of-the-art research modems.

To demonstrate the functionality of the proposed testbed (low-cost testing environment) as an emulator, we have used two low-cost UW acoustic modems (Modem-A and Modem-B). The electroacoustic transducers and two sensors (temperature and salinity) are submerged in an aquatic environment. Modem-A transmits the data from the sensors. The data from the sensors is received by Modem-B and transferred to a personal computer (PC) working as a LabVIEW server. Finally, the real-time data from the sensors (temperature and salinity) are monitored on a graphical user interface. The validation results show that the proposed testbed environment requires less development time, low cost and provides (local and remote) monitoring. It is important to note that the functionality of the testbed has been validated using the proposed low-cost modems. However, the proposed testbed environment can also be used to test various types of modems.

Finally, the validation of the proposed energy efficient module is performed in several steps. Initially, the hypothesis is verified using MATLAB (algorithmic level testing). Then, a model is designed and simulated in Simulink (functional level testing). Finally, an electronic circuit is built and experimentally tested in Multisim to validate the feasibility of the concept (circuit level testing). Consequently, the results obtained by simulations (algorithmic as well as functional level) and circuit implementation show that the proposed integrated system is an energy-efficient and cost-effective solution as compared to existing solutions.

Resumen

La naturaleza ha dotado al lecho oceánico de inmensos recursos que ofrecen un gran potencial para el crecimiento económico. El avance de la tecnología está facilitando a los investigadores la exploración de los océanos, llevando a un gran avance en las comunicaciones industriales y militares. Las comunicaciones submarinas han llamado considerablemente la atención en los últimos años debido a una variedad de aplicaciones, algunas de ellas son: la vigilancia de la calidad del agua, el cambio climático, la contaminación y los arrecifes de coral, datos útiles para investigación oceanográfica, la exploración en alta mar y los fines militares [1].

Tradicionalmente, en comunicaciones submarinas se usan diferentes tecnologías, como ondas electromagnéticas (EM), ondas ópticas u ondas acústicas, teniendo cada tipo sus propias ventajas y desventajas. Las ondas EM, que son utilizadas principalmente en las comunicaciones terrestres, son absorbidas en el agua y sólo pueden ser utilizados en distancias cortas [1]. Para superar este problema, se requiere más potencia de transmisión junto con una gran antena, lo cual no es factible ya que los sistemas de comunicación submarinos funcionan con baterías. Por otro lado, las ondas ópticas son útiles para las comunicaciones de alta velocidad, pero debido al fenómeno de dispersión y absorción, y sobre todo el requisito de la comunicación por visión directa (LOS, de Line Of Sight), se limitan a distancias muy cortas [2, 3]. Como contraposición de los dos anteriores, los sistemas acústicos subacuáticos poseen una comunicación más eficiente, ya que la atenuación de la señal es menor por tratarse de frecuencias más bajas 3-30 kHz. De esta forma, las ondas acústicas pueden cubrir largas distancias desde cientos de metros hasta kilómetros con una compensación por las tasas de datos [4, 5].

- Redes inalámbricas submarinas (UWSN)

La tecnología de las redes inalámbricas submarinas de sensores (WSN) está suficientemente madura en los entornos terrestres, pero debido a las duras condiciones del medio marino, las redes de sensores inalámbricos submarinas (UWSN) se encuentran en una fase de desarrollo [4-8]. Una UWSN es una infraestructura que combina diferentes tipos de sensores con tecnología inalámbrica para diversas funciones como detección, procesamiento y comunicación. Más específicamente, las redes inalámbricas submarinas de sensores (UWSN) se utilizan ampliamente en muchas aplicaciones relacionadas con la monitorización del ecosistema, la búsqueda de pecios, el mantenimiento de infraestructuras, la seguridad y la defensa, entre otras.

En comparación con la WSN terrestre, el diseño de una UWSN requiere más tiempo y es más costoso debido a las duras condiciones del entorno marino. Por ejemplo, en lo referente a las pruebas de campo, hacerlas para las UWSNs no sólo son más costosas, sino que requieren mucho tiempo y esfuerzo para su instalación. Como resultado, los sistemas desplegados en este momento tienen muchas limitaciones y se está llevando a cabo una amplia investigación para diseñar un banco de pruebas adecuado. Factores como el tiempo de modelado, el costo, los recursos de despliegue o la fiabilidad (etc.), dificultan cualquier avance importante. Los emuladores se utilizan para evaluar los componentes de hardware de sistemas de comunicación UW antes de su despliegue en entornos reales, mientras que los simuladores se utilizan para verificar los algoritmos y protocolos [63]. Algunas herramientas de simulación han sido diseñadas

específicamente para cumplir los requisitos de los escenarios submarinos, mientras que otros, que en realidad fueron desarrollados para la comunicación terrestre, han sido modificados para ser usados en aplicaciones submarinas. En comparación con los simuladores, los sistemas basados en emuladores son más precisos y requieren menos tiempo de configuración que en los entornos acuáticos reales. Son válidos para ser usados en la validación de varios tipos de sistemas de comunicación submarina, como a bordo de vehículos autónomos submarinos (AUV, Autonomous Underwater Vehicle), vehículos autónomos de superficie (ASV, Autonomous Surface Vehicle), vehículos operados a distancia (ROV, Remotely Operated Vehicle), etc.

- Módems acústicos submarinos (UAM)

El módem acústico submarino (UAM) [9, 10] es uno de los elementos clave de una UWSN responsable de la comunicación, esto es, de la transmisión y recepción de señales en el canal acuático, mediante ondas acústicas. Los módems (dentro de los nodos sensores) pueden clasificarse en dos categorías principales: (*i*) módems comerciales [11-27] y (*ii*) módems de investigación [28-60].

Se han diseñado muchos módems comerciales y de investigación para diferentes aplicaciones. Los módems comerciales pueden comunicarse a mayores distancias con fiabilidad, pero son caros y de menor rendimiento energético. Por otra parte, los módems para investigación tienen características diversas y se diseñan utilizando un procesador de señales digitales (DSP) y una matriz de puertas lógicas programables en campo (FPGA). Además del empleo de un DSP (que tiene un costo elevado) y de una FPGA (que requiere mucha energía), el uso de un microcontrolador es también una práctica común, de menor costo, pero proporciona una potencia de cálculo limitada. Por lo tanto, hay una necesidad práctica de un módem acústico subacuático de bajos consumo y coste de propósito general para su uso en UWSNs. Los principales elementos de un UAM son: (*i*) transductor acústico, (*ii*) circuito de comunicación, y (*iii*) unidad de control. El transductor acústico convierte la energía eléctrica en energía acústica y viceversa para transmitir y recibir datos en el canal marino. Los circuitos de comunicación se encargan de varias tareas, como amplificación de la señal, modulación, demodulación, filtrado, procesamiento de la señal, etc. Finalmente, el control como su nombre indica, se utiliza para controlar la funcionalidad del módem.

Para el diseño del módem, se pueden elegir varias plataformas de hardware. Los DSP (Digital Signal Processor) son las principales plataformas utilizadas en el diseño UAM, pero son caros [34]. Otra opción es la FPGA (Field-Programmable Gate Array) que puede ser reprogramada, pero consume más energía [53] [64]. El ordenador personal (PC) o el portátil también han sido utilizados con fines de prueba, pero su despliegue en pruebas de campo no es factible. También existen diseños basados en microcontroladores (o MCU, Microcontroller Unit), debido a que son más pequeños y menos costosos. El inconveniente de diseños basados en MCU es su limitada potencia de cálculo, que inhabilitan para ser utilizados en aplicaciones finales [56].

Otro de los factores determinantes del UAM es la modulación empleada. Se han utilizado diversos esquemas de modulación en los módems acústicos submarinos. Una de las más empleadas, OFDM, requiere una alta potencia de cálculo y amplificadores lineales debido al alto valor de la relación potencia de pico a potencia media [65, 66]. Por su parte, la modulación FSK es resistente al ruido y a las variaciones de la intensidad de la señal, y relativamente fácil de implementar, pero debido a los requerimientos de gran ancho

de banda, no se prefiere en módems de alta velocidad [67]. Los sistemas de comunicación basados en modulación ASK son simples de diseñar y de bajo coste, pero su eficiencia energética es baja y muy susceptible a interferencia por ruido [80]. Por último, la modulación QPSK es eficiente en cuanto al ancho de banda, pero no en cuanto a la potencia en comparación con otros esquemas de modulación [52]. La familia de técnicas de espectro ensanchado (SS, Spread Spectrum) mantienen una comunicación segura y sin interferencias, pero son complejas de implementar [35].

- Arquitectura del módem UAM diseñado

Se ha planteado la arquitectura del módem desde una división en 3 bloques: (i) transductores, (ii) módulo analógico y (iii) módulo digital.

(i) La misión principal de los transductores es adaptar la señal eléctrica que se quiere transmitir a formato acústico y propagarla en el agua, y viceversa en la operación de recepción. Un principio físico que se puede aprovechar para realizar esta conversión de señal es el fenómeno piezoeléctrico, que ocurre en algunos materiales cristalinos. El efecto radica en que, al someter estos cristales bajo tensiones mecánicas, como es el caso de una onda acústica (que ejerce variaciones de presión en el agua al propagarse), su masa adquiere una polarización eléctrica y como consecuencia, aparecen cargas eléctricas en su superficie, generándose una diferencia de potencial.

Un tipo de cristal piezoeléctrico muy usado en acústica submarina es el material cerámico, que posee bajas pérdidas y altos coeficientes de acoplo [85]. Los fabricantes, diseñan los transductores acústicos con diferentes formas (por ejemplo, cilíndrica y esférica) y diferentes diagramas de radiación (por ejemplo, directivo u omnidireccional). El principal obstáculo para usar estos materiales de alta calidad es el coste. Debido a la orientación del trabajo realizado, que persigue un bajo coste de implementación, los transductores empleados no superan los 50 USD. Se discutirán las razones en el apartado 3.3.1 respecto del modelo empleado ($SMC3631T20111$).

Además del tipo de material y prestaciones en la conversión acústico-eléctrica, su diseño final debe permitir la comunicación full dúplex, es decir, que se pueda enviar a la vez que se recibe. Debido a la operación que realizan, deben estar sumergidos en el medio marino, fuera del encapsulado que protege el resto del módem.

(ii) Las funciones que tiene asignadas el segundo módulo, analógico, son: modulación, demodulación y amplificación. De esta forma, el módulo analógico es responsable de todas las tareas relacionadas con el procesamiento de la señal. La amplificación está dividida entre un preamplificador y un amplificador de potencia. Debido a la robustez, la inmunidad al ruido y la búsqueda de una implementación simple de bajo coste, se utiliza un esquema de modulación FSK de fase continua en el módem [5].

El circuito del modulador FSK, está diseñado con un generador de funciones monolíticas [88]. La frecuencia portadora se fija mediante un condensador y resistencias. El condensador, que persigue el sincronismo, se conecta a los terminales de un oscilador controlado por voltaje (VCO, Voltage-Controlled Oscillator), y las resistencias se conectan a terminales de interruptores de corriente a tierra, permitiendo así versatilidad a la hora de seleccionar diferentes portadoras.

El demodulador FSK, está diseñado a partir de un decodificador de tonos [89]. El rango de frecuencias de trabajo es 0.01–300 kHz, que cubre la mayor parte de la banda acústica empleada en comunicaciones submarinas. Los elementos de ajuste del demodulador FSK son elementos discretos: una resistencia y varios condensadores.

Respecto a la amplificación usada, hay un preamplificador, basado en un transistor de efecto campo (FET, Field-Effect Transistor), junto con un amplificador de potencia, que se ha decidido usar de clase AB en esta tesis.

La elección de un transistor FET como etapa de previa de amplificación, es debida principalmente al bajo nivel de ruido generado, frente a otras soluciones, como transistor bipolar (BJT, Bipolar Junction Transistor) o basado en circuito integrado.

Por otra parte, con solo esta etapa previa, la señal modulada no tiene suficiente potencia como para ser transmitida a distancias útiles en el medio marino debido a múltiples fenómenos físicos, como la absorción. Esto lleva al uso de una etapa de potencia adicional, en la que el principal enemigo es su alto consumo. Por ello se clasifican los amplificadores según su eficiencia energética y se toma una decisión final. Los Clase A, tienen como principal ventaja ser simples de diseñar y un comportamiento muy lineal pero debido a su baja eficiencia (35% aproximadamente), no es una buena elección cuando la fuente principal de energía son baterías que es el caso del UAM a diseñar. Los amplificadores Clase B, suben su eficiencia hasta un 80%, pero amplifican solo el semiciclo positivo de la señal de entrada, así que tampoco se recomiendan [91]. Los amplificadores Clase AB, superan la limitación de los B al tener amplificación en todo el rango de la señal de entrada, por lo que son una buena elección. Respecto al resto de clases de amplificadores, los Clase C se desestiman en este diseño porque tienen problemas de linealidad y los Clase D, que son de bajo coste y tienen la mejor eficiencia en su operación, producen interferencias electromagnéticas, necesitando de una red de adaptación de impedancias [92].

(iii) Por último, el módulo digital realmente es un controlador digital, que gobierna las funciones de varios bloques, y está implementado en una plataforma bajo coste basado en SBC (Single Board Computer), junto con un microcontrolador. En este trabajo, se han empleado como SBC la plataforma de hardware libre Raspberry Pi, y para el caso del microcontrolador, el chip Atmega328P.

La elección de Raspberry Pi se debe fundamentalmente a dos razones: su versatilidad (puede correr Linux o librerías de Windows 10 para IoT, Internet Of Things), y su bajo coste. El sistema operativo Linux proporciona una gran variedad de aplicaciones de acceso gratuito, que incluyen tanto de desarrollo como de validación y funciones de E/S de la placa. En este sentido, dispone de puertos USB, y conexión Ethernet 10/100 Mbit/seg para las comunicaciones con el exterior, además de 40 puertos de propósito general programables para periféricos. Específicamente, el modelo usado fue Raspberry-Pi 2 Model B+, equipado con una CPU de 4 núcleos ARM Cortex, a una frecuencia de operación de 900 MHz y una memoria RAM de 1 GByte.

Por otra parte, el microcontrolador Atmega328P es un chip de 8 bit, con un conjunto reducido de instrucciones (RISC, Reduced Instruction Set Computer). Posee 32 kB de memoria Flash, una memoria EEPROM de 1 kB y una interfaz UART operando a 16 MHz, muy útil para comunicaciones.

La división de tareas entre ambos es lógica: todas las tareas de alto nivel las realiza la Raspberry Pi, mientras los procesos más cercanos al hardware, o de comunicaciones con el exterior, las realiza el microcontrolador Atmega328P.

- Entorno de desarrollo y pruebas del módem diseñado

Los bloques a diseñar y probar son: (i) los transductores, (ii) la etapa de amplificación (preamplificador y amplificador de potencia), (iii) modulador y demodulador, y por último, (iv) el módulo digital (SBC y MCU).

En el desarrollo de todas las partes (i)-(iv) se ha empleado una placa hardware de desarrollo de la empresa National Instruments (NI), denominada ELVIS (Educational Laboratory Virtual Instrumentation Suite) en su versión II+. ELVIS es una placa de prototipado avanzada, e integra 12 instrumentos de laboratorio muy comunes, como monitorización para osciloscopio, analizador lógico, o funciones de multímetro entre otras. Se puede conectar al PC usando un puerto USB, para depuración. Dispone de un software de prueba para la placa, escrito en LabView (Laboratory Virtual Instrument Engineering Workbench) que es un lenguaje de programación visual creado por NI. Los objetos usados, se denominan Instrumentos Virtuales (VIs) y están compuestos de dos elementos: el panel frontal, y diagrama de bloques. El panel frontal, integra los controles de entrada y las salidas (indicadores, gráficos, …). El diagrama de bloques contiene el código fuente en formato gráfico. Las ventajas de uso de LabVIEW abarcan aprendizaje rápido, flexibilidad en el diseño y un buen soporte tanto para el software como para el hardware.

(i) La caracterización de los transductores, exige una primera fase de análisis de su respuesta en frecuencia dentro de la banda de operación prevista. A través del módulo ELVISmx Impedance Analyzer, de LabVIEW, se ha obtenido del transductor su impedancia. Concretamente, los parámetros medidos abarcan su módulo y fase, en función de la frecuencia. Los datos obtenidos de hacer el barrido en frecuencia se guardaron en una hoja de cálculo para su análisis posterior.

(ii) En el caso de las etapas amplificadoras (previa y de potencia), una vez montadas en la placa ELVIS, se observó su salida a través del osciloscopio, validando los valores del diseño.

(iii)-(iv) Para probar la modulación, y el módulo de control digital, primero se almacenó una secuencia digital en la Raspberry Pi para posteriormente aplicarla al modulador (a través del microcontrolador) y generar la señal modulada FSK, observándola en el osciloscopio. De esta forma, se comprueba la operación del modulador. Para verificar la operación inversa, del demodulador, se aplicó la señal FSK al bloque demodulador, probando que se obtenía la secuencia binaria original.

La prueba final que validaba la operación del módem completo se realizó con dos módems -A y B- que se comunicaban (A era transmisor y B receptor) dentro de un tanque de agua que simulaba las condiciones del medio marino. Diferentes velocidades de transmisión entre 100-1200 bps fueron probadas, con resultados satisfactorios (ver apartado 3.4.4).

- Herramienta web para banco de pruebas en UWSN

Como trabajo adicional al módem desarrollado, se ha creado una herramienta web de bajo costo para evaluar el rendimiento de una red UWSN y/o sus componentes. El objetivo final es presentar un emulador de coste reducido y sencillo de usar para investigar la funcionalidad de las redes UWSN o de sus componentes por separado, que incluyen módems, sensores, diferentes modulaciones… siempre dentro de un entorno controlado de laboratorio.

El sistema de prueba también es capaz de simular el canal acústico submarino, la propagación de las ondas, así como diferentes modelos matemáticos y protocolos. Como mejora y novedad, se ha dotado al sistema de una herramienta software que permite el acceso remoto para controlar el experimento a través del navegador web.

La estructura del sistema es una combinación de hardware y software que usa instrumentación virtual para probar diferentes tipos de módems. De esta forma, el sistema mantiene un coste reducido y una puesta en marcha y configuración sencilla, en comparación con otros sistemas existentes [62]. Los dos elementos principales del sistema de prueba son: (i) el interfaz hardware que se usa como emulador del sistema de comunicaciones inalámbrico submarino, y (ii) el módulo software, que actúa como simulador, usado para evaluar las ecuaciones del modelo de propagación, los algoritmos y obtener los resultados de las simulaciones realizadas.

 (i) En su parte hardware, el sistema de prueba consiste en un tanque de agua que tiene capacidad para almacenar 400 litros, y probar así el sistema de comunicación UW de bajo costo. Los módems acústicos (que operan entre 30,5 - 32,5 kHz) tienen implementada una modulación FSK, y son utilizados en este banco de pruebas como una capa física [31].

Cada módem está equipado con transductores submarinos para la transmisión y recepción acústica en el canal de agua. El módem A, posee sensores de temperatura y salinidad del agua, y transmite acústicamente estas lecturas para obtener dichos datos en tiempo real del sistema, utilizando el transductor de transmisión. Por otra parte, el módem B recibe los datos del canal acuático usando su transductor de recepción, y los pasa al servidor de LabVIEW (está conectado por un puerto de comunicación estándar) ejecutando un instrumento virtual (VI) para su posterior procesamiento [94].

En la parte de la red de datos, existe un servidor LabVIEW que está conectado a la red local de red / Internet para compartir información con otros clientes a través de un navegador web. Además de compartir los datos de forma remota, este servidor realiza la vigilancia y almacenamiento en la terminal local de dichos datos recibidos.

(ii) Respecto al software del banco de pruebas, también está diseñado en LabVIEW. Una de las principales ventajas de LabVIEW es que ya posee incorporadas funciones para controlar los instrumentos utilizando una amplia variedad de interfaces: bus de interfaz de propósito general (GPIB), bus serie universal (USB), la red de área local (LAN), un circuito integrado (I2C), un interfaz serie de periféricos (SPI, Serial Peripheral Interface), un grupo de acción de prueba conjunta (JTAG) etc. Aparte de esto, permite usar funciones matemáticas, estadísticas y de procesamiento de señales para el análisis de datos y señales.

Los datos adquiridos también pueden visualizarse mediante el panel frontal y almacenarse a través de Microsoft Access® y otras bases de datos. LabVIEW también proporciona una interfaz para diversas aplicaciones de control de códigos fuente, validación de datos y otros instrumentos de gestión. Los resultados de las pruebas también pueden generarse utilizando Microsoft Office®, o hipertexto con plantillas de informes en lenguaje HTML. Otra función que lo hace especialmente útil en desarrollo es que el código LabVIEW creado se puede desplegar en un destino a partir de la creación de ejecutables e instaladores independientes. Además, las aplicaciones creadas en LabVIEW también pueden ser controladas y monitorizadas remotamente.

Existen tres conjuntos de objetos de programación en LabVIEW: (i) herramientas paleta, (ii) paleta de control e indicador, y (iii) paleta de funciones. La paleta de herramientas (i) está disponible en ambos paneles frontales y en la ventana del diagrama, mientras que los controles (ii) están disponibles en el panel frontal y la paleta de indicadores, y las funciones (iii) están disponibles sólo en la ventana del diagrama. Las funciones y los controles están conectados entre sí en función del tipo de dato del objeto. Como material de soporte, LabVIEW proporciona herramientas de depuración, como VI Analyzer, que ayuda a mejorar y encontrar fallos en los VI.

- Resultados del banco de pruebas web

Tal y como se ha indicado anteriormente, el banco de pruebas puede funcionar como (i) emulador o como (ii) simulador.

Como (i) emulador, se han utilizado dos módems acústicos UW de bajo coste [31]. Los transductores y los sensores de temperatura y salinidad están sumergidos en un entorno acuático. El módem transmisor (módem A) recoge los datos de temperatura y salinidad del agua, mediante sensores conectados a él, y transmite estos datos por medio del transductor correspondiente en el agua. En el otro extremo, el módem receptor (módem B) recibe los datos mediante su transductor de recepción y los transfiere al ordenador personal que actúa como servidor LabVIEW. Finalmente, los valores de temperatura y salinidad en tiempo real son monitoreados en pantalla a través de una interfaz gráfica (GUI, Graphical User Interface). Los resultados obtenidos se encuentran en el apartado 4.4.1.

En el funcionamiento como (ii) simulador, la plataforma de prueba desarrollada se basa en un entorno GUI sobre lenguaje LabVIEW [94], comúnmente usado por la comunidad científica. Usando LabVIEW, los investigadores pueden fácilmente diseñar, implementar, simular, probar y evaluar el rendimiento de los algoritmos de comunicaciones UW. Los parámetros definidos del sistema se pueden configurar en tiempo real para obtener los resultados deseados. Los resultados gráficos de las simulaciones pueden ser monitorizados y controlados localmente, así como de forma remota mediante servicios web.

Se consideraron tres parámetros importantes en simulación: la velocidad del sonido, el ruido ambiente y la atenuación de la onda sonora propagada.

Para simular la velocidad del sonido, se creó un GUI donde el usuario tiene control para variar la temperatura y la salinidad. Como resultado se dan curvas de la velocidad del sonido según la profundidad.

En el segundo caso del ruido ambiente, son bastantes los factores que intervienen [105-106]: velocidad del viento, frecuencia de la onda acústica, efecto de las turbulencias, de las olas, etc. Todos fueron implementados en un GUI para que el usuario pueda habilitarlos u obviarlos, antes de obtener las curvas típicas de evolución de la atenuación por ruido ambiente (dB) según la frecuencia.

Por último, para el caso de la atenuación de la onda acústica con la distancia, el interfaz GUI recoge controles para que el usuario pueda fijar el rango de transmisión (distancia máxima) y el factor de ensanchamiento (cilíndrico/esférico o valor intermedio) típico de la conocida fórmula de Thorp. Se da como salida diferentes curvas: atenuación total, o componentes individuales de atenuación por absorción / ensanchamiento.

- Integración del modulador digital con amplificador Clase-D

Mientras que en el capítulo 3 el objetivo principal era obtener un módem UAM de bajo coste, ahora se plantea mejorar la eficiencia energética del módem. Para ello, se presenta la integración de un modulador digital y un amplificador Clase-D para mejorar la eficiencia energética del sistema.

El sistema integrado propuesto proporciona amplificación, así como el desplazamiento de fase que sufre una señal modulada en fase o PSK. Para validad su correcto funcionamiento, se ha llevado a cabo su simulación en el software matemático MATLAB®, así como un modelo diseñado y probado en Simulink®. Finalmente, se construye un circuito prototipo que ha sido probado previamente usando el software Multisim®. Los resultados experimentales del prototipo muestran que el sistema propuesto es un sistema eficiente en energía y solución rentable en comparación con los diseños existentes en la actualidad.

El amplificador de potencia es el módulo más exigente en cuanto a energía en los dispositivos móviles, los aparatos portátiles, transceptores estáticos, e incluso nodos usados en redes acústicas UW. Estos dispositivos incorporan un modulador, típicamente con una modulación de ancho de pulso (PWM, Pulse Width Modulation) y un amplificador de potencia Clase-D, para mayor eficiencia [109]. Esta clase de amplificadores, son los más eficientes en términos de potencia, con valores del orden del 90% en diseños prácticos [109], y se prefieren en aplicaciones en las que la autonomía es esencial.

La estructura de bloques de un amplificador tradicional Clase-D consiste en un modulador analógico de una portadora digital seguido de un circuito de conmutación que impulsa la corriente de una fuente de alimentación de corriente continua (DC, Direct Current). Esta corriente pasa a la carga a través de un filtro que recupera la señal en banda base. Debido a su complejidad, los amplificadores de Clase-D no son apropiados para señales pequeñas, pero en aplicaciones de potencia, son la mejor opción por sus bajas pérdidas. En muchas de sus aplicaciones, estos amplificadores se utilizan en sonido de alta fidelidad (hi-fi, High Fidelity) y que opera en una banda de audio entre 20 Hz-20 kHz, usando como filtro recuperador un filtro paso bajo (LPF, Low Pass Filter). En nuestro caso, como el amplificador está destinado a estar en la etapa de salida de un sistema de comunicación ultrasónica, el filtro LPF queda sustituido por un filtro paso banda (BPF).

Como resumen, en esta tesis se propone una técnica para integrar el modulador de un transmisor y el modulador de pulsos (PWM) de un amplificador Clase-D para mejorar la eficiencia general del sistema. Este

conjunto integrado, funciona como un mezclador ascendente (supradino), un modulador de fase (PM), y un modulador digital binario de fase (BPSK) según ciertas condiciones. En nuestro diseño propuesto, dicha integración permite las siguientes funciones: (*i*) amplificar la señal, (*ii*) realizar el filtrado y (*iii*) generar la señal modulada PSK.

- Objetivos de la tesis. Conclusiones finales

En esta tesis se plantean distintos objetivos, que se han plasmado en las correspondientes contribuciones científicas. En primer lugar, identificar las limitaciones de los módems acústicos submarinos comerciales y de investigación de última generación a través de un estudio exhaustivo. El resultado del estudio realizado es un análisis/comparación minuciosa en términos de características y prestaciones (como el rango operativo, la velocidad de datos, la frecuencia central, el ancho de banda, la tasa de bits erróneos, el consumo de energía, etc.).

Sobre la base de los resultados del estudio realizado, la segunda contribución ha consistido en el diseño un módem acústico de bajo costo para las comunicaciones submarinas de corto alcance utilizando un enfoque modular que puede configurarse para diversas aplicaciones. Como ya se ha comentado, respecto a la implementación concreta del módem en este trabajo de tesis, tras analizar diferentes variables, opciones hardware disponibles, y esquemas de modulación, se propone un esquema de bajo coste basado en SBC (Raspberry Pi), junto con un microcontrolador (Atmega328P). El resto de los elementos del módem y los amplificadores están diseñados con componentes discretos. Los transductores electroacústicos se han fabricado con elementos piezoeléctricos, lo que ha reducido el costo total. Además de la reducción del costo del diseño, el costo de verificación/prueba del diseño es igualmente importante.

Con el fin de reducir ese costo, la tercera contribución de esta tesis ha consistido en la creación un banco de pruebas de comunicaciones acústicas submarinas basado en la web y una plataforma de simulación. El banco de pruebas funciona como un emulador para probar diferentes tipos de módems en una instalación de laboratorio controlada y simula el canal submarino así como modelos de propagación de sonido. La accesibilidad remota al banco de pruebas mediante un navegador web reduce aún más el costo total de las pruebas.

La eficiencia energética desempeña un papel importante en entornos de difícil acceso como es el caso submarino, ya que estos sistemas funcionan con acumuladores eléctricos (batería) y a menor consumo, mayor autonomía. El amplificador de potencia es el módulo que más energía requiere y suele estar compuesto por un amplificador de clase D (que es el más eficiente en términos de energía). En la práctica común se utilizan dos módulos diferentes, para la modulación (como la modulación por desplazamiento de fase o por desplazamiento de frecuencia, etc.) y la amplificación (como el amplificador de clase D) en un módem de acústica submarina. Por consiguiente, se realizan dos modulaciones; una en el modulador propiamente dicho y otra en un amplificador de clase D, que está basado en un modulador de anchura de impulsos (PWM).

La cuarta contribución de esta tesis está basada en la idea de aprovechar la modulación de fase residual propia de la PWM para integrar modulador y amplificador de potencia. De esta manera se consigue la

modulación PSK y la amplificación en solo módulo, lo que simplifica considerablemente el esquema de bloques del transmisor y mejora su eficiencia energética.

A fin de validar el módem de bajo costo propuesto, se han realizado pruebas a nivel de componentes y a nivel de sistema. Para las pruebas de nivel de componentes, cada módulo, como el módulo analógico (modulador, demodulador y amplificador), el controlador digital (Raspberry Pi y microcontrolador) y los transductores subacuáticos, se han probado individualmente en una instalación de laboratorio controlada. A continuación, los módulos individuales se integran para realizar pruebas de nivel de sistema en un entorno acuático a diferentes velocidades de datos con un alcance fijo de 1 metro y una frecuencia central de 31,5 kHz. Las velocidades de transmisión utilizadas para las pruebas a nivel de sistema son de 100, 300, 600 y 1200 bits por segundo (bps). Los resultados obtenidos muestran que el módem propuesto podría comunicarse a mayores velocidades con menos errores de transmisión que otros módems de investigación de última generación.

Para demostrar la funcionalidad del banco de pruebas propuesto (entorno de pruebas de bajo costo) como emulador, hemos utilizado dos módems acústicos UW de bajo costo (Módem-A y Módem-B). Los transductores electroacústicos y dos sensores (temperatura y salinidad) se sumergen en agua para emular el entorno submarino. El Modem-A recoge los datos y los transmite. El módem-B actúa de receptor y transfiere los datos recibidos a un ordenador personal que funciona como servidor LabVIEW. Por último, los valores de temperatura y salinidad en tiempo real se supervisan en una interfaz gráfica de usuario. Los resultados de la validación muestran que el entorno del banco de pruebas propuesto requiere menos tiempo de desarrollo y es de bajo costo. Es importante señalar que la funcionalidad del banco de pruebas se ha validado utilizando los módems de bajo costo propuestos. Sin embargo, el entorno del banco de pruebas propuesto también puede utilizarse para probar diversos tipos de módems.

Por último, la validación del modulador/amplificador integrado propuesto se ha realizado en varios pasos. Inicialmente, la hipótesis se ha verifica utilizando MATLAB (prueba de nivel algorítmico). A continuación, se ha diseñado un modelo en Simulink que ha permitido, mediante simulación, realizar pruebas funcionales. Finalmente, se ha diseñado un circuito electrónico y se ha probado experimentalmente en Multisim para validar la viabilidad del concepto (prueba de nivel de circuito). Los resultados obtenidos por las simulaciones (tanto a nivel algorítmico como funcional) y la implementación del circuito muestran que el sistema integrado propuesto es una solución energéticamente eficiente y de menor costo que las soluciones existentes.

Acknowledgements

I would like to express my sincere respect and gratitude to my thesis supervisor, Prof. Dr. Pablo Otero for his expert guidance, support and patience over the years. He is always a great source of new ideas and motivation.

I am deeply indebted to my co-supervisor (late) Prof. Dr. Javier Poncela for his mentorship and keen interest throughout the course of this study. Unfortunately, before completion of the present thesis, he left us forever. His untimely demise left us in depression and agony which is difficult to overcome.

But at this juncture, I am grateful to my new thesis co-supervisor Prof. Dr. Miguel-Ángel Luque-Nieto, who always stood beside me, supported and encouraged me till the last moment.

I am thankful to the Research Institute of Oceanic Engineering, the University of Malaga, and the Spanish Government for their support towards my doctoral research.

Lastly and most importantly, I would like to thank my parents, their love and prayers helped me remain focused during my studies. I am thankful to my family members, without their help I would not have accomplished my goals. I am grateful to my colleagues and friends for their help and support during the studies.

This page intentionally left blank

Table of Contents

List of Tables

List of Figures

xx

List of Abbreviations

ADC	Analog to digital converter
ARM	Advanced RISC machines
ASK	Amplitude shift keying
ASV	Autonomous surface vehicle
AUV	Autonomous underwater vehicle
BASS	Broadband acoustic spread spectrum
BER	Bit error rate
BJT	Bipolar junction transistor
BPF	Band-pass filter
BPSK	Binary phase shift keying
CDMA	Code-division multiple access
CMOS	Complementary metal–oxide–semiconductor
CRC	Cyclic redundancy check
DAQ	Data Acquisition System
DDS	Direct digital synthesis
DSP	Digital signal processor
DSSS	Direct sequence spread spectrum
FET	Field effect transistor
FPGA	Field programmable gate array
FSK	Frequency shift keying
GPIB	General-purpose interface bus
GPIO	General-purpose input-output
GPL	Graphical programming language
GUI	Graphical user interface
HTML	Hypertext markup language
I2C	Inter-integrated circuit (serial bus)
JTAG	Joint test action group
LabVIEW	Laboratory virtual instrument engineering workbench
LAN	Local area network

LNA	Low-noise amplifier
LPF	Low-pass filter
MACA	Multiple access with collision avoidance
MFSK	Multiple frequency shift keying
MOSFET	Metal oxide semiconductor field effect transistor
NI-ELVIS	National instruments educational laboratory virtual instrumentation suite
OFDM	Orthogonal frequency division multiple access
OOK	On–off keying
PC	Personal computer
PCB	Printed circuit board
PDM	Pulse density modulation
PLL	Phase-locked-loop
PM	Phase modulator
PPC	Passive phase conjugation
PPM	Pulse position modulation
PPT	Parts per thousand
PSK	Phase shift keying
PWM	Pulse-width modulation
QAM	Quadrature amplitude modulation
QPSK	Quadrature phase shift keying
RF	Radio frequency
RFID	Radio frequency identification
ROV	Remotely operated underwater vehicle
RX	Receive
S2C	Sweep spread carrier
SBC	Single board computer
SDR	Software-defined radio
SNR	Signal-to-noise-ratio
SPI	Serial peripheral interface
SS	Spread spectrum
SWiG	Subsea wireless group

TCP	Transmission control protocol
TX	Transmit
UAM	Underwater acoustic modem
UAN	Underwater acoustic network
UDP	User datagram protocol
USB	Universal serial bus
UW	Underwater
UWSN	Underwater wireless sensor network
VCO	Voltage controlled oscillator
VI	Virtual instruments
WSN	Wireless sensor network

Chapter 1: Introduction

1.1.   Underwater communication

Nature has bestowed the ocean bed with immense resources that offer a great potential towards economic growth. Advancement in technology is facilitating the researchers to explore oceans, leading to a breakthrough in industrial and military communication and other applications. Underwater communication has drawn considerable attention in past few years due to a variety of applications, some of them include: monitoring of water quality, climate change, pollution and coral reefs, oceanographic data collection, offshore exploration, and military purposes [1].

Traditionally, the electromagnetic, optical and acoustic waves are used in underwater (UW) communication such that each has its own advantages and disadvantages. The electromagnetic waves, which are effectively used in terrestrial communications, are absorbed in water and can only be used for short distances [1]. To overcome this issue, more transmission power along with a large antenna is required, which is not feasible as the underwater communication systems are battery powered. Optical waves are useful for high-speed communications, but due to the scattering and absorption phenomenon, and requirement of line-of-sight communication, they are limited to very short distances [2, 3]. As compared to the above two, for underwater systems, acoustic communication is auspicious as the signal attenuation is less at lower frequencies $3-30\ kHz$ and the acoustic waves can cover long distances in the order of several hundred meters with a tradeoff for data rates [4, 5].

1.1.1.   Underwater wireless sensor network

The technology in wireless sensor network (WSN) is mature enough in terrestrial environments but due to the tough aquatic conditions, underwater wireless sensor network (UWSN) is in a developing stage [4-8]. UWSN is a combination of wireless and sensor technologies having sensing, processing and communication facilities used to explore the unseen world below the surface of water. Compared to terrestrial WSN, designing UWSN is more time consuming and expensive due to harsh conditions of the aquatic environment. Underwater acoustic modem (UAM) [9, 10] is one of the key elements of a UWSN responsible for communication in an aquatic channel using acoustic waves. The acoustic

modems (sensor nodes) can be classified into two main categories: (i) commercial modems [11-27] and (ii) research modems [28-60].

A typical UWSN architecture consists of several components as shown in Figure 1.1. The UWSN can be used in many scenarios from water pollution monitoring to explore the hidden aquatic world. As mentioned in Section 1.1, acoustic waves are generally considered more suitable for a UWSN. The sensor nodes have sensing, processing and underwater acoustic communication facilities and are deployed autonomously and form a stand-alone cluster [61]. Figure 1.1 shows two clusters, consisting of nodes (acoustic modems) are deployed at the bottom of the seabed. The deployed nodes operate in a horizontal direction and communicate with the center node. Subsequently, the center node passes the data vertically to the gateway buoy, connected with the satellite via a microwave link. The autonomous underwater vehicles (AUVs) also communicate acoustically with the nearest UWSN. There is an acoustic link, available from the buoy to the ship. Furthermore, the ship can communicate from the shore using radio waves. It is important to note that several UWSN configurations are possible, depending upon a particular application scenario.
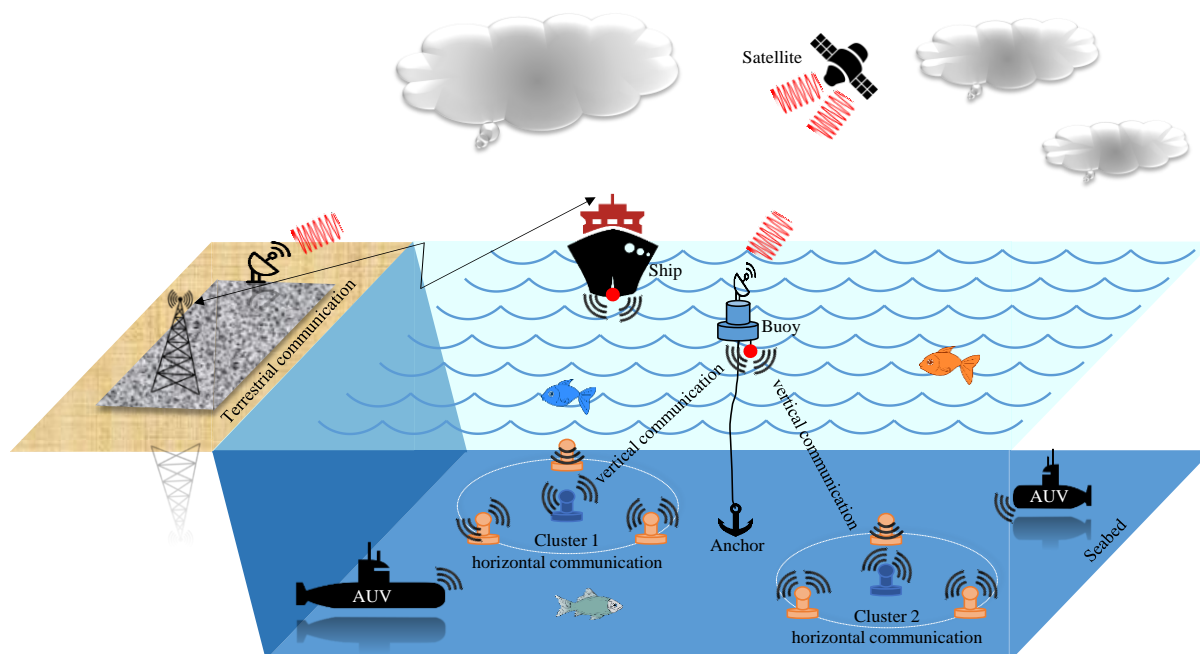
Figure 1.1. Underwater wireless sensor network.

1.1.2. Testing of underwater communication systems

UWSNs have been an area of interest for researchers for the past few decades. Despite their commercial and military importance, their practical deployment and testing remains an open research area .In recent years, several UW communication testbed designs have been proposed in general as well as for specific applications. The dynamic nature of an UW channel remains a challenge for the scientific community in the designing the testbeds [62]. These testbeds can be categorized based on (i) size i.e., small, medium, and large; and (ii) cost of development and deployment which can be low, medium or high.

The in-field testing of UWSNs is not only expensive but requires a lot of time and effort to setup. As a result, the systems deployed at the moment have many limitations and extensive research is being carried out to design a suitable testbed. Factors such as modeling time, cost, deployment resource and

reliability etc., hinder any major breakthrough. Emulators are used to evaluate hardware components of UW communication systems before deployment in real environments, while simulators are used to verify the algorithms and protocols [63]. Some simulation tools have been designed specifically to fulfill the requirements of UW scenarios, while others, which were actually developed for terrestrial communication, have been modified to be used in UW applications. Compared with simulators, the emulator-based systems are more accurate and require less setup time than real-aquatic environments. They can be used to test various kinds of UW communication systems, AUV, autonomous surface vehicle (ASV) and remotely operated vehicle (ROV) etc.

1.2. Underwater acoustic modems

An acoustic modem converts digital data into acoustic waves and transmits underwater, similarly at the other end, the signals in the form of acoustic waves are received by the other modem and converted back into digital data. As said previously, the UAMs can be of commercial or research type. Commercial modems [11-27] are industrial grade designs used for high-speed and reliable communication, but they consume high energy and are expensive. They can communicate at distances up to several km [19, 21, 26], consume more power –up to 300 W [22]–, are large in size and weights –up to 25 kg [12]–. Their cost is in the order of several thousand dollars [60]. Being trade secrets, the manufacturers do not provide complete details of design parameters, therefore alteration or improvement in the modem design for further research is difficult or sometimes impossible. To the contrary, several underwater acoustic modem designs have been proposed in recent years by the scientific community i.e., research modems [28-60] that have exploited diverse alternatives with varying success. The comparative analysis of commercial and research modems based on their characteristics and design constraints, in order to describe the current trends and more promising techniques is provided in the Chapter 2 of this thesis.

A typical UAM consists of four main modules as shown in Figure 1.2. Every modem is built using a hardware platform that works as a brain to control the functionality of other modules. The modems are usually battery operated and ports are used to connect various types of sensors and configuration. The modulator (mix carrier and signals) i.e., modulation and demodulator (also known as detector) is used to recover the original signal. The power amplifier is used for the excitation of underwater transducers, and the pre-amplifier increases the voltage level of the input signal that is readable for the demodulator. The underwater transducers are used to transmit and receive acoustic signals in the water channel.
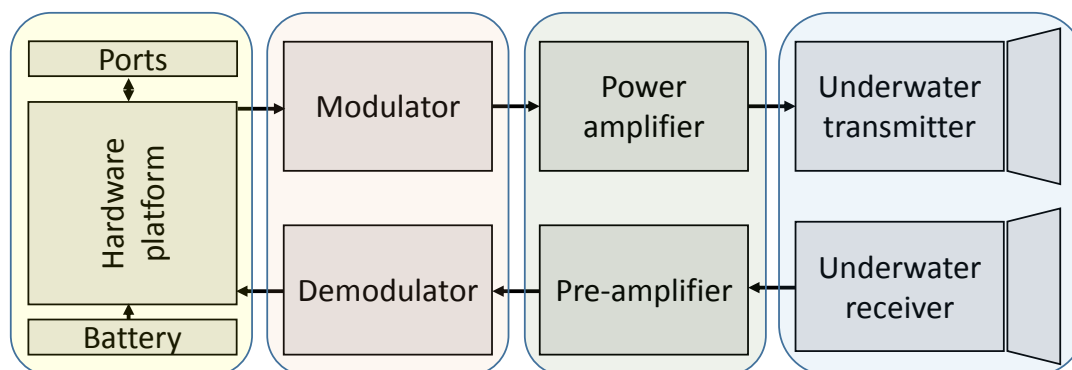
Figure 1.2. A typical underwater acoustic modem.

1.2.1. Hardware platforms

The UW acoustic modems are based on single or a combination of multiple hardware platforms including, digital signal processor (DSP), field programmable gate array (FPGA), ARM Cortex processor, microcontroller (MCU) and laptop / personal computer (PC) based - software defined radio (SDR) etc. Many modems designs are based on DSPs due to their sophisticated signal processing techniques. Typically, a DSP converts the analog data into digital, applies complex mathematical algorithms to process the digital data, and then convert it into analog form. The functionality of the system can be modified or upgraded by programming. The DSP architecture is optimized to perform many mathematical operations in a short span. DSPs are reliable solutions with the limitations of cost-effectiveness [34].

The hardware architecture and operations of FPGAs are not fixed and can be programmed according to the application using hardware descriptive language (HDL). The design can be modified or updated by simply changing the code without making any change in the hardware. Parallel processing is one of the leading features of FPGAs which is useful in high-speed large data processing, especially in video streaming. In spite of design flexibility and availability, FPGAs are power hungry devices and can quickly dissipate the power of the system [53, 64]. MCUs are smaller in size and lower cost to perform general purpose tasks. They are easily available, programmable and can be used in a variety of applications. The MCUs have several general purpose input output (GPIO) software configurable pins which can be used either as input or output. The use of MCU reduces the overall cost and development time, but due to their limited functionality, they cannot be used in high applications [56]. In many cases, the selection of a particular hardware platform depends on a number of factors, and no single platform is an ideal solution. The combination of these platforms is often more appropriate in many applications, which can be seen in state-of-the-art modems discussed in chapter 2.

1.2.2. Communication schemes

On the communication front, the modulation schemes used in UW acoustic modems working in variable aquatic environment include; orthogonal frequency division multiplexing (OFDM), frequency shift keying (FSK), amplitude shift keying (ASK), quadrature phase shift keying (QPSK), direct sequence spread spectrum (DSSS) [10], and two the proprietary schemes only used in commercial modems are sweep spread carrier modulation scheme (S2C) [19] and broadband acoustic spread spectrum (BASS) [21]. The OFDM is a digital multi-carrier modulation technique which encodes digital data over multiple carrier frequencies. It is a special case of FDM, which combines modulation and multiplexing. It provides effective use of spectral efficiency and is useful for high data-rate communication. OFDM implementation requires high computational power and linear amplifiers due to high peak-to-average power ratio [65] [66].

In FSK modulation, the carrier frequency varies according to the input signal. At the transmitter side, the logic high and low states are represented by two different frequencies with the same amplitude. The receiver typically consists of phase-locked-loop (PLL) [56]. FSK is resilient to noise and signal strength variations, and relatively easy to implement, but due to high bandwidth requirements, it is not preferred in high speed modems [67]. ASK is a form of amplitude modulation in which the carrier wave variation represents the digital data. The amplitude of the carrier signal represents $logic - 1$ and

$logic - 0$ for data inputs, keeping the frequency and phase constants. ASK based communication systems are simple to design and comparatively inexpensive but its power efficiency is low and susceptible to noise interference. The QPSK is an alternative to the PSK modulation scheme having four values of phase angles of the carrier wave to represent digital information. QPSK is bandwidth efficient modulation but not power efficient as compared to other modulation schemes [52]. The spread spectrum (SS) has two flavors, frequency hopping (FH) and direct sequence (DS). In FHSS, the signal is transmitted by quickly switching a carrier wave between many frequencies using pseudo-random sequence, while DSSS makes rapid phase transition to the data to make it larger in bandwidth. SS is secure and non-interference communication but complex to be implemented [35].

1.2.3. Amplifiers

Typically class-B, AB and D amplifiers are used for the excitation of piezo-electric transducers of a UAM. Class-B amplifiers are easy to design, but efficiency is not suitable for these kinds of applications because it uses only the positive side of the input signal. To overcome this issue, class-AB amplifier can be used, but again it suffers big energy losses due to a simultaneous operation of both transistors [56]. The block diagram of a class-D amplifier is significantly more complicated compared to that of a class B or AB amplifier, but it provides best efficiency and cost effective, however, there are some drawbacks, e.g., electro-magnetic-interference (EMI) and impedance matching issues. An audio class-D amplifier usually receives a line signal at its input and its first stage consists in a modulator (typically pulse-width, pulse-density or sigma-delta modulators). If the amplifier is to be used at ultrasonic frequencies, the carrier clock has to be raised beyond the typical values of audio frequencies, which are a few hundred kHz. Thus, the carrier frequency of the internal modulator should be higher than about $1\,MHz$, which yields higher switching losses and, at a minimum, makes power efficiency questionable. Therefore, when a class-D amplifier is used to transmit digital data, this modulator could be integrated with the corresponding stage of the modem, so that only one modulation process is carried out [68].

Concerning its output, class-D amplifiers incorporate an output low pass filter subject to strict requirements of losses, frequency band and impedance matching. Differential output is preferred to single-ended output in terms of deliverable power from a nominal DC voltage and transients in the filter inductors, but the number of components in the final stage doubles. In addition, the highly reactive input impedance of the ultrasonic underwater projectors results in a cumbersome design and causes that amplifiers and projectors are somehow matched and different models are not easily interchangeable. Regarding the receiving transducers, the main problem is again impedance matching [31, 69]. In the receiving side of a communication system it is common to find a first stage consisting in a low-noise amplifier (LNA), even at frequencies well below the RF, the reason being to get a clear signal. Impedance matching between the ultrasonic transducer and the LNA is mandatory in order to maximize the power delivered to the demodulator [52].

1.2.4. Transducers

A transducer is a device that converts electrical energy into other types of energy, usually the physical attributes that can be used for different purposes. An underwater acoustic transducer is one of the core elements of an UAM which not only converts electrical energy into acoustic energy (as transmission)

but also converts acoustic energy into electrical energy (as receiver). Underwater transducers use a broad spectrum of frequencies from $1\ Hz\ to\ 1\ MHz$ for acoustic communication [70]. Due to the absorption of sound in water, low frequencies below $100\ Hz$ are used for long distance communication (several thousands of kilometers), while $10\ kHz$ to several hundred kHz are used for normal operation depending upon the depth of the water [70].

Piezo-electric materials are favorable in the designing of acoustic transducers due to their less electrical losses and high coupling coefficient. Piezo-electric materials are available in different types e.g., (piezo-electric ceramics, single crystal, composite material and polymer) [71]. Acoustic transducers can deliver power from few W to several hundred kW. Shallow waters require low power but high frequency, while the high power and low frequencies are used at deep seas. From the vibration point of view, the transducers are available in (i) longitudinal vibration that are extensively used in sonars, (ii) cylindrical type transducers (made by piezo-electric ceramic tube or ring), and in (iii) spherical transducers (made by hollow piezo-electric) used in hydrophones. The size and vibration modes of these transducers vary and depend upon the application [72].

1.3. Research motivation

The previous sections have discussed the basic concepts of underwater acoustic communication and its testing requirements. Particularly, various attributes of an underwater modem, which is the most critical component of underwater acoustic communication, have been discussed. Now, it is important to present a typical underwater acoustic communication scenario in terms of design, testing, deployment and operation, as discussed in Section 1.3.1. The application scenario in Section 1.3.1 enables us to identify the critical factors which play an important role in the success of an underwater communication application. Subsequently, Section 1.3.2, briefly overviews the current practices to handle the identified factors. Consequently, the research gap is identified in Section 1.3.3.

1.3.1. A typical underwater acoustic communication scenario

The process starts with the design/selection of an appropriate modem, depending upon the application type. For example, commercial modems are generally used in all those applications where reliability and high data rates are key concerns[21]. However, the design cost of commercial modems is the real hindrance in their overall adoption for low-budget underwater projects. There are very few research modems which are available to the public and can be used in a low cost scenario [31] [60]. Once the design of UAM is completed, it is required to be tested comprehensively before its actual deployment. The testing can be performed in a real aquatic environment (in-field testing) as well as in the laboratory. The in-field testing is expensive and time consuming as all the laboratory facilities are required on the test site. Although, the laboratory testing is relatively less expensive and less time consuming, a physical access to the laboratory is essential for the testing of modems. After the successful design and testing, the modems are deployed for a particular application/mission. The deployed modems are battery operated and work for a specific amount of time. Therefore, the replacement of batteries is essential after a certain period of time for the successful continuation of the mission. It is important to note that the initial deployment of modems as well as the replacement of batteries are expensive [5].

From the aforementioned application scenario, it is clear that the design cost, testing cost and energy efficiency of a UAM are critical factors. An alternative solution is to design low cost modems with a

relatively larger battery time such that the modems are deployed initially. The deployed modems work for a specific lifetime (depending upon their battery capacity) and replaced with new modems. It implies that instead of replacing the batteries, the complete modems can be replaced. However, this alternative scenario is only feasible when we really have low cost modems along with a relatively low testing cost. Furthermore, the low-cost modems should be energy efficient so that they can work for a longer period of time after their deployment.

1.3.2. Limitations of current practices

The current practices on the design of UAM reveal that either they are expensive (in the order of several thousand USD) [21, 26], or the design information is not available for further research [36]. The detailed performance comparison for various types of commercial and research UW modems is presented in Chapter 2 of this thesis. In the context of UW testing, the in-field testing of UAM has been performed in SUNRISE [73] and SUNSET [74] frameworks. It has been shown in [73] and [74] that the in-field testing support in SUNRISE and SUNSET frameworks is costly and can only be feasible in large-scale scenarios [73] [74]. On the other hand, the laboratory testing has been performed in [75] and [76] to reduce the overall testing cost significantly. However, a physical access to the laboratory is essential in [75] and [76]. Moreover, only an authorized (limited) number of people can benefit from the laboratory. A remote-access facility may solve this issue which in turn will reduce the overall testing cost. Finally, in order to make the UAM energy efficient, certain techniques have been proposed [44, 59]. However, these techniques are mostly implemented at application level (system level). A low cost deployment solution (*deploy-and-forget scenario*) as discussed in Section 1.3.1 is only feasible when the energy efficiency techniques should be implemented at the physical layer (in the design of modem) along with the application/system level techniques.

1.3.3. Research gap

From the discussion in Section 1.3.2, it is clear that some low cost physical layer techniques are needed in the design of a UAM. However, it is always a tradeoff between the cost and various performance factors such as range, data rates and reliability. Moreover, a low-cost remote monitoring and controlling facilities for the testing of modems is needed. A remote monitoring allows the designer to remotely access the lab facility, irrespective of time and duration. It ultimately results in a more comprehensive and thorough testing with a reduced cost. In addition to the low cost design and testing techniques, an energy efficient technique is needed at physical level such that the design of a UAM is modified at component level. The modified UAM should present a better energy efficiency performance.

1.4. Research objectives

In order to address the limitations of current practices (mentioned in Section 1.3.2) and the identified research gap (mentioned in Section 1.3.3), the main objectives of this research are as follows:

a) To propose hardware/software solutions for cost-effective underwater acoustic communication modems to be used in low-budget applications.
b) To implement an economical underwater acoustic communication systems testbed that can be used locally as well as remotely to evaluate the performance for higher layers (such as MAC and Network).

c) To explore physical layer techniques for underwater acoustic communications that require low energy consumption for long-life underwater acoustic modems.

1.5. Contributions to the dissertation

In order to achieve the objectives mentioned in Section 1.4, this dissertation has four contributions to implement the physical layer techniques for cost-effective and energy efficient underwater acoustic communication modem.

a) ***State-of-the-art underwater acoustic modems.*** The purpose is to provide a taxonomy to classify the existing underwater acoustic modems by dividing them into two major groups: (*i*) commercial modems and, (*ii*) research modems. In each category, the performance has been compared in terms of certain performance attributes. These performance attributes are data rate, range, center frequency, bandwidth, transmission power, modulation schemes and bit-error rate. Furthermore, a statistical analysis of the presented modems has allowed us to extract various design challenges. Moreover, the detailed performance comparison may enable the researchers and practitioners of this domain to select an appropriate UAM as per their requirements and a particular application scenario.

b) ***Design of a low cost underwater acoustic modem.*** The objective is to design a cost-effective underwater acoustic modem using a modular approach that can be replicated or modified for further improvements. Contrary to the traditional hardware platforms in UAM such as DSP and FPGA, the proposed design revolves around a single-board computer along with a microcontroller. The other components of the modem (such as modulator, demodulator, amplifiers and transducers) are designed with discrete components to reduce the overall design cost. Basic functionality of the modem has been tested (both at component level as well as at system level) in an aquatic environment to verify the design.

c) ***A web-based underwater communication testing system.*** The goal is to develop a web-based underwater communication testbed and simulation platform. The distinguished features of the proposed testbed are less development time, low-cost and remote monitoring facility. In other words, the proposed UW communication testbed is not only economical but requires low setup and learning time for test setup. The remote monitoring and controlling facility using a web browser is an additional characteristic of the testbed to access the facility without physical access. The cost-effective emulator is designed to test underwater modems and sensors in an aquatic laboratory environment. The graphical easy-to-use simulator has been designed in LabVIEW to simulate underwater acoustic channel and sound propagation models. The simulator has remote accessibility via web browser.

d) ***Integration of a digital modulator and a class-D amplifier.*** The idea of this integration of a digital modulator and a class-D amplifier is to improve the energy efficiency of the underwater communication system to prolong the battery life. The concept is verified using MATLAB, modeled in Simulink and implemented as an electronic circuit using Multisim. The proposed integration is energy-efficient as well as cost-effective.

1.6. Dissertation organization

The dissertation consists of six chapters and organized as follows:

Chapter 1 describes an overview of underwater acoustic communication. First, we provide the background knowledge followed by the research objectives. We also describe the contributions and organization of the dissertation then outline of the dissertation is presented. The list of related publications is provided at the end of the chapter.

Chapter 2 provides an overview of state-of-the-art underwater acoustic modems in terms of their fundamental characteristics. The commercial and research underwater acoustic modems are classified in tabulated form. In each category, we define certain performance attributes such as operating frequency, range, data rate, hardware platform, modulation scheme etc. The performance of various commercial and research modems is discussed in terms of defined attributes. Furthermore, a statistical analysis is performed to compare various performance parameters of commercial and research modems and results are presented in graphical form. From the statistical analysis, certain design challenges are extracted. The extracted design challenges are low cost UAM design, cost efficient underwater testing and energy efficient techniques at physical level. This chapter has set a stage for the remaining chapters of this thesis. The design challenges, extracted in this chapter, have been addressed with various physical layer techniques in Chapter 3, Chapter 4 and Chapter 5 of this thesis. The contents of this chapter have been published in [77].

Chapter 3 contains the second contribution of the thesis i.e., the design of a low-cost UAM for short range underwater acoustic communications. The proposed modem is designed in this chapter is designed using a low-cost single board computer (Raspberry-Pi) and a microcontroller. The remaining modules (modulator, demodulator and amplifiers) are designed from discrete components and the transducers are made from piezo-ceramic elements to reduce the overall cost of the modem. The modular architecture and main blocks of the proposed modem are described. Each module has been tested separately before integration. Experimental setup and results along with discussions are presented to verify the functionality of the modem. The chapter ends with a comparison with similar modem designs. The contents of this chapter have been published in [31].

Chapter 4 is the design of a web based underwater acoustic communication testbed and simulation platform. The experimental setup has been used to evaluate the performance of underwater modems using a water tank in a controlled laboratory setup. Simulations of underwater sound propagation, attenuation and ambient noise models have been performed locally as well as using a web based browser. A detailed discussion of underwater communication testbeds has been provided. The contents of this chapter have been published in [69].

Chapter 5 is the integration of digital modulator with class-D amplifier. A mathematical model is presented to integrate the pulse width modulator of a class-D amplifier and binary phase shift keying modulator. This technique is used to reduce the size and increase power efficiency of the transmitter. An electronic circuit has been designed and successfully tested to validate the experimental results. The contents of this chapter have been published in [78].

Chapter 6 summarizes the research and provides conclusions with the future directions.

1.7. Related publications

Following are the related publications. To avoid the use of double numeration of the same cite and clarity, we have used the same reference numbers as used in the bibliography.

[9]   M. Y. I. Zia, A. M. Khan, P. Otero, and J. Poncela, "Investigation of underwater acoustic modems: Architecture, test environment & performance," in 3rd International Conference on Computing for Sustainable Global Development (INDIACom), 2016, pp. 2031-2036.

[31]   M. Y. I. Zia, P. Otero, and J. Poncela, "Design of a Low-Cost Modem for Short-Range Underwater Acoustic Communications," Wireless Personal Communications, vol. 101, pp. 375-390, 2018, doi: 10.1007/s11277-018-5694-5.

[69]   M. Y. I. Zia, P. Otero, A. Siddiqui, and J. Poncela, "Design of a Web Based Underwater Acoustic Communication Testbed and Simulation Platform," Wireless Personal Communications, pp. 1-23, 2020, doi: 10.1007/s11277-020-07203-7.

[77]   M. Y. I. Zia, J. Poncela, and P. Otero, "State-of-the-Art Underwater Acoustic Communication Modems: Classifications, Analyses and Design Challenges," Wireless Personal Communications, 2020, doi: 10.1007/s11277-020-07431-x.

[78]   M. Y. I. Zia, R. Tierno, M.-Á. Luque-Nieto, and P. Otero, "An Energy-Efficient Integration of a Digital Modulator and a Class-D Amplifier," Electronics, vol. 9, p. 1319, 2020, doi:10.3390/electronics9081319.

Chapter 2: State-of-the-Art Underwater Acoustic Modems [*]

Chapter 1 has described two motivating factors for this thesis: (*i*) cost-effective and (*ii*) energy efficient techniques for underwater acoustic communication modems. Since acoustic waves are suitable in underwater communication due to low attenuation of sound in water, many commercial manufacturers and research organizations have designed acoustic modems for underwater applications. Hence there is a need for a comprehensive comparative analysis to find state-of-the-art.

This chapter provides a comprehensive statistical analysis of state-of-the-art underwater acoustic modems. Main characteristics of commercial and research modems are presented in tabular form including the following parameters: operating range, modulation schemes, data rates, center frequency, bandwidth, bit-error-rate, and power consumption. These parameters are jointly analyzed to highlight the gap between commercial and research products and summarized at the end of the chapter.

This chapter is organized as follows: Section 2.1 describes the fundamental features of underwater acoustic modems. Section 2.2 presents state-of-the-art commercial and research underwater acoustic modems. Statistical analysis of various parameters of commercial and research modems is performed in Section 2.3. Section 2.4 provides a discussion on the characteristics of the modems. Section 2.5 identifies the design challenges and Section 2.6 concludes the chapter.

2.1. Introduction

A typical UWSN consists of various sensor nodes (modems) that collect, store, and share data wirelessly below the water surface. The operating range, data rate, cost and power consumption of these modems vary, depending on the applications for which they are deployed. In UW communications, water is the transmission medium. Electromagnetic waves in water suffer from excessive absorption in the communication link [1]. To achieve high-speed data communication, optical waves are a good choice with the constraints of scattering, absorption, limited to short distances and require line-of-sight alignment of agents [2, 3]. As compared to electromagnetic and optical waves, acoustic propagation is better in water and it can cover far greater distances, in the order of several kilometers [4, 5]. We present a comprehensive comparative analysis of underwater acoustic modems to find state-of-the-art in this chapter.

There are some surveys available on UWSNs [4-8], and some on UAMs [9, 10]. A background of UWSN is presented in [4] which mainly focuses on the applications of UWSN though some opportunities are also highlighted in the research. The characteristics of terrestrial and UWSNs in terms of cost, deployment, communication, and power consumption are described in [5]. Furthermore, the research challenges of UWSN at different layers are main targets of the article. The architecture and fundamental aspects of UWSN are presented in [6] that address the challenges for efficient communication in UWSNs. A cognitive underwater acoustic network (UAN) is proposed in [7] to efficiently utilize spectrum resources with the features of UW channel and acoustic modems along with the challenges and possible solutions are also discussed in the paper. The advances and challenges in UW acoustic communications are discussed in [8] which focus on UW communication, algorithms and networking protocols and provide ideas and developments that are likely to be the foundation of future UW communication networks. Recent developments in UW acoustic modems are presented in [9] where various parameters of UW acoustic modems are compared including hardware platform, operating range, data rate, etc. The investigation is based on a limited dataset of UW acoustic research modems. Analysis of commercial and research UW acoustic modems is presented in [10].

While the surveys, presented in [4-10] provide a good insight on the problem, there are certain limitations. For example, there is a lack of detailed explanation for sensor nodes in [4-8]. Similarly, the work in [9, 10] is based on relatively smaller data sets of acoustic modems without any statistical analysis. It implies that their study is based on a limited number of UW acoustic modems and a deficit of graphical analysis. Therefore, it is essential to perform a comprehensive analysis of commercial as well as research underwater acoustic modems in terms of various attributes. The results are required to be analyzed statistically so that a meaningful conclusion can be made.

The analysis presented in this chapter aims to provide a comprehensive overview on state-of-the-art commercial and research underwater acoustic modems. Commercial modems are designed to meet industrial requirements, while the research modems are developed by the scientific community. A set of characteristics has been devised for analysis due to their inherent interest. For example: the operating range of a UAM has direct impact on the length of one hop; the modulation schemes used may be adapted to the characteristics of the transmission signal and its propagation within the oceanic medium; the choice of center frequency and bandwidth directly affects the range and data rates of the modems;

the power consumption indicates the energy efficiency of the modem. The design challenges faced by modem designers e.g., cost-effectiveness and energy efficiency are discussed at the end of the chapter.

2.2. Commercial and research modems

The details of state-of-the-art commercial and research modems are presented in this section. Subsection 2.2.1 explains the characteristics of commercial modems [11-27], while the properties of research modems are described in Subsection 2.2.2 [28-60]. The common parameters used for both classifications include: operating range, data rates, modulation schemes, center frequency, bandwidth, power consumption and bit-error-rate. Some exclusive parameters of commercial modems, e.g., working depth, weight and operating temperature, and of research modems, e.g., hardware platforms, and amplifiers are also discussed.

2.2.1. Commercial modems

The state-of-the-art UW commercial modems recently developed and available in the market are alphabetically arranged in Table 2.1[11-27]. The first and second columns represent the manufacturer and model number respectively. The third – fifth columns show the range, modulation schemes and data rates. Operating depths (typical and maximum) are shown in sixth and seventh columns. The eighth – tenth columns show the center frequency, bandwidth and bit-error-rate. Power consumptions during transmission (typical and maximum), receiving and standby are shown in columns eleventh – fourteenth. Fifteenth column shows the weight and operating temperatures (minimum and maximum) are shown in sixteenth and seventeenth columns. First we describe the different models designed by each manufacturer, then the analysis is carried out.

SeaModem is an open source hardware/software platform designed by AppliCon [11] using DSP for low-cost UW communication systems. It works in the frequency band of $25 - 35\,kHz$, with selectable multiple frequency shift keying (MFSK) modulation scheme. The modem has a range of up to $400\,m$ distance in shallow water with claimed data rates of $750, 1500,$ and $2250\,bps$. It can deliver up to $40\,W$ during transmission. Cyclic redundancy check (CRC) is used to detect errors; however, convolutional codes and Viterbi decoding algorithms are used for error correction in a received bit stream [11]. It has a network capability with capacity for up to 15 modems and operates at $12\,V_{DC}$.

AquaSeNT [12] has designed three types of acoustic modems. Their first model, AM-AUV, as the name indicates, is specially designed for AUVs. It works in the frequency range of $21 - 27\,kHz$, and consists of a discrete digital-analog board fixed in a metallic frame to avoid electromagnetic interference. The second model, AM-D2000, has the capability of vertical communication in deep waters down to $2000\,m$, thus making it suitable for data telemetry from sea floor to the surface. It operates in the frequency range of $9 - 15\,kHz$. The third model, AM-OFDM-13A is designed for shallow waters, especially for horizontal communication, and uses the frequency band $21 - 27\,kHz$. Its transducer is omni-directional, and four hydrophones make it a multi-channel receiver. These modems communicate up to $5000\,m$ using OFDM modulation with data rates in the range of $375 - 9000\,bps$. They are powered by a $12 - 16\,V$ supply.

Table 2.1: Underwater acoustic commercial modems.

Manufacturer	Model number	Range (m)	Modulation scheme	Data rate (bps)	Depth (m) Typical	Depth (m) Max.	C.F. (kHz)	BW (kHz)	Bit error rate	Power consumption (W) TX	TX_{max}	RX	Standby	Weight (kg)	Temp. (°C) Min.	Temp. (°C) Max.
AppliCon [11]	SeaModem	400	MFSK	750, 1500, 2250	-	-	30	10	-	-	40	-	-	0.53	-	-
	AM-AUV	5000	OFDM	375, 750, 1500	-	-	24	6	-	-	25	0.8	0.12	-	-	-
AquaSeNT [12]	AM-OFDM-13A	5000	OFDM	1500, 3000, 4500, 6000, 9000	-	200	24	6	-	-	25	0.8	0.12	9.5	-	-
	AM-D2000	5000	OFDM	375, 750, 1500	-	2000	12	6	-	-	25	0.8	0.12	24.2	-	-
Aquatec [13]	AQUAmodem 500	250	PPC	25-100	-	200	29	4	-	-	-	-	-	-	0	40
	AQUAmodem 1000	5000	FSK, DPSK SS	300-2000	-	1000	9.75	4.5	-	20	20	0.6	0.005	-	-5	40
Blueprint Subsea [14]	SeaTrac X150	1000	SS	100	100	2000	28	8	-	6	6	-	0.6	0.72	-5	40
	SeaTrac X110	1000	SS	100	100	2000	28	8	-	6	6	-	0.6	0.69	-5	40
	SeaTrac X010	1000	SS	100	300	300	28	8	-	6	6	-	0.6	0.3	-5	40
Desert Star [15]	SAM-1	1000	PPM	150	300	300	37.5	9	-	16	32	0.17	-	0.23	0	70
Develogic [16]	HAM.NODE	1950	OFDM, MFSK	7000	750	6000	3.5, 10.5, 15.5, 23	2, 5, 9, 12	-	30	250	-	0.03	13.6	-	-
	HAM.Base	1200	OFDM, MFSK	10000	750	6000	52.5	25	-	30	250	-	0.01	-	-	-
DiveNET [17]	Microlink	1000	BPSK	78	-	300	20	20	10^{-6}	6	-	0.33	-	0.16	-5	50
	Sealink C	8000	BPSK	88	300	400	10	10	10^{-6}	10	-	0.4	-	0.33	-5	50
	Sealink R	2500	BPSK	560, 1200	300	300	27.5	35	10^{-5}	10	-	0.4	-	0.36	-5	50
	Sealink S	8000	BPSK	80	300	400	10	10	10^{-6}	10	-	0.4	-	0.36	-5	50
DSPComm [18]	Aquacomm	3000	DSSS, OFDM	100, 240, 480	-	-	23	14	10^{-6}	-	30	-	-	-	-5	50
	Aquacomm Gen2	8000	DSSS, OFDM	100-1000	-	-	23	14	10^{-6}	10	30	-	-	-	-5	50
Evologics [19]	S2CM HS	300	S2C	62500	200	200	160	80	10^{-10}	3.5	10	0.8	0.0005	1.12	0	60
	S2CM 48/78	1000	S2C	31200	200	2000	63	30	10^{-10}	18	55	0.8	0.0025	1.12	0	60
	S2CM 42/65	1000	S2C	31200	200	2000	53.5	23	10^{-10}	18	35	0.8	0.0025	1.21	0	60
	S2CM 18/34	3500	S2C	13900	200	2000	26	16	10^{-10}	35	55	0.8	0.0025	1.26	0	60
	S2CR 48/78	1000	S2C	31200	200	2000	63	30	10^{-10}	18	60	1.1	0.0025	2.25	0	60
	S2CR 42/65	1000	S2C	31200	500	2000	53.5	23	10^{-10}	18	60	1.1	0.0025	2.3	0	60
	S2CR 40/80	2000	S2C	27700	500	2000	51	26	10^{-10}	40	60	1.1	0.0025	1.39	0	60
	S2CR 18/34	3500	S2C	13900	200	2000	26	16	10^{-10}	35	80	1.3	0.0025	2.44	0	60
	S2CR 18/34D	3500	S2C	13900	6000	6000	26	16	10^{-10}	35	80	1.3	0.0025	6.5	0	60
	S2CR 15/27	6000	S2C	9200	200	6000	21	12	10^{-10}	15	40	1.1	0.0025	2.99	0	60
	S2CR 12/24	6000	S2C	9200	200	6000	18.5	11	10^{-10}	15	40	1.1	0.0025	2.99	0	60
	S2CR 7/17	8000	S2C	6900	200	6000	12	10	10^{-10}	40	80	1.1	0.0025	2.99	0	60

Table 2.1: Underwater acoustic commercial modems (continued).

Manufacturer	Model number	Range (m)	Modulation scheme	Data rate (bps)	Depth (m) Typical	Depth (m) Max.	C.F. (kHz)	BW (kHz)	Bit error rate	TX	TX$_{max}$	RX	Standby	Weight (kg)	Temp Min.	Temp Max.
Kongsberg [20]	cNode MiniS 34-180	1000	FSK	6000	-	4000	26	10	-	-	100	-	0.1	4	-5	55
	cNode MiniS 34-40V	4000	FSK	6000	-	4000	26	10	-	-	100	-	0.1	4.6	-5	55
LinkQuest [21]	UWM1000	350	BASS	17800	200	200	35.7	17.9	10^{-9}	1	2	0.75	0.008	4.2	-5	45
	UWM2000	1500	BASS	17800	2000	4000	35.7	17.9	10^{-9}	2	8	0.8	0.008	4.8	-5	45
	UWM2000H	1500	BASS	17800	2000	2000	35.7	17.9	10^{-9}	2	8	0.8	0.008	4.8	-5	45
	UWM2200	1000	BASS	35700	1000	2000	71.4	35.7	10^{-9}	6	6	1	0.012	3.0	-5	45
	UWM3000	3000	BASS	5000	2000	7000	10	5	10^{-9}	3	12	0.8	0.008	4.1	-5	45
	UWM3000H	3000	BASS	5000	2000	7000	10	5	10^{-9}	3	12	0.8	0.008	4.1	-5	45
	UWM4000	4000	BASS	8500	3000	7000	17	8.5	10^{-9}	7	7	0.8	0.008	4.1	-5	45
	UWM10000	10000	BASS	5000	2000	7000	10	5	10^{-9}	40	40	0.9	0.009	21	-5	45
Oceania [22]	GPM 300	5000	DSSS	10-1200	1000	1000	-	-	10^{-4}	-	300	1.8	-	7	0	50
Sercel [23]	MATS 3G 12 kHz	15000	FSK / PSK	20, 100, 200 / 850, 2100, 3600, 5500, 7400	-	6000	12.5	5	-	-	75	0.6	0.04	-	-10	50
	MATS 3G 34 kHz	5000	FSK / PSK	20, 150, 300 / 1000, 3000, 6400, 9200, 13000, 15000, 24600	-	6000	34.5	9	-	-	75	0.6	0.04	-	-10	50
Sonardyne [24]	Modem 6 Sub-Mini	2000	QPSK	200-9000	1000	1000	26.8	11.5	-	-	-	-	-	3.2	-5	40
	Modem 6 Mini	3000	QPSK	200-9000	3000	3000	26.8	11.5	-	-	50	0.5	0.3	5.1	-5	40
	Modem 6 Standard	5000	QPSK	200-9000	3000	5000	26.8	11.5	-	-	-	-	-	23.8	-5	40
Subnero [25]	M25M	3000	OFDM, FSK	15000	-	-	25	16.6	-	-	-	-	-	-	-	-
Teledyne Benthos [26]	903 ATM-903	6000	MFSK / PSK	140-2400 / 2560-15360	-	-	11.5, 18.5, 24.5	5	10^{-7}	-	20	0.6	0.01	-	-	-
	910 ATM-915	6000	MFSK / PSK	140-2400 / 2560-15360	500	500	11.5, 18.5, 24.5	5	10^{-7}	-	20	0.6	0.01	10.8	-	-
	910 ATM-916	6000	MFSK / PSK	140-2400 / 2560-15360	500	500	11.5, 18.5, 24.5	5	10^{-7}	-	20	0.6	0.01	4.5	-	-
	920 ATM-925	6000	MFSK / PSK	140-2400 / 2560-15360	2000	2000	11.5, 18.5, 24.5	5	10^{-7}	-	20	0.6	0.01	10.8	-	-
	920 ATM-926	6000	MFSK / PSK	140-2400 / 2560-15360	2000	2000	11.5, 18.5, 24.5	5	10^{-7}	-	20	0.6	0.01	4.1	-	-
	960 ATM-965	6000	MFSK / PSK	140-2400 / 2560-15360	6000	6000	11.5, 18.5, 24.5	5	10^{-7}	-	20	0.6	0.01	16.3	-	-
	960 ATM-966	6000	MFSK / PSK	140-2400 / 2560-15360	6000	6000	11.5, 18.5, 24.5	5	10^{-7}	-	20	0.6	0.01	4.1	-	-
Tritech [27]	Micron	500	SS	40	750	750	24	8	-	7.9	7.9	0.72	-	0.24	-10	35

Aquatec [13] has presented two products, AQUAmodem 500 and 1000. AQUAmodem 500, operates in the frequency range of $27-31\ kHz$ for short range, up to $250\ m$. The data rate is low in the range of $25-100\ bps$. It can be used in a variety of applications, including diver status monitoring, subsea pipeline monitoring, etc., and uses passive phase conjugation (PPC) modulation scheme. The second model, AQUAmodem 1000, is tailored for long range, high data rate and deep water communication. It uses frequencies from $7.5-12\ kHz$ with FSK and DPSK spread spectrum (SS) modulation schemes. Its communication range is from $250-5000\ m$, with data rates in the range of $300-2000\ bps$. It can be deployed at a depth of $1000\ m$.

A SeaTrac series of underwater acoustic modems are introduced by Blueprint Subsea [14]. The three models of SeaTrac ($X150, X110$, and $X010$) are based on the SS modulation scheme. The modems operate in the frequency range of $24-32\ kHz$ and can communicate up to $1000\ m$, with the data rate of 100 bps. The operating depth varies in the range of $100-300\ m$, which can be extended up to $2000\ m$ by using suitable casing [14]. Due to light weight, the modems can be used in small to medium scale remotely operated underwater vehicles (ROVs) or AUVs etc. The modems are powered by $9-28\ V_{DC}$ supply and consume $6\ W$ during transmission.

A low-cost miniature acoustic modem, SAM-1, has been introduced by Desert Star Systems [15] to operate in a variety of underwater environments. It works in the frequency range of $33-42\ kHz$ and uses pulse position modulation (PPM) scheme. The modem operates in (i) data mode: to transmit and receive data, and (ii) control mode: to configure modem parameters. The typical communication range of the modem is reported as $250\ m$, however it can communicate up to $1000\ m$ under a quiet, deep water environment with a data rate of $150\ bps$. The depth rating is $300\ m$. The modem is considered as energy efficient and uses low power during standby mode.

Develogic has designed powerful acoustic modems for underwater communication [16]. They can be operated with a variety of transducers and different frequency bands from $750-6000\ m$ deep sea. OFDM and MFSK modulation schemes are used in the modems using DSP. The HAM.NODE can operate up to $1950\ m$ with data rate $7000\ bps$, while HAM.Base can work up to $1200\ m$ with data rate $10,000\ bps$. During normal operation they consume $30\ W$ which can be increased up to $250\ W$ in high power transmission mode.

DiveNET has introduced miniature and compact underwater acoustic modems [17]. Its product Microlink is considered as a world smallest UW acoustic modem that can operate up to $1000\ m$ range with $78\ bps$ data rate in shallow waters [17]. Another model Sealink-R can work up to $2500\ m$ with 560 and $1200\ bps$. Sealink-C and Sealink-S can operate up to $8000\ m$ with 88 and $80\ bps$ respectively. Binary phase shift keying (BPSK) modulation scheme is used in the modems. Typically they can be deployed up to $300\ m$ deep waters which can be extended up to $400\ m$ in Sealink-C and Sealink-S. The bit error rate (BER) of each model is 10^{-6}, while power consumption during transmission is $6-10\ W$ and less than $0.4\ W$ during reception.

The acoustic modems designed by DSPComm are based on DSP and used in reliable UW communication [18]. The first model AquaComm can communicate up to $3000\ m$ with data rates 100, 240, and 480 bps, while the second model AquaComm Gen2 can communicate up to $8000\ m$ using data rates from $100-1000\ bps$. DSSS and OFDM modulation schemes are used in the frequency band

of $16-30\ kHz$. BER of the modems is in the range of 10^{-6}. The modems operate from $5-9\ V_{DC}$, and consume $10\ W$ during normal operation that can be increased up to $30\ W$ in high power transmission mode.

The Evologics modems use a proprietary modulation scheme; sweep spread carrier (S2C) [19]. Their variety of models work in the range of $300-8000\ m$ with data rates from $6900-62,500\ bps$. One of the models S2CM-HS operates in the frequency band of $120-200\ kHz$ with a high data rate, i.e., $62,500\ bps$, for the range of $300\ m$. This is the fastest and most reliable modem reported among all UW modems. The other two groups consist of $S2CM-xx/yy$ and $S2CR-xx/yy$ series. Series $S2CM-xx/yy$ consists of three models, which operate in the range of $1000-3500\ m$, with the data rate from $13,900-31,200\ bps$, while series $S2CR-xx/yy$ has eight models that operate in the range of $1000-8000\ m$ using data rates of $6900-31,200\ bps$. The BER of all models is 10^{-10}, while the operating depth is in between $200-6000\ m$. The power consumption depends upon the model, as mentioned in Table 2.1.

cNode Modem MiniS is designed by Kongsberg for point-to-point UW acoustic communications [20]. The two models use FSK modulation and operate in the frequency range from $21-31\ kHz$. The modems are powered by $24\ V_{DC}$ supply. The maximum transmit power can be extended up to $100\ W$, while they consume $0.1\ W$ during reception. The modems communicate at 6000 bps and can be deployed at $4000\ m$ deep water. The operating range of MiniS 34-180 is $1000\ m$, and MiniS 34-40 V can work up to $4000\ m$.

LinkQuest's UW acoustic modems are popular due to their high data rate, low BER and power consumption [21]. The modem design is based on state-of-the-art DSP technology. It uses proprietary modulation scheme broadband acoustic spread spectrum (BASS) and it is categorized as the best-selling UW acoustic modem in the world. Hundreds of modem nodes are deployed in the world largest UW acoustic network [21]. Eight models of the series work in the range of $350-10,000\ m$ with data rates from $5000-35,700\ bps$. They can be classified into three groups, as mentioned in Table 2.1. The communication range of UWM1000–UWM2000H is from $350-1500\ m$, with a data rate of $17,800\ bps$. Modem UWM2200 operates at $1000\ m$ with $35,700\ bps$, which is the highest data rate among all models. The third group consists of modems UWM3000–UWM10000; they communicate from $3000-10,000\ m$, with a data rate of $5000-8500\ bps$. The BER of all models is below 10^{-9}. The power consumption during transmission is $1-7\ W$, except for one model, which consumes up to $40\ W$ for long range communication.

The GPM300, a long range UW acoustic modem designed by Oceania [22], can communicate up to $5000\ m$ with data rates from $10-1000\ bps$. The modem can be used in a variety of applications, including voice and data transmission. In calm and deep underwater environments, the theoretical range of the modem for data transmission, as reported by the manufacturer, is up to $45,000\ m$ with a very low data rate of $10\ bps$ [22]. At an increased data rate, $1000\ bps$, it can communicate up to $5000\ m$, while actual range depends on deployment and environmental conditions [22]. Direct sequence spread spectrum (DSSS) modulation scheme is used in the modem, and its BER is in the order of 10^{-4}. One of the major features of the modem is the maximum power, that can be adjusted up to $300\ W$.

Sercel has introduced a multi-modulation acoustic telemetry system (MATS3G) modems based on state-of-the-art DSP technology [23]. The two models can be used in a variety of UW applications, such as AUV, command and control, and underwater monitoring systems using FSK/PSK modulation schemes. In low noise environments, the maximum communication range of the modems is from $5000 - 15,000\,m$, with data rates from $850 - 24,600\,bps$. The modems consume up to $75\,W$ during transmission, and can be deployed at a depth of $6000\,m$.

Sonardyne [24] has introduced three underwater modems; Sub-Mini, Mini, and Standard working in the range of $2000 - 5000\,m$. They use a QPSK modulation scheme and typically operate in the frequency range from $21 - 32.5\,kHz$. The modems operate at data rate from $200 - 9000\,bps$ and can be deployed at the depth from $1000 - 5000\,m$. The power consumption of Mini modem is $0.5\,W$ during reception, however it can consume up to $50\,W$ during high power transmission. RS-232 and RS-485 protocols are available with host communication.

The software defined modem Subnero [25] is based on DSP & FPGA designed to perform high performance underwater acoustic communications and navigation. It works in the frequency band from $20 - 30\,kHz$ with bandwidth up to ⅔ of carrier frequency [25]. It supports various software defined modulation schemes including PSK-OFDM, Incoherent OFDM and FH-BFSK. The communication range of the modem reaches up to $3000\,m$, depending upon the aquatic conditions with a data rate of $2000 - 10,000\,bps$. The key features of the modem include support of multiple logical channels with configurable modulation and acoustic channel diagnostics. It claims to be able to operate in highly noisy environments, such as those with presence of sea creatures and shipping activity.

Teledyne Benthos offers a variety of low BER underwater acoustic modems [26]. These modems operate in various frequency ranges: low frequency $9 - 14\,kHz$, medium frequency $16 - 21\,kHz$, and high frequency $22 - 27\,kHz$. MFSK and MPSK modulation schemes are used in the modems. The typical operating range of the different models is from $2000 - 6000\,m$, which can be increased further using a repeater. The modems are capable of operating at different data rates from $140 - 15,360\,bps$. Depending upon the model, Benthos modems can be deployed at varying depths, i.e., shallow water, deep water from $500 - 6000\,m$. The modems provide high reliability, with a BER in the order of 10^{-7}. RS-232 and RS-485 interfaces are available for data connection.

Micron modem is a low-power acoustic modem designed by Tritech [27] for low data rate UW communications. It can be used as a stand-alone system or can be used to control an AUV. The major features of the modem include its compact size and multi-path noise cancelation. The modem operates in the $20 - 28\,kHz$ frequency range using a robust SS modulation scheme. The communication range (horizontal) of the modem is up to $500\,m$, with a data rate of $40\,bps$. It consumes around 8 W during transmission and can be deployed at a depth of $750\,m$.

Based on the above descriptions, we proceed to analyze state-of-the-art underwater acoustic commercial modems. In the corresponding figures we have arranged the modems on the horizontal axis; the parameter of interest is shown on the vertical axis.

a) **Range.** The operating range of UW commercial modems is from $250-15,000\ m$, as illustrated in Figure 2.1. The modems are shown on the horizontal axis and the values of operating range are displayed by blue dots on the vertical axis using a logarithmic scale. From the figure, it is clear that many modems provide similar ranges. The operating range of 40.0% modems is from $250-2000\ m$, 49.1% from $2500-6000\ m$, and only 10.9% operate in the range of $8000-15,000\ m$. The median operating range of commercial modems is $3000\ m$, shown by a blue dotted line; the standard deviation is $2910\ m$.
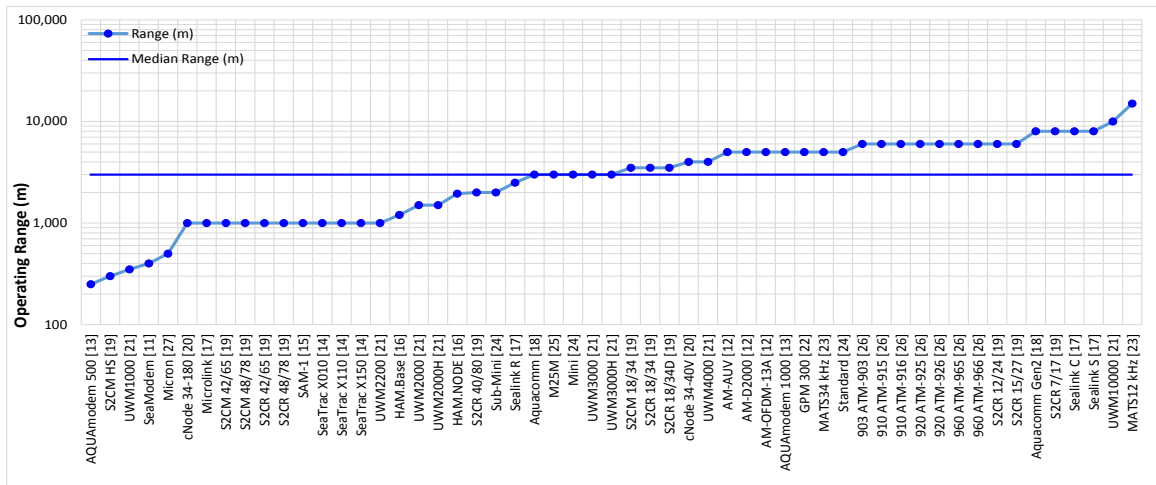

Figure 2.1. Operating range of commercial modems.

b) **Data rates.** Figure 2.2 shows the data rates that vary from $10-62,500\ bps$. The horizontal axis indicates the model and the data rate values are shown on the vertical axis on a logarithmic scale. The light blue line joining the blue dots is representing the trend. The data rate of 48.4% of the modems is from $10-1000\ bps$, 29.7% from $1500-10,000\ bps$, 10.9% from $13,900-17,800\ bps$, and 10.9% can communicate from $27,700-62,500\ bps$.
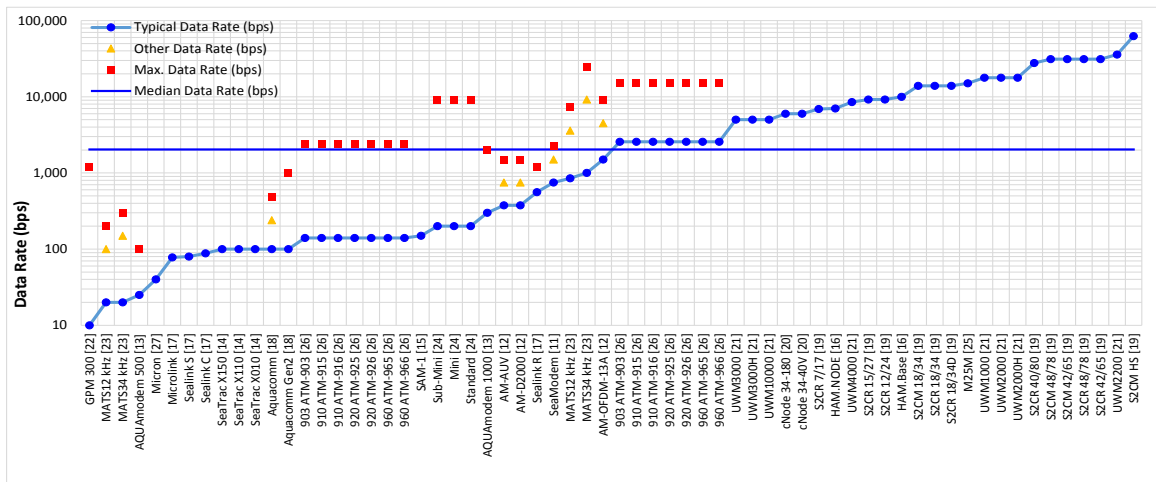

Figure 2.2. Data rates of commercial modems.

The median value of the data rate is 2030 *bps* and the standard deviation is 11,764 *bps*. Out of the total, 48.4% modems have the capability to communicate at higher data rates; the maximum data rate of these modems is shown by red squares in Figure 2.2. The median value of the maximum data rate is 2400 *bps*.

c) *Modulation schemes.* The modulation schemes used by commercial modems are shown in Figure 2.3. The modems developed by various manufacturers are arranged on the horizontal axis, while the vertical axis is representing two scales. On the left hand side, the number of modems using particular modulation schemes are shown by blue bars; on the right hand side the percentage of the modems using that modulation scheme is illustrated by red triangles. The most common modulation schemes used in UW commercial modems are FSK and PSK, which are being used in 22.9% in each of these modems. OFDM and SS are also used in 11.4% in each of the modems. The two proprietary modulation schemes S2C and BASS are respectively used in 17.1% and 11.4% of the modem designs [19, 21]. 1.4% modems are based on PPC and the same 1.4% modems use pulse position modulation (PPM).
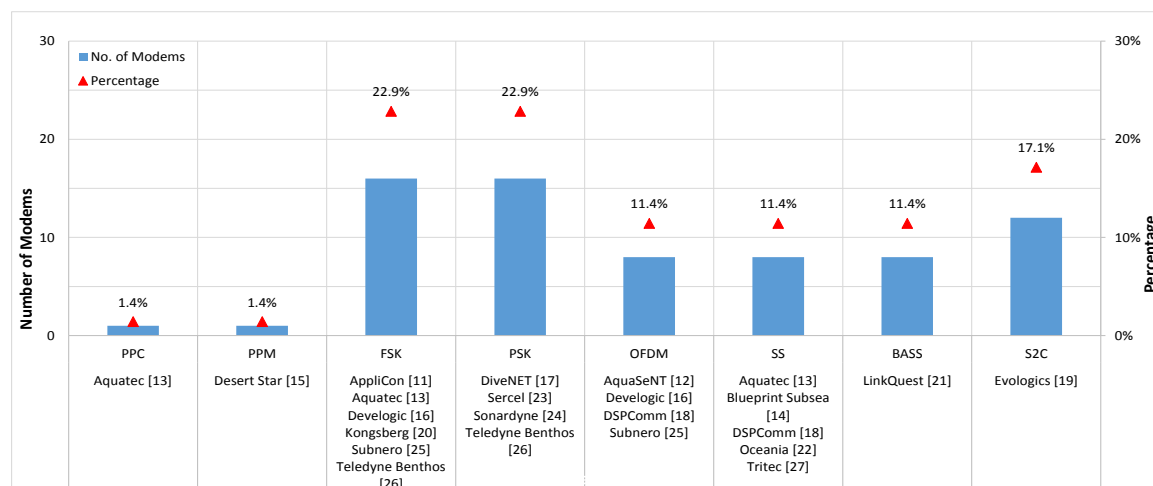

Figure 2.3. Modulation schemes of commercial modems.

d) *Working depth.* Working depth of the modems is from $100 - 6000\ m$, as shown in Figure 2.4 using blue dots on a logarithmic scale on vertical axis, while the modems are placed on horizontal axis.
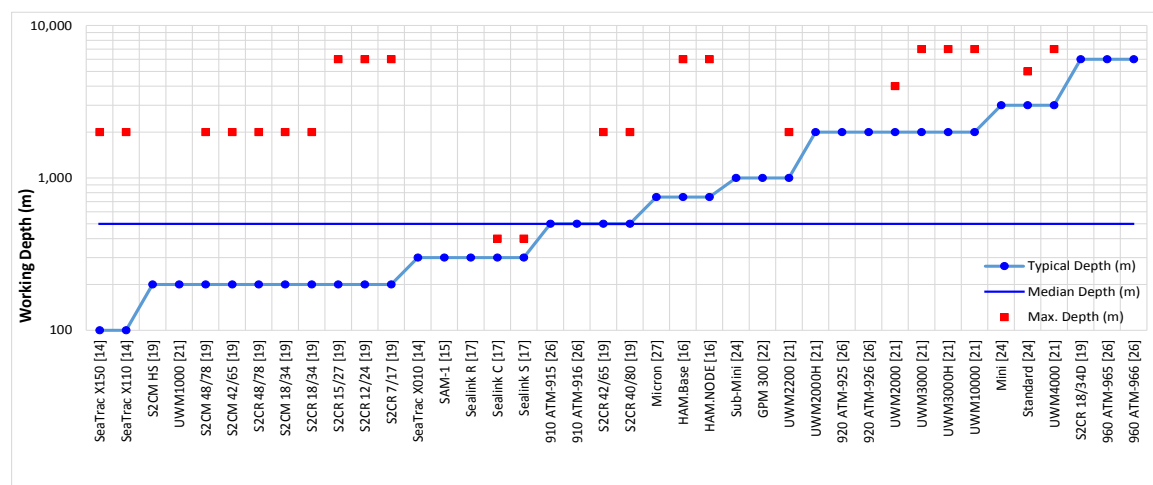

Figure 2.4. Working depth of commercial modems.

The working depth of 42.5% modems is from $100-300\ m$, 42.5% from $500-2000\ m$, and 15.0% from $3000-6000\ m$. The median working depth is $500\ m$, as shown by the blue dotted line; the standard deviation is $1598\ m$. For normal deployments, the modem casing employs delrin material. For deep water deployments different material casings, e.g., aluminum alloy, stainless steel, or titanium, are used [19]. The maximum working depth of commercial modems is from $400-7000\ m$ as shown by red squares in the figure with a median value of $2000\ m$.

e) **Center frequency and bandwidth.** The center frequency used in the commercial modems is from $3.5-160\ kHz$ as shown by blue dots in Figure 2.5. The modems are arranged on the horizontal axis, while center frequency is shown on the vertical axis on a logarithmic scale. The frequency range from $3.5-20\ kHz$ is being used by 36.4% modems, $21-71.4\ kHz$ by 61.4% modems and only 2.3% modems operate at $160\ kHz$. The median value of the center frequency is $24\ kHz$, as shown by a dotted blue line, and the standard deviation is $25\ kHz$. The BW used by commercial modems is in the range of $2-80\ kHz$ as shown in Figure 2.5. The vertical red bars indicate the spans of bandwidth for each modem. The BW from $2-10\ kHz$ is being used in 56.8% modems, $11-20\ kHz$ in 27.3%, $23-36\ kHz$ in 13.6% and 2.3% modems use $80\ kHz$. The median value of BW is $10\ kHz$, and the standard deviation is $13\ kHz$.
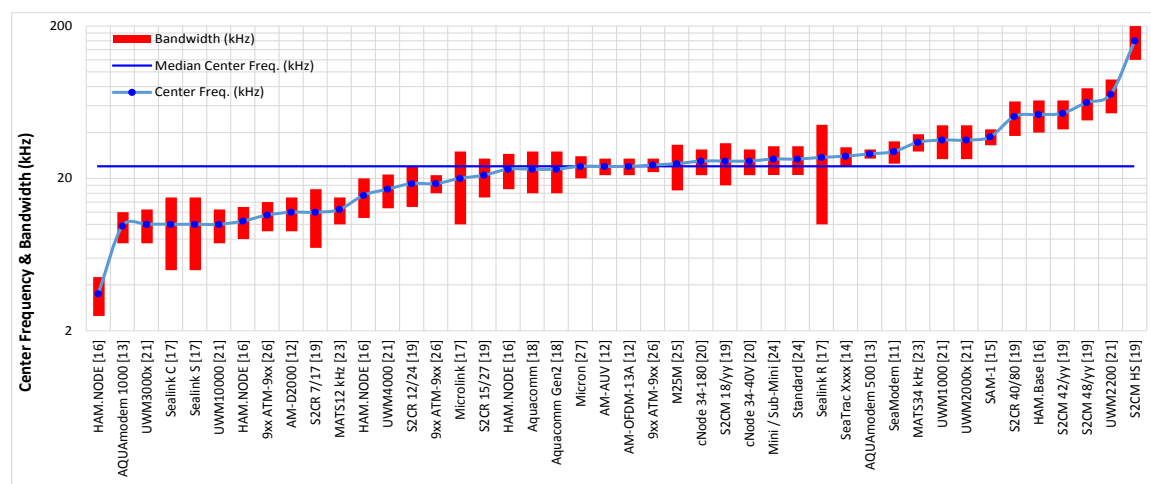

Figure 2.5. Center frequency and bandwidth of commercial modems.

f) **Transmission power.** The power consumption of commercial modems during normal transmission is in the range of $1-40\ W$. Figure 2.6 shows the modems on the horizontal axis and the transmission power is plotted on the vertical axis using blue dots. During normal operation, 39.4% modems use $1-8\ W$, 36.4% use $10-20\ W$ and 24.2% consume $30-40\ W$. The median power consumption during normal transmission is $10\ W$, shown by blue dotted line, and the standard deviation is $12\ W$. In high power transmission, the power can be doubled in most of the cases and, in some modems, it can be increased up to $300\ W$ [22]. In Figure 2.6 the maximum power consumption is shown by red squares. During high power transmission, the median is $37.5\ W$, represented by a red dotted line, and the standard deviation is $65\ W$.
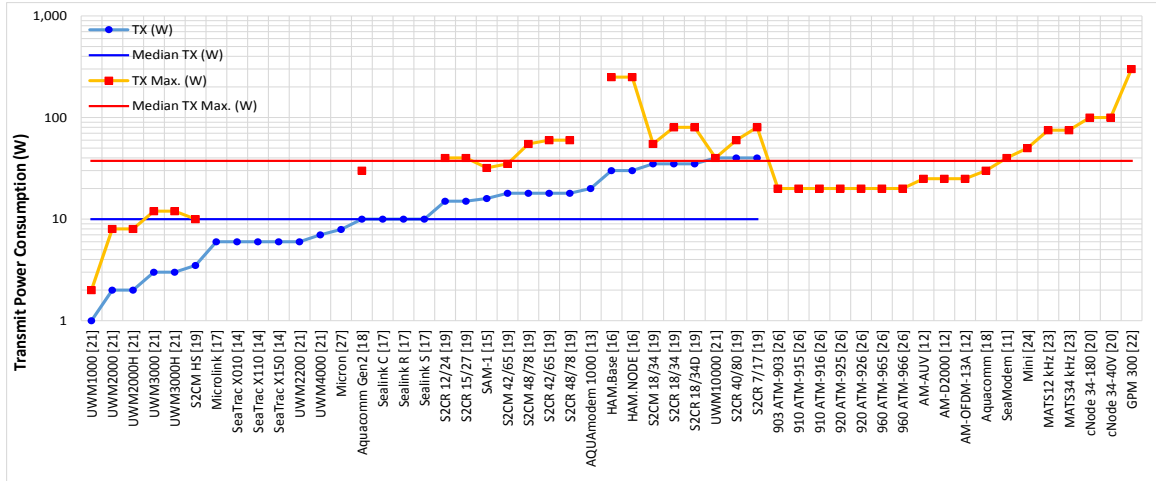
Figure 2.6. Transmission power of commercial modems.

g) ***Receive and standby powers.*** Figure 2.7 depicts the power consumption during reception and standby modes. The modems are placed on the horizontal axis and power consumption is plotted on the vertical axis on a logarithmic scale. During reception, commercial modems consume power from $0.168 - 1.8\ W$, shown as red squares. Around 75.6% of the commercial modems consume less than $1\ W$ during reception and the remaining 24.4% consume from $1.0 - 1.8\ W$. The median power consumption is $0.8\ W$, shown by the red dotted line, and the standard deviation is $0.3\ W$. In Figure 2.7, the power consumption during standby mode of commercial modems is from $0.0005 - 0.6\ W$ shown by blue dots. 49% modems consume less than $9\ mW$, while consumption of 51% modems is from $10 - 600\ mW$. The median value is $10\ mW$ and standard deviation is $158\ mW$.
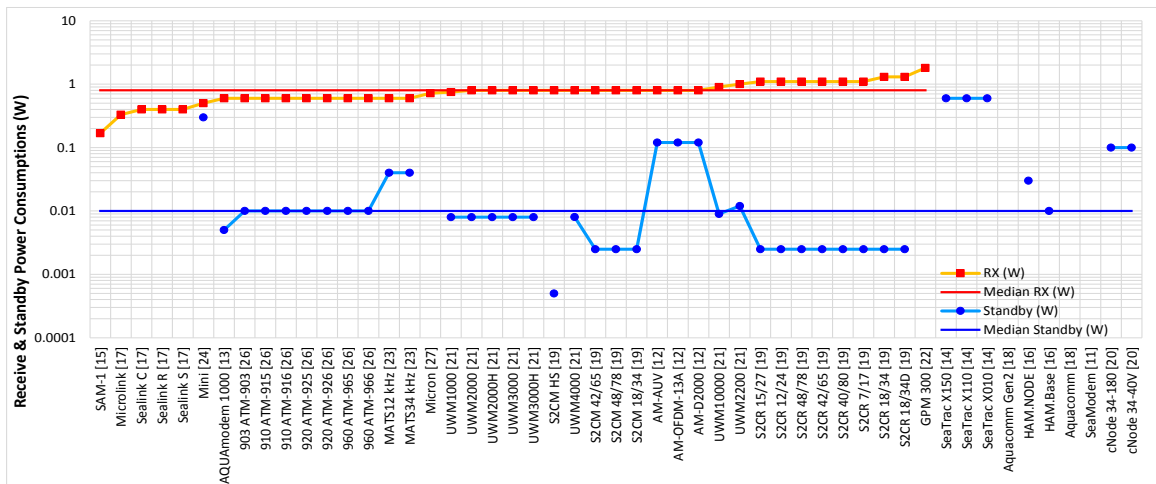
Figure 2.7. Receive and standby power of commercial modems.

h) ***Weight.*** The weight varies in between $0.16 - 24.2\ kg$. In Figure 2.8, modems are shown on the horizontal axis and their weight is depicted on the vertical axis using blue dots. The weight of 46.7% modems is less than $3\ kg$, 37.8% from $3.0 - 9.5\ kg$, and 15% modems are in the range of $10.8 - 24.2\ kg$. The median weight is $3.2\ kg$, a blue dotted line, and the standard deviation is $6\ kg$.

Figure 2.8. Weight of commercial modems.

i) **_Operating temperature._** The overall operating temperature range is from $-10\ to\ 70\ °C$, as shown in Figure 2.9. The modems are placed on the horizontal axis and the temperature range is plotted on the vertical a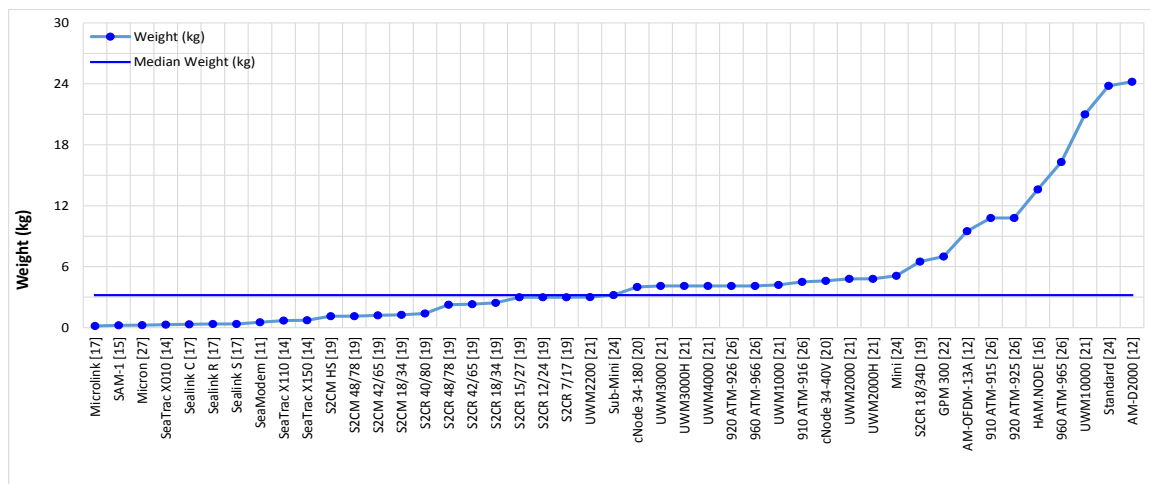xis. At the lower half, the minimum operating temperature range is shown; it is $-10\ to\ 0\ °C$, shown by blue dots, with a median of $-5\ °C$ and standard deviation of $3\ °C$. The maximum operating temperature range is from $35\ to\ 70\ °C$, shown by red squares, with a median of $50\ °C$ and standard deviation of $8\ °C$.
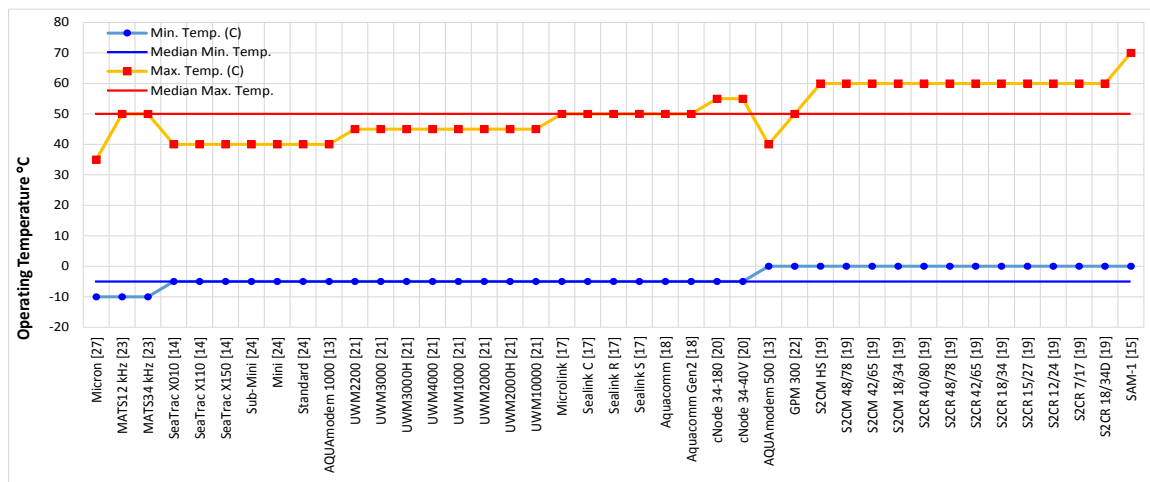
Figure 2.9. Operating temperature of commercial modems.

j) **_Bit error rate._** Figure 2.10 shows the BER values in the range of $10^{-4}\ to\ 10^{-10}$. Modems are arranged on the horizontal axis and their BER values are plotted as red dots; percentage is represented by the height of the bars. From the figure, it can be seen that Oceania [22] has BER 10^{-4} with 1.8% of the total designs, DiveNET Sealink R [17] has BER 10^{-5} with 1.8% of the total designs, DiveNET Sealink models C, S, Microlink [17], and DSPComm [18] modems has BER 10^{-6} with 9.1%. Teledyne Benthos [26] has BER 10^{-7}, which is 12.7% of the designs, and LinkQuest [21] has BER 10^{-9} with 14.5%. Evologic [19] represent 21.8% of the total modems, are the most reliable ones, having a BER value of 10^{-10}. For the remaining 38.2% of modem designs, the BER value is not reported by the manufacturers.

Figure 2.10. BER of commercial modems.

2.2.2. Research modems

The state-of-the-art of UW research modems are presented in Table 2.2 [28-60]. First and second columns represent the modem reference and hardware platform. Third–fift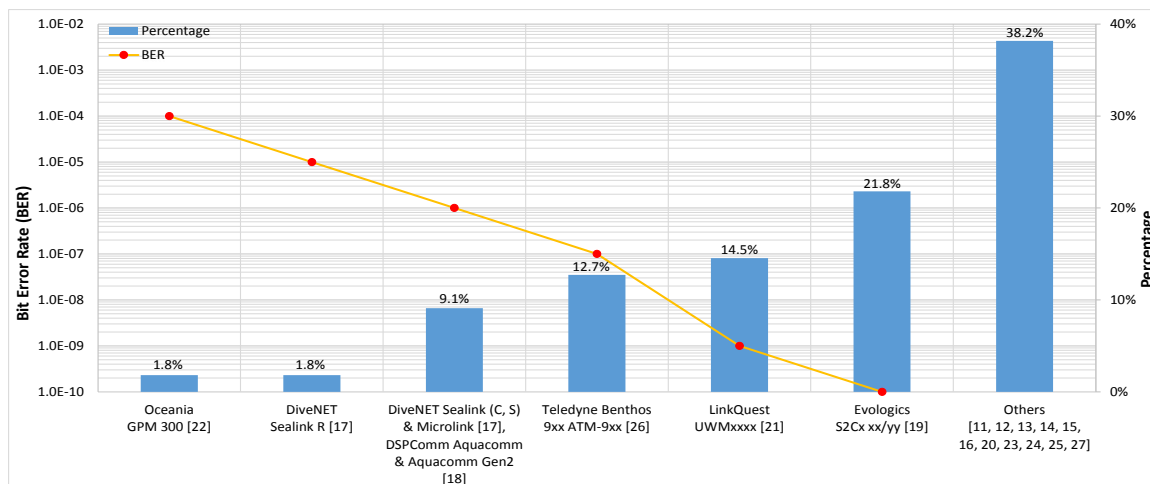h columns show the operating range, modulation schemes, data rates respectively. Center frequency and bandwidth are listed in sixth and seventh columns. Bit-error-rate and amplifier types are described in eighth and ninth columns respectively. Tenth–twelfth columns show the transmit, receive and standby powers respectively.

It is important to note that during the discussion on commercial modems in Section 2.2.1, we have first discussed the individual models from various manufacturers. Subsequently, a comparative analysis of various models from different manufacturers is presented in Table 2.1 and Figures 2.1–2.10. However, in case of research modems, the detailed description on each modem is available in corresponding references [28-60].

Our objective in this section is to critically analyze the results of different research modems in terms of various performance attributes. However, the interested readers may consult the corresponding article on each research modem for more details. The performance attributes of research modems including operating range, data rates, modulation schemes, hardware platforms, center frequency, bandwidth, power consumption, amplifiers and bit-error-rate are discussed in the following. In the figures, we have arranged the modems in the horizontal axis; the corresponding parameter of interest is shown on the vertical axis.

Table 2.2: Underwater acoustic research modems.

UW research modems	Hardware platform	Range (m)	Modulation scheme	Data rate (bps)	C.F. (kHz)	BW (kHz)	Bit error rate	Amplifier	Power consumption (W)		
									TX	RX	Standby
[28]	SDR (Laptop)	200	OFDM, DSSS	104k, 260k / 104k, 260k	100 / 100	24 / 24	2.0×10^{-5} / 2.0×10^{-2}	BII-5002	-	-	-
[29]	DSP, ARM Cortex	100 / 10	MFSK / OFDM	208 / 1230, 2480, 3730	12.5 / 12.5	3 / 3	-	-	-	-	-
[30]	MCU	1	FSK	1200	41.5	3	-	-	-	-	-
[31]	Raspberry Pi, MCU	-	FSK	1200	31.5	2	-	Class AB	1.5	-	-
[32]	SDR (NI USRP 2930)	2	OFDM	-	30	4	1.0×10^{-3}	GST YE5873A	-	-	-
[33]	SDR (Beaglebone Black)	90	FSK	1000	19	2	-	Class D	3	-	-
[34]	DSP	1000	QPSK	770	12	-	5.0×10^{-3}	-	-	-	-
[35]	MCU	9	FSK	2000	22	16	-	-	0.77	0.53	-
[36]	-	25	QPSK	1200	10	2	-	-	-	-	-
[37]	DSP, FPGA	-	M-ary SS / MFSK	48-500 / 80-1200	11.5	5	-	Class D	20	1.2	0.02
[38]	DSP, FPGA	2000	FSK	500	23	6	-	-	-	-	-
[39]	Laptop, DAQ	2	OFDM	-	15	6	-	KRONE-HITE	50	-	-
[40]	SDR (Laptop)	10 / 50	FSK	20-600	16.5 / 15	2 / 2	-	Class AB	19	-	-
[41]	Raspberry Pi, ARM	20	FSK	20	33	6	-	-	-	-	-
[42]	MCU, FPGA	20	OOK	1M / 512k / 256k	1000 / 1000 / 1000	-	3.0×10^{-3} / 2.3×10^{-5} / 1.0×10^{-8}	THS7001	-	-	-
[43]	SDR (PC Intel Core-II)	1	GMSK	7500, 10000, 15000	137.5	75	-	-	-	-	-
[44]	SDR (ARM Cortex)	140	FSK	10-200	21	2	-	Class D	8	0.3	0.06
[45]	-	100	OOK	1M	1000	250	-	-	-	-	-
[46]	ARM Cortex	60 / 500	ASK	500 / 5000	70	-	1.3×10^{-2} / 4.0×10^{-2}	-	8 / 8	-	-
[47]	DSP, ARM	5000	OFDM	3041	8	4	1.8×10^{-5}	-	120	-	-
[48]	DSP, ARM	10000	OFDM	4000	-	4	1.0×10^{-4}	-	-	-	-
[49]	DSP, FPGA	-	MFSK / MPSK	1000 / 10000	-	-	-	-	0.8 / 1.5	-	-
[50]	SDR (Laptop)	800	OFDM	1875, 2500, 3750, 5000 / 3750, 5000, 7500, 10000	17.5 / 35	5 / 10	-	-	-	-	-
[51]	DSP, ARM Cortex	3000	OFDM	710 / 10	7 / 7	2 / 2	-	KRONE-HITE	-	-	-
[52]	SDR (DSP)	8000	QPSK	8000	-	-	-	-	-	-	-
[53]	SDR (DSP, FPGA, SBC)	400	OFDM	400, 9000	30	12	1.3×10^{-3}	-	-	-	-
[54]	ARM Cortex	100 / 500	ASK	1000 / 1000	70 / 26	-	-	-	-	-	-
[55]	DSP	212	MCSS	300	25	10	-	-	0.97	-	-
[56]	MCU	240	FSK	1000	85	1	-	Class B	0.108	0.024	-
[57]	ARM Cortex	70	ASK	200	70	-	3.9×10^{-4}	-	4.5	-	-
[58]	DSP	3000	OFDM	3200, 6400	18	6	-	-	-	-	-
[59]	MCU	1.2	ASK	2000	-	-	-	-	-	-	-
[60]	FPGA	350	FSK	200	35	6	1.0×10^{-2}	Class AB,D	7	0.75	-

a) **Range.** The operating range of UW research modems is from $1-10,000\ m$ shown by blue dots in Figure 2.11 using logarithmic scale. The blue dotted line at $100\ m$ is the median, and the standard deviation is $2272\ m$. 52.9% modems work in the range of $1-100\ m$, 29.4% from $140-1000\ m$, 11.8% from $2000-5000\ m$, and 5.9% work in the range of $8000-10,000\ m$.
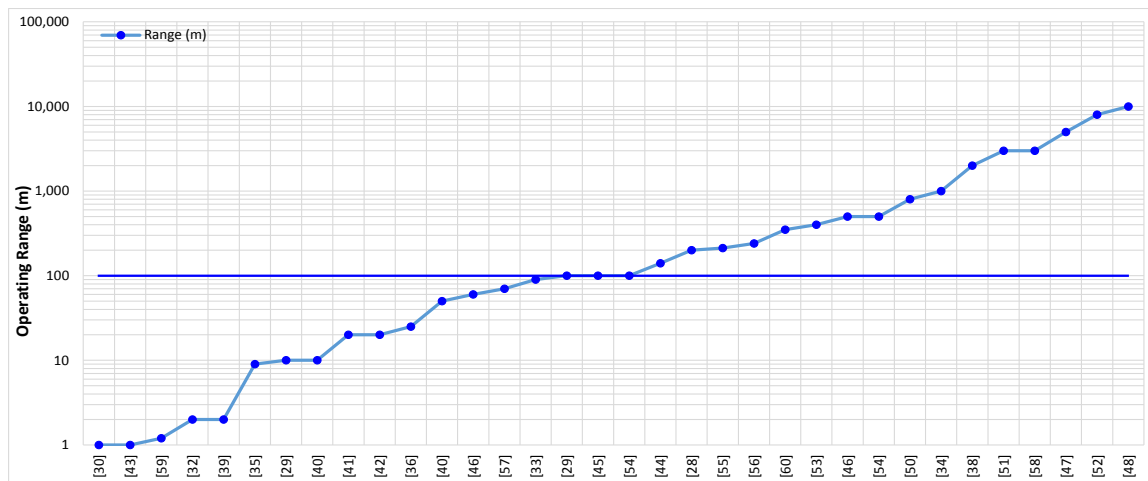

Figure 2.11. Operating range of research modems.

b) **Data rates.** The data rates vary from $10-1,000,000\ bps$, as shown in Figure 2.12, where a logarithmic scale has been used in the vertical axis. The graph is smoothly increasing at the beginning, while after $10,000\ bps$ it rises sharply. The nominal value of the data rate of 38.5% research modems is from $10-770\ bps$, 48.7% from $1000-10,000\ bps$, and 12.8% from $100,000-1,000,000\ bps$. The median data rate of research modems is $1200\ bps$, indicated by the blue dotted line, and the standard deviation is $233,035\ bps$. There are 12.8% modems that also communicate at higher data rates, shown by orange triangles, with a median value of $7500\ bps$. Out of the total, 28.2% of the modems have the capability to communicate at maximum data rates; shown by red squares in Figure 2.12. The median value of the maximum data rates is $5000\ bps$.
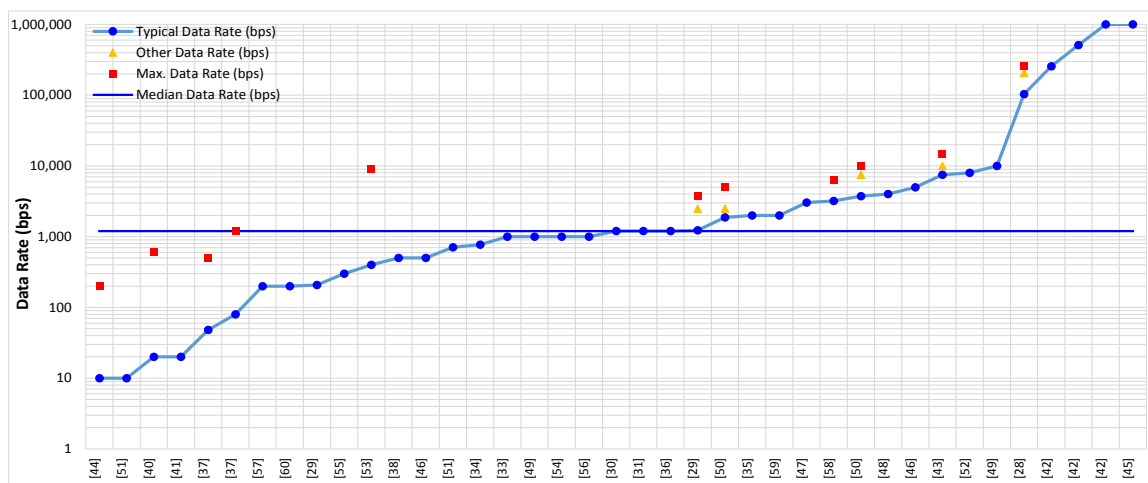

Figure 2.12. Data rates of research modems.

c) **Modulation schemes.** Figure 2.13 illustrates the modulation schemes employed in modems. The number of modems are represented by blue bars while the percentage of the modulation scheme

used in each modem is shown by red triangles. The most common modulation scheme used in research modems are frequency shift keying (FSK) or multiple frequency shift keying (MFSK) used in 36.8% of the modem designs. Orthogonal Frequency Division Multiplexing (OFDM) is used in 26.3%, amplitude shift keying (ASK) or on-off keying (OOK) is used in 15.8% designs. Spread Spectrum (SS) is used in 10.5%, and a variety of phase shift keying (PSK) used in 10.5% designs.
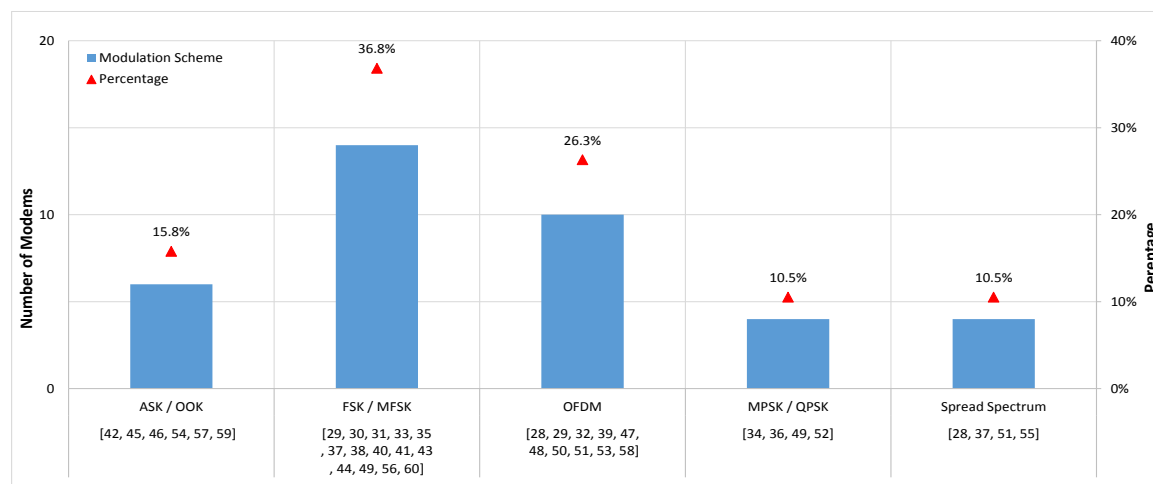

Figure 2.13. Modulation schemes of research modems.

d) *Hardware platforms.* Research modems use single or a combination of hardware platforms as shown in Figure 2.14. The bar graph represents the number of modems, while the red triangles show the percentage. DSP is a leading hardware platform used in 26.7% of the modems, while Advanced RISC machines (ARM) is present in 20%. Laptop or single board computer (SBC) based designs along with data acquisition system (DAQ) are a part of 15.6% designs. MCU and FPGA are present in 13.3% each of the modem designs. BeagleBone/Raspberry-Pi are used in 6.7% modem designs. In 4.4% of the designs, the information of hardware platforms is not available.
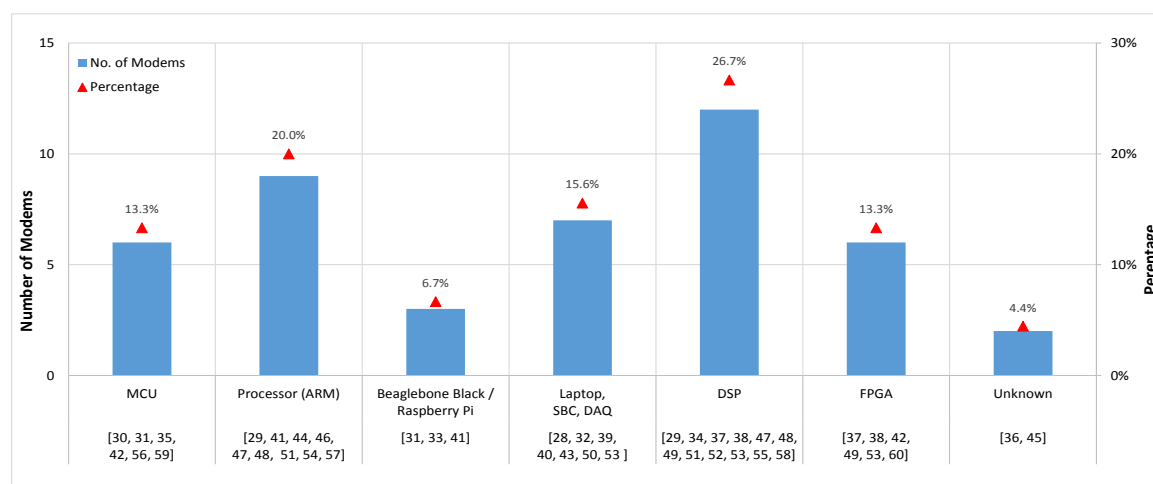

Figure 2.14. Hardware platforms of research modems.

e) *Center frequency and bandwidth.* Research modems use center frequency in the range of $7 - 1000 \, kHz$ (see Figure 2.15) displayed on the vertical axis using blue dots on a logarithmic scale. 36.4% of the modems use center frequency from $7 - 19 \, kHz$, 39.4% from $21 - 41.5 \, kHz$, and

18.2% of use $70 - 137.5\ kHz$. Only 6.1% modems use $1000\ kHz$. The median value of the center frequency is $26\ kHz$ and the standard deviation is 232 kHz. The BW is from $1 - 250\ kHz$ shown by red vertical bars (indicate the span for each modem) in Figure 2.15. The BW of 73.1% of the modems is from $1 - 6\ kHz$ and 19.2% use $10 - 24\ kHz$. The values $75\ kHz$ and $250\ kHz$ are equally used in the rest of 3.8% modem designs. The median value of the BW is $5\ kHz$ and the standard deviation is $49\ kHz$.
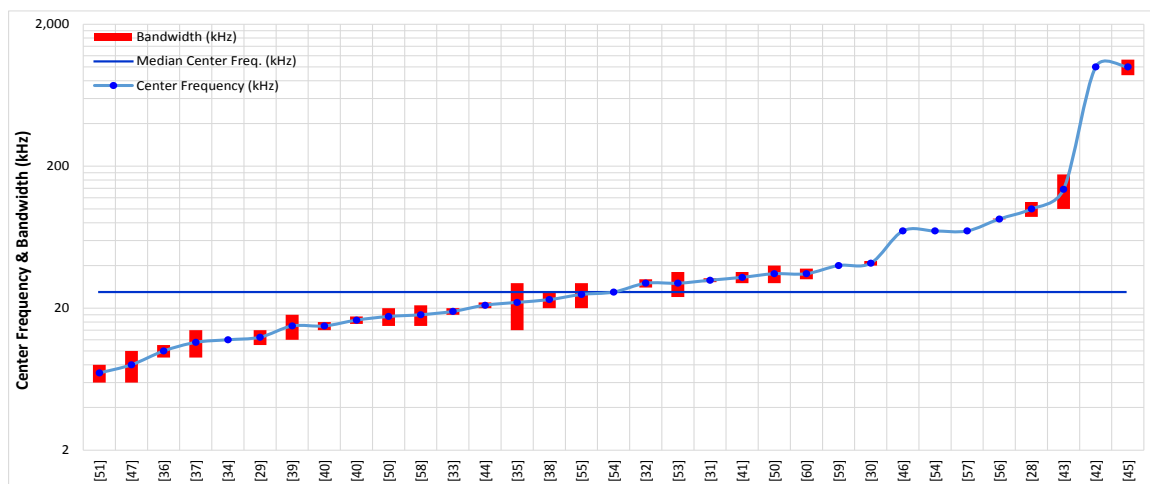

Figure 2.15. Center frequency and bandwidth of research modems.

f) ***Power consumption.*** The power consumption is presented in Figure 2.16. During transmission, research modems use $0.1 - 120\ W$ power, shown by blue dots on a logarithmic scale. During normal operation, 53.3% modems use $0.1 - 4.5\ W$, 33.3% use $7 - 20\ W$, 6.7% of the modems use a power from $50\ W$ and the same 6.7% modems use $120\ W$. The median transmission power during normal transmission is $4.5\ W$ (blue dotted line) and the standard deviation is $30\ W$. The power consumed during reception is from $0.02 - 1.2\ W$, shown by red squares, and the standby power consumed is from $20 - 60\ mW$, shown by green triangles. In both cases, the available data is insufficient to perform further analysis, however the values are mentioned just to have an idea.
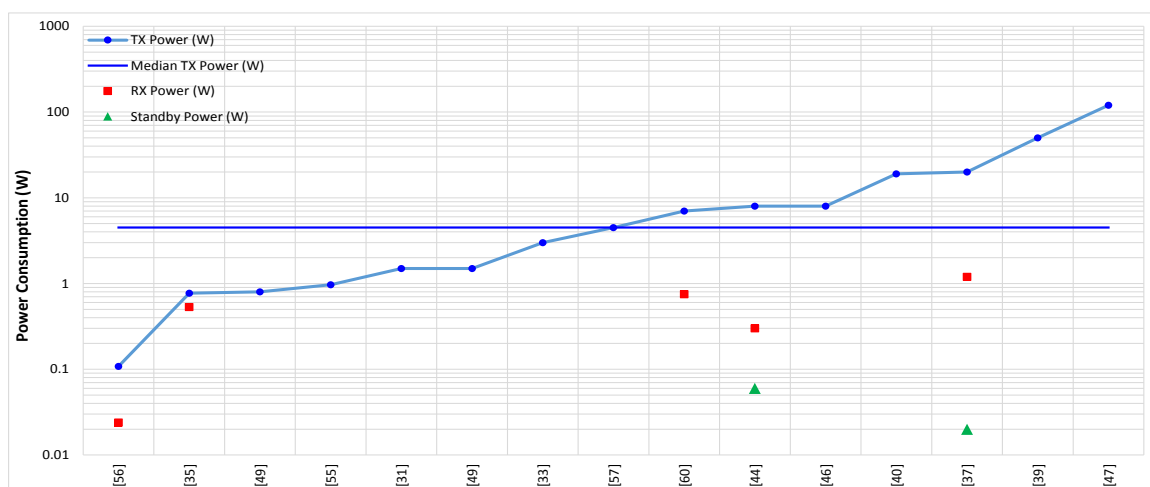

Figure 2.16. Power consumption of research modems

g) *Amplifiers.* Figure 2.17 illustrates the power amplifiers used in UW research modems. The number of modems is represented by blue bars and the percentage is shown by red triangles. Class-D amplifiers are used in 11.8% designs [33, 37, 44, 60], while class-AB amplifiers are used in 8.8% designs [31, 40, 60]. KRONE-HITE [39, 50] is used in 5.9% and other types amplifiers class-B, BII-5002, GST YE5873A, THS7001 are used in 2.9% in each of the modems [28, 32, 42, 56]. The analysis is based upon limited data, because 61.8% of the modem designers did not provide information about amplifiers.
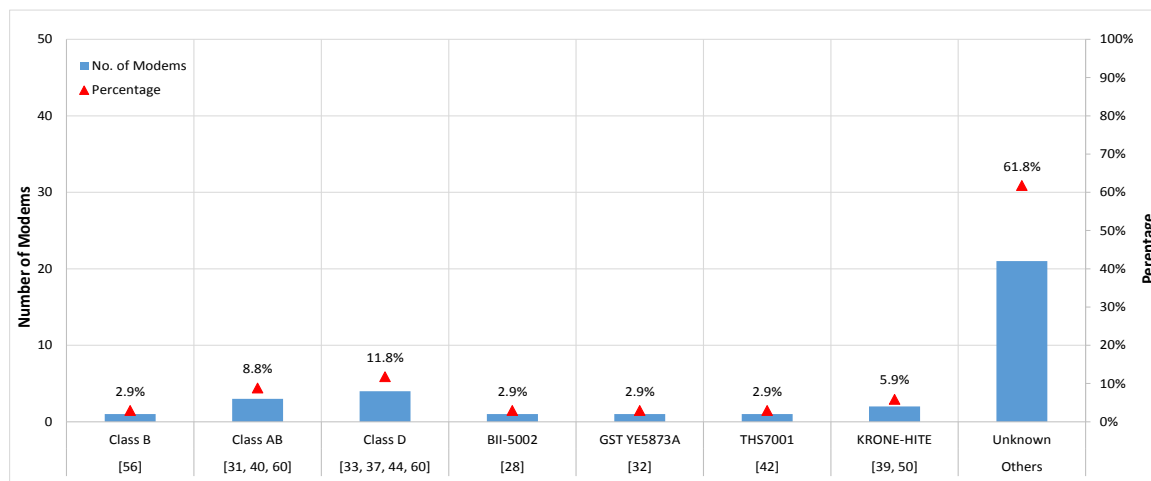
Figure 2.17. Amplifiers used in research modems.

h) *Bit error rate.* The BER varies in the range of $10^{-2} - 10^{-8}$. In Figure 2.18 the BER values are plotted on the vertical axis as red dots, while the percentage of modems with a particular BER is shown by blue bars. The BER of 8.3% of the modems [28, 46, 60] is 10^{-2}, while 11.1% of the modems [32, 34, 42, 54] have a value of BER 10^{-3}, another 5.6% [48, 57] have a BER in the range of 10^{-4}, 8.3% of the modems [28, 42, 47] have a BER of 10^{-5}, and the last 2.8% modem [42] has a BER of 10^{-8}. The BER values of the remaining 63.9% are not available.

Figure 2.18. BER of research modems.

2.3. Comparative analysis of commercial and research modems

Main features of commercial and research underwater acoustic modems are discussed in Section 2.2, while common parameters are analyzed in this section. The data rates, center frequency, bandwidth and power consumption of c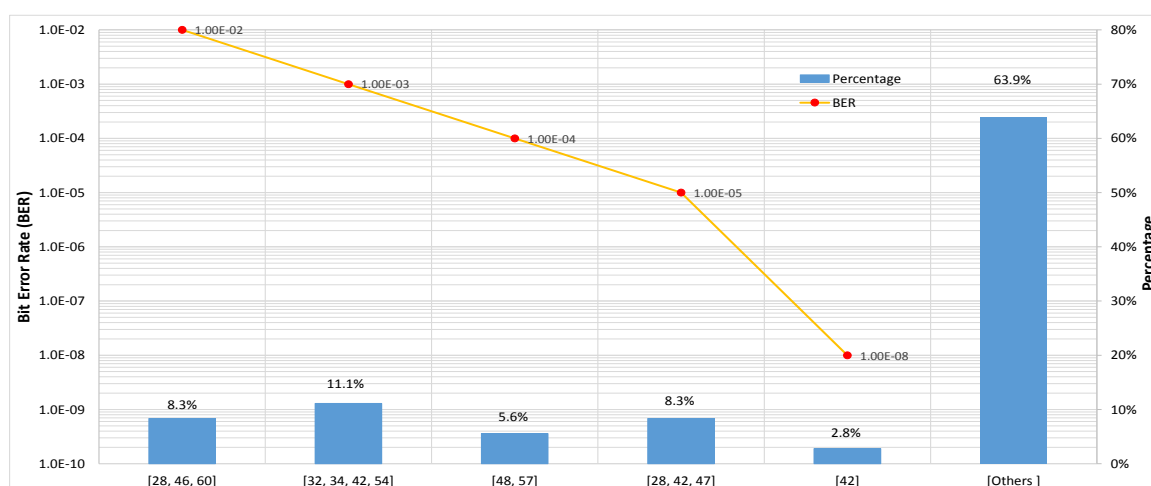ommercial and research modems are compared in Figures 2.19–2.22. Commercial modems are shown by red triangles, while blue dots are used for research modems. These parameters are plotted against the operating range of the modems on the horizontal axis. The modulation schemes and bit-error-rates of the modems are analyzed in Figures 2.23–2.24. It is important to mention that these parameters are related with each other, while they are analyzed individually in the following section for better comparison between commercial and research modems.

2.3.1. Range and data rate

The range vs data rate graph of commercial and research modems is presented in Figure 2.19. The data rates of commercial modems are from $10-62,500\ bps$, while research modems communicate from $1-1,000,000\ bps$ illustrated in Figure 2.1 using red triangles and blue dots respectively. The corresponding median value of data rates of commercial and research modems are $2030\ bps$ and $1200\ bps$ respectively while almost half of the modems can communicate up to $1\ kbps$ in each case.

The horizontal axis represents the range; the data rates of commercial modems are shown by red triangles and for research modems blue dots are used. The median operating ranges of commercial modems and research modems are $3000\ m$ and $100\ m$ respectively, which indicates the commercial modems can communicate at distances $30\ times$ larger than research modems. The median values of the data rate of commercial modems is $2030\ bps$, and for research modems is $1200\ bps$. The red and blue range-rate trends are used for commercial and research modems respectively. The analysis shows that commercial modems can communicate at a speed $1.7\ times$ higher than research modems.
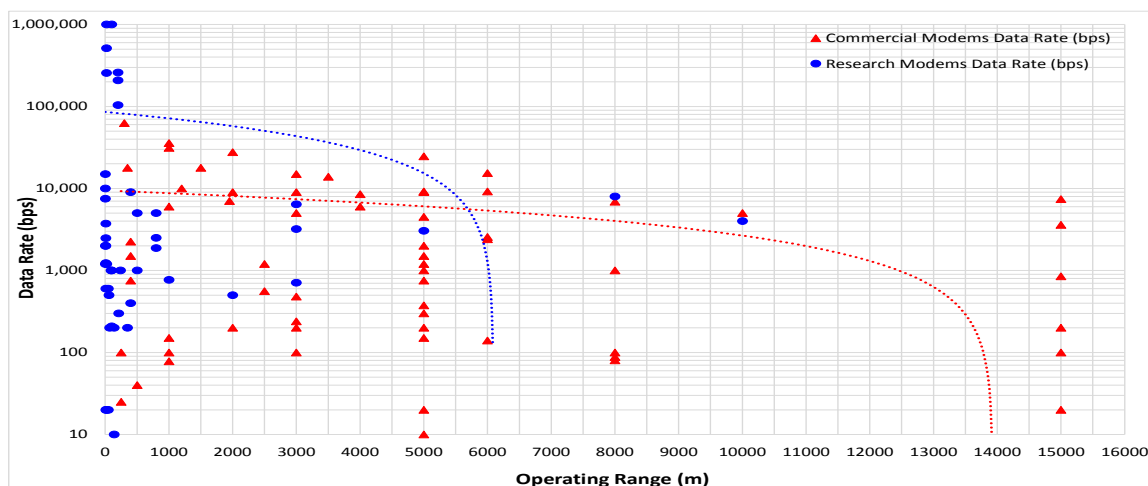
Figure 2.19. Data rates of commercial and research modems.

It would seem that commercial modems outperform research modems in this category, but the largest data rates happen to be obtained by research modems, though at smaller distances. Commercial modems concentrate in the range of several kilometers, and, in that range, they outperform, on average, known research modems. The further ranges are achieved by commercial modems for a handful of manufacturers (Evologics, Sercel, LinkQuest), standing out the systems from Evologics [19], which

obtain the best ratios for range vs data rate. Modems with better features are based on software defined radio schemes, or use OFDM modulation, and incorporate automatic adaptive coding or modulation techniques [48, 52].

2.3.2. Center frequency

The center frequency vs range graph is presented in Figure 2.20. The center frequency of the acoustic signal used by commercial modems is $3.5 - 160\ kHz$, while research modems operate from $7 - 1000\ kHz$. The center frequency of commercial modems is shown by red triangles, while blue dots are used for research modems. The median values of commercial and research modems are 24 and 26 kHz respectively. From the analysis it is found that approximately half of the modem designs operate beyond the human auditory field i.e., from $21 - 70\ kHz$. Modems using low values of center frequency can communicate at larger distances, while data rate increases with the increase of center frequency values.

The range is plotted on the horizontal axis and the center frequency is shown on the vertical axis using logarithmic scale. For commercial modems red triangles and for research modems blue dots are used. The median value of the center frequency used by commercial modems is 24 kHz, while the median value of the center frequency used by research modems is 26 kHz. The figure shows that research modems attempt to explore further frequency bands, possibly with the aim of identifying and measuring channel characteristics that can be used to develop systems with higher data rates. The commercial modems, however, most of them lie comfortably in the range of $20 - 30\ kHz$, which, being a lower frequency band, allows more easily for larger ranges. We can notice that those modems with higher center frequency are, in essence, those modems with larger data rates (see Figures. 2.2 and 2.5).
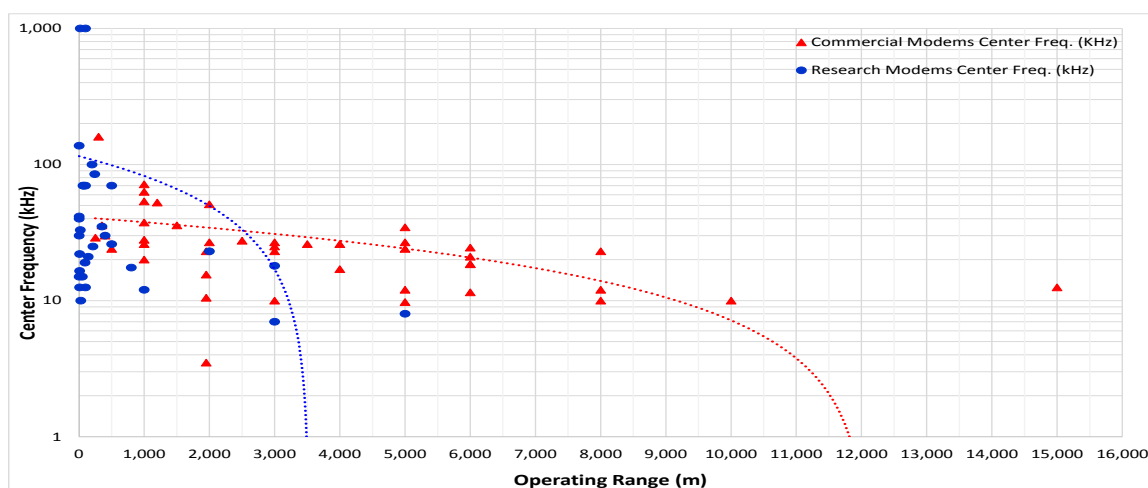
Figure 2.20. Center frequency of commercial and research modems.

2.3.3. Bandwidth

The bandwidth vs range graph is shown in Figure 2.21. The range is plotted on the horizontal axis and the bandwidth is shown on the vertical axis, on a logarithmic scale. As usual, red triangles are used to represent the commercial modems to show the bandwidth from $2 - 80\ kHz$, while for research modems blue dots are used from $1 - 250\ kHz$. The median BW of commercial modems, $10\ kHz$, is twice the BW used by research modems, 5 kHz. The conclusions inferred from this comparison are similar to the ones

obtained from the analysis of the center frequency. While commercial modems employ larger BW in their comfort range area, research modems target more experimental designs, and use larger bandwidths, though at shorter distances. The figure also shows that the modems with larger bandwidth are targeted for operating in the short-range.
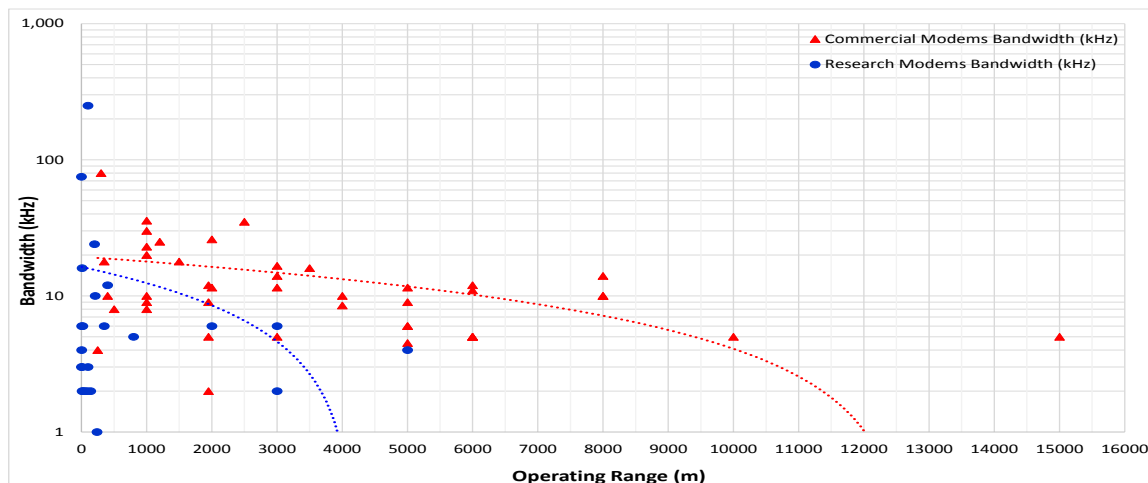
Figure 2.21. Bandwidth of commercial and research modems.

2.3.4. Transmission power

The transmission power vs range is presented in Figure 2.22. The transmission power of research modems is shown by blue dots, and commercial modems are depicted by red triangles; the maximum transmission power of commercial modems is illustrated by green squares. The same colors are used for each group to plot the trend lines. The figure gives an impression that commercial modems consume more power as compared to the research modems, but in truth they do so while communicating at large distances. As the operating range of research modems is smaller, so, obviously, they require less power. The median value of the transmission power of commercial modems is $10\ W$, higher than the corresponding value of research modems, which is $4.5\ W$. Median value of the maximum transmission power of commercial modems is $37.5\ W$.

Figure 2.22. Power consumption of commercial and research modems.

2.3.5. Modulation schemes

The modulation schemes are displayed in Figure 2.23. Red and blue bars are used to indicate the number of commercial and research modems, respectively; red triangles and blue dots are used to represent the percentage of modems using a particular modulation scheme (commercial and research, respectively).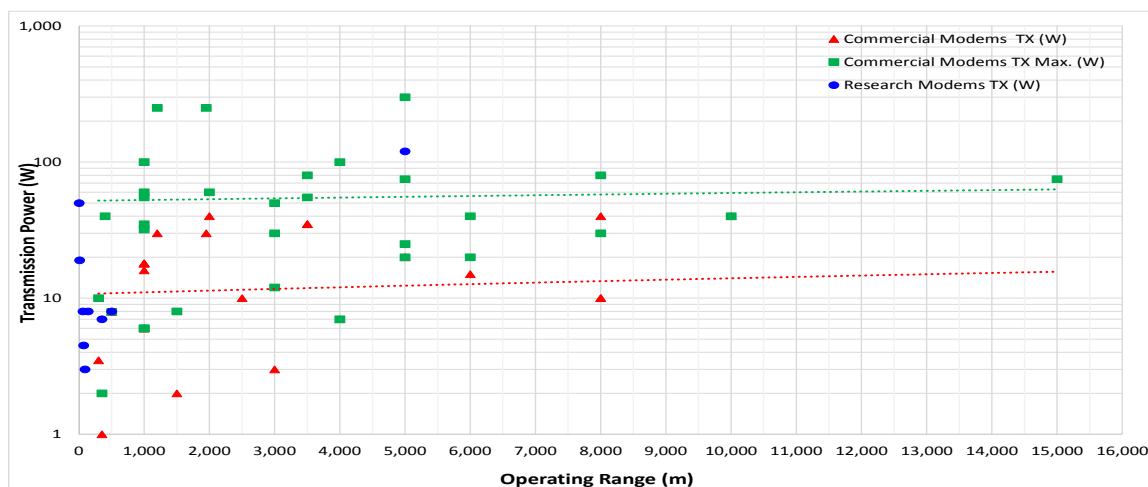 The common modulation schemes used by commercial and research modems include FSK, PSK, OFDM, and SS. FSK is used in 22.9% commercial and 36.8% research modems, while PSK is used in 22.9% commercial and 10.5% research modems. OFDM in 11.4% commercial and 26.3% research modems and finally SS is used in 11.4% commercial and 10.5% of research modems.
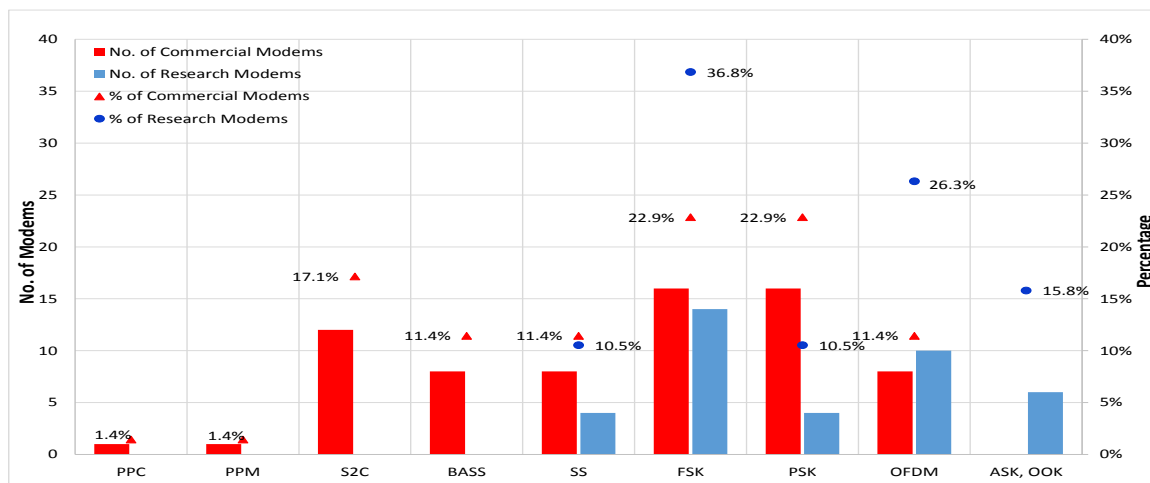
Figure 2.23. Modulation schemes of commercial and research modems.

On the left side of the figure we see only commercial modems. The unique modulation schemes PPC and PPM are used in 1.4% in each design, while 28.5% commercial modems are based on proprietary modulation schemes i.e., 17.1% S2C and 11.4% BASS. The modulation scheme ASK/OOK is used in 15.8% of research modems. It is normal that research modems are more speculative, in the sense that different variations are tried, searching for better performance in specific scenarios.

2.3.6. Bit error rate

The BER of commercial and research modems are shown in Figure 2.24. Red triangles and blue dots are used to represent the BER values and bars of the same color show the percentage of each group. The striped square depicts the common BER values shared between both categories. From the graph, we can see that the BER value 10^{-2} is achieved by 8.3% of research modems [28, 46, 60], while BER 10^{-3} is present in 11.1% designs [32, 34, 42, 54]. The BER 10^{-4} is common in both categories for 1.8% of commercial modems [22] and 5.6% of research designs [48, 57]. BER 10^{-5} is present in 1.8% of the commercial [17] and 8.3% research modems [28, 42, 47]. BER $10^{-6}\ to\ 10^{-7}$ is only available in 9.1% [17, 18] and 12.7% [26] commercial designs, while BER 10^{-8} is obtained by only 2.8% of the research modems [42]. BER $10^{-9}to\ 10^{-10}$ is achieved by 14.5% and 21.8% of commercial modems respectively [19, 21]. The BER values for remaining 38.2% commercial and 63.9% research modems are not reported.

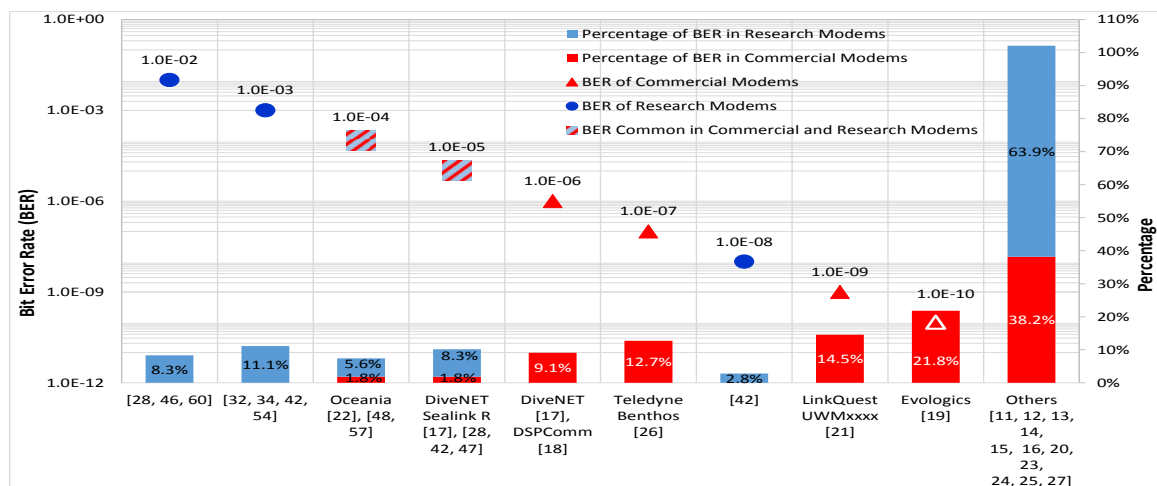Figure 2.24. Bit error rates of commercial and research modems.

The BER is a parameter of paramount importance for the performance analysis of a system. The graph clearly shows that commercial modems implement stronger data protection mechanisms, as would be expected from industrial enterprises, where reliability in the communication is paramount. However, many research modems aim only to characterize the behavior of the channel for specific modulation schemes, which causes this apparently larger transmission error rates. The best BERs are achieved by LinkQuest [21] and Evologics [19] which claim astonishing values 10^{-9} and 10^{-10} respectively.

2.4. Discussion

The comparative results of commercial and research modems are summarized in Table 2.3. First column shows the parameter of interest while the second and third columns represent the values of commercial and research modems respectively. The communication range of commercial modems is from $250-15,000$ m, while the research modems can communicate from $1-10,000$ m. From the statistical analysis we see that the median range of commercial modems is 3000 m, as compared to that of research modems 100 m, i.e., commercial modems can communicate 30 times greater than research modems. To communicate at longer distances, the commercial modems consume more power that increases the cost and size, however, to save the cost and power the range of research modems is kept limited depending upon the application.

The data rate of commercial modems is in the range of $10-62,500$ bps, while research modems achieve data rates from $1-1,000,000$ bps. It feels that research modems have greater data rate, but the statistical analysis shows that the median data rate of commercial modems is 2030 bps, larger than the 1200 bps of research modems, hence commercial modems are 1.7 times faster than research modems. The variation in data rate is due to the application where the modems are used. There is always a tradeoff between different parameters like operating range, data rate and power consumption. Commercial modems from different manufactures e.g., Oceania [22] communicate at 10 bps up to the distance 5000 m and consume power up to 300 W, while the EvoLogics [19] with higher data rate 62,500 bps can communicate up to 300 m using 10 W power.

Table 2.3: Commercial and research acoustic modems

Parameter		Commercial modems	Research modems
Median range (m)		3000	100
Median data rate (bps)		2030	1200
Percentage of modulation schemes	PPC	1.4	-
	PPM	1.4	-
	S2C	17.1	-
	BASS	11.4	-
	SS	11.4	10.5
	FSK	22.9	36.8
	PSK	22.9	10.5
	OFDM	11.4	26.3
	ASK/OOK	-	15.8
Percentage of hardware platforms	DSP	27.2	26.7
	Processor/MCU	-	33.3
	Laptop/SBC	-	22.3
	FPGA	-	13.3
	Unknown	72.8	4.4
Median center frequency (kHz)		24	26
Median bandwidth (kHz)		10	5
Median transmit power (W)		10	4.5
Minimum BER		10^{-10}	10^{-8}

The modulation schemes used in both commercial and research modems include FSK, PSK, OFDM and SS. They are used in 68.6% of commercial and 81.5% of research modems. 28.5% commercial modems use proprietary modulation schemes; however, ASK/OOK is used in 13.2% of research modems. The main purpose to use FSK and PSK modulation schemes is reliability and ease of implementation, while ASK/OOK is used for research purposes only.

The use of DSP as hardware platform in commercial modems is 27.2%, while it is used in 26.7% of research designs. The processor/MCU is used in 33.3%, laptop/SBC in 22.3%, and FPGA is used in 13.3% of research modems. In case of research modems the information regarding the hardware platforms is available, while commercial products do not disclose it due to trade secret.

The center frequency used in commercial modems is from $3.5 - 160$ kHz, with a median of 24 kHz, while the center frequency research modems is from $7 - 1000$ kHz, with a median of 26 kHz. The median values of center frequency for both the commercial and research modems are almost similar, however some higher ranges are also used for experimental purposes. Similarly, the bandwidth of commercial modems is from $2 - 80$ kHz with a median of 10 kHz, while research modems use $1 - 250$ kHz bandwidth with a median value of 5 kHz i.e., the median bandwidth of commercial modems is almost twice of the research modems.

The power consumption of commercial modems during normal transmission is in the range of $1 - 40$ W with a median value of 10 W. The power is almost doubled in many cases for high power transmission and in some modems it can reach up to 300 W [22]. The median value of the maximum transmission power of commercial modems is 37.5 W. The power consumption of research modems is in the range of $0.1 - 120$ W with median 4.5 W. The median transmission power of commercial modems during normal transmission is 2.2 times greater than research modems, which allows them to communicate up to larger distances.

The BER of commercial modems is in the range of 10^{-4} to 10^{-10}, while research modems achieve BERs from 10^{-2} to 10^{-8}. The data reliability, in terms of BER, for commercial devices is 100 times better than for research modems. The commercial modems are designed for error free and reliable data transmission, however the purpose of research modems is mainly a low cost setup for experimentation.

2.5. Design challenges

From the analysis of the underwater acoustic modems we found that commercial modems are superior to the research modems in terms of operating range, data rates and reliability. On the other hand commercial modems are (i) expensive to be used in an economical research project, (ii) their in-field testing is costly and time consuming, and (iii) they are less energy-efficient compared to the research modems. We address each of the design challenges in the following.

2.5.1. Low-cost modem

A UAM is an essential component of an UWSN i.e., used for monitoring of an aquatic environment, coral reefs, coastal surveillance, etc. The design of UAM is a challenging research problem due to the varying water environment. Moreover, the cost of UAM is an impediment to use it in a large UWSN. Hence, an economical UAM is required to encourage research in this area. In this research, a low-cost modem prototype for short-range underwater acoustic communications is presented in chapter 3. As compared to the available solutions, cost-effectiveness is a novelty of the modem. Furthermore, design parameters are available that could be modified or replicated for further research. The cost of the modem has been reduced by, (a) using custom-made underwater acoustic transducers using the piezo-ceramic material, (b) electronic circuitry, designed by discrete components and (c) low-cost hardware platform, to control the functionality of the modem. Each module is tested individually and the overall performance of the modem is evaluated by experiments in an aquatic environment. The outcomes of the research are useful for the scientific community and provide guidelines, to design a low-cost underwater acoustic modem.

2.5.2. Cost effective testing system

UWSNs are playing a vital role in exploring the unseen underwater natural resources. However, performance evaluation of UWSNs is still a challenging research problem. Various techniques such as, in-field testing, simulation and emulation have been used for the purpose, but they all have limitations. For example, in-field testing is expensive as well as extensive; similarly, a simulation model based on assumptions may not provide precise results. Consequently, it is crucial to have a solution that is reliable, inexpensive and requires less effort to validate the functionality of UWSNs and their components. In this research, a testbed is proposed in chapter 4 that evaluates the UW communication

system in a controlled aquatic environment and simulates the UW channel and sound propagation models. The constraint of physical access to the testbed facility is resolved by using a web-based monitoring and controlling graphical user interface (GUI).

2.5.3. Energy efficiency

Power consumption is a major constraint for autonomous long-life underwater sensor networks. The critical key metric for batteries is the capacity charge per kg. Though many of the current research efforts in batteries are aimed for cheap long-life rechargeable batteries, for underwater deployed sensors it is hard to think of scenarios where recharges will be of true usefulness. For non-rechargeable batteries, the Li-thionyl chloride is the best choice, achieving an energy density of up to $550\ Wh/kg$ [79]. The power stage of the modem transmitter should be a class-D amplifier, as it results in the better power efficiency of all power amplifier classes and, consequently, the lowest dissipation at similar transmitted power. Class-D amplifiers are a mature technology at audio frequencies and the effort to shift the band to ultrasonic frequencies is not weighty. These points make class-D the most convenient technology in underwater communications because it produces less heat, which means space and cost savings, and extends the lifetime for the same battery capacity [68]. An integration of a digital modulator with a class-D amplifier is presented in chapter 5 to address the issue of energy efficiency. Theoretically the proposed solution has been verified using MATLAB and Simulink and for validation, an electronic circuit has been built and tested using Multisim.

2.6. Conclusion

This chapter presents a comprehensive analysis on state-of-the-art commercial and research underwater acoustic modems. The common attributes of commercial and research modems such as operating range, data rates, center frequency, bandwidth, power consumption, modulation schemes and bit-error-rates are first separately explained in tabular form as well as graphically then jointly analyzed. Some exclusive parameters of commercial modems e.g., working depth, weight, and operating temperature and of research modems e.g., hardware platform and amplifier type are also graphically explained.

From the statistical analysis it is found that on average, the operating range of commercial modems is tens of times greater than of research modems, however they consume more power to achieve long distance communication. Due to the use of proprietary modulation schemes the data-rate of commercial modems is also double compared to the research modems with remarkable reliability. Commercial modems can be deployed in deep waters and use special materials and metal alloy casings to sustain the water pressure. These characteristics make them expensive to be used in economical projects.

This chapter has identified three main design challenges: (i) the need of a low-cost acoustic modem for economical underwater applications. (ii) cost-effective testing system to validate the modems in a controlled laboratory environment, and (iii) energy-efficient design to prolong the battery life. The next three chapters are going to address these challenges. Initially, Chapter 3 presents a low-cost underwater acoustic modem design, then Chapter 4 explains a web-based cost-effective emulator and simulator that can be used to test the functionality of underwater wireless sensor networks and its components. Finally, Chapter 5 presents an integration of a digital modulator and a class-D amplifier to improve the energy efficiency of the system.

Chapter 3: Design of a Low Cost Underwater Acoustic Modem [*]

The main features of state-of-the-art commercial and research underwater acoustic modems are presented, and their characteristics are analyzed in chapter 2. From the statistical analysis it is concluded that the operating range, data rate and reliability of commercial modems are much better than research modems, but their cost is one of the major constraints to be used in an economical project. In addition, commercial modems consume more energy compared to the research modems.

To overcome the issue of the cost and to promote the research in underwater communication, a low-cost underwater acoustic modem design is presented in this chapter using a modular approach that can be used in a variety of applications after suitable modifications. The modem has been tested in a controlled laboratory setup to validate the basic functionality, however, the same design can be used in the field with suitable modifications.

This chapter is organized as follows: Section 3.1 provides the introduction of a low-cost underwater acoustic modem. Section 3.2 presents related work. The architecture of underwater acoustic modem is provided in Section 3.3. Section 3.4 explains the experimental results with discussions. We conclude the chapter in Section 3.5.

3.1. Introduction

The WSNs are becoming a popular research area among the scientific community due to their variety of applications. This technology is mature enough in terrestrial environment, but due to the tough aquatic conditions, UWSNs are in their developing stages. A UWSN is a combination of wireless and sensor technologies having sensing, processing and communication facilities. Some applications of UWSN include; water pollution monitoring, oceanographic data collection, disaster alerts, coral reef, AUV etc. [6]. The design of UWSN depends on the application and may have different requirements e.g., stationary or mobile, long range, high data rate, low-power etc. The performance of UWSN may vary in different areas and times due to changes in the physical conditions of aquatic environment. An UWSN deployed in a coastal area may not provide satisfactory results in deep water [5].

UAMs are the essential component of any UWSN use for communication below the water surface. Hence, to design a general purpose modem, to be used in UWSNs, is still a big challenge. The main elements of a UAM are: (*i*) acoustic transducer, (*ii*) communication circuitry, and (*iii*) control unit. The acoustic transducer converts electrical energy into acoustic energy and vice versa to transmit and receive data in the water channel. The communication circuitry is responsible for several tasks, such as signal amplification, modulation, demodulation, filtering, signal processing, etc. Finally, the control unit, as the name indicates, is used to control the functionality of the modem.

The modem design is based on several hardware platforms. DSPs are the leading platforms used in the design of modems but they are expensive [34]. Another choice is the FPGA that can be reprogrammed but consumes more power [53] [64]. Personal computer (PC) or laptop have also been used for testing purposes, but their field deployment is not feasible [ref]. The MCU based designs although smaller and less expensive but due to limited computation power they cannot be used in high end applications [56].

Various modulation schemes have been used in underwater acoustic modems. An OFDM implementation requires high computational power and linear amplifiers due to high peak-to-average power ratio [65, 66]. The FSK modulation is resilient to noise and signal strength variations, and relatively easy to implement, but due to high bandwidth requirements, it is not preferred in high speed modems [67]. The ASK based communication systems are simple to design and comparatively inexpensive but its power efficiency is low and susceptible to noise interference [80]. The QPSK modulation is bandwidth efficient but not power efficient as compared to other modulation schemes [52]. The SS technique is secure and non-interference communication but complex to be implemented [35].

After the study of various environment variables, constraints, variants, available hardware options and modulation schemes to design an underwater acoustic modem i.e., cost effective as well as power efficient, a novel short-range UW acoustic modem design is presented in this chapter. The proposed modem is based on a single board computer (SBC); Raspberry-Pi running Linux operating system to support various protocol stacks [81]. Low level functionality of the modem is controlled using a microcontroller Atmega328P [82]. The modulator, demodulator, and amplifiers are designed with discrete components. The transducers are made by low cost piezo-ceramic elements. The modem has

been tested in an aquatic environment at different data rates. Design parameters of each block have been provided to replicate or modify the design in future for further improvements.

3.2. Related work

In the last couple of years, several efforts have been made to design a cost-effective and energy-efficient UAM. A number of researchers, currently active in the field, have proposed several UAM designs using different hardware platforms depending upon the application, cost, flexibility and computational power. Similarly, a number of modulation schemes have been implemented in different $sub-GHz$ frequency bands for UW communication. In this section overview of low-cost UAM designs have been presented. Moreover, modem designs that are based on FSK modulation scheme have been the focus in order to provide a better comparison with the proposed modem.

A power efficient and low-cost UW sensor node called the Proteus II is described in [83] by W. A. van Kleunen et al. The system is based on dual ARM Cortex-M4 processors. One of the two controls modem functionality and the other processor is responsible for network protocols. Several sensors are attached with the modem including a temperature sensor and an accelerometer. For sensors configuration and network debugging, a $433\ MHz$ radio is available. The modem uses FSK modulation scheme in the band of $20-22\ kHz$, because it is computationally less complex. Hamming code is used for error correction mechanism. The maximum communication distance of the modem in a small artificial lake is reported as $140\ m$ with the data rate of $150\ bps$. While testing in a highly reflective environment i.e., concrete walls and floors, the packet delivery rate of $30-40\%$ is achieved. Energy consumption during transmission is $8\ W$, reception is $300\ mW$ and in idle mode, the modem utilizes only $60\ mW$.

W. bin Abbas et al. [40] designed a low-cost SDR based underwater acoustic modem. The acoustic modem includes a laptop, which runs an SDR, and hydrophone designed by the piezo-ceramic cylinder. An open-source SDR; GNU radio is used for modulation and demodulation. FSK modulation scheme is used in the frequency range of $14-16\ kHz$, because sound card is used to operate the hydrophone. Class-AB amplifier is used to deliver power up to $19\ W$ to drive the $43\ \Omega$ load. An additional step-up transformer is used after the power amplifier to provide impedance matching and to increase voltage for improved performance. The authors experienced several problems in the receiver design and after many attempts, a low pass filter with a cutoff frequency of $20\ kHz$ and a pre-amplifier with automatic gain control (AGC) has been implemented to avoid signal saturation in the sound card. The modem has been tested in a swimming pool and a lake using data rate $100\ bps$. In the swimming pool, due to longer delay spread, 80% packet receiving rate (PRR) was possible at a distance of $24\ m$, while in the lake experiment, at a distance of $25\ m$, $70\%\ PRR$ was reported.

An ultra-low power underwater acoustic modem is presented by A. Sanchez et al. in [56]. The suggested architecture consists of a low-power MCU and peripherals for efficient energy consumption. The novelty of the modem is the use of radio-frequency identification (RFID) technology in underwater acoustic communication. An ultra-low power asynchronous wake-up scheme consumes $10\ \mu W$ and recognizes 8 or $16-bit$ patterns without the MCU involvement. To reduce the overall cost of the modem, instead of using a hydrophone, a less-expensive commercially available transducer Humminbird $XP\ 9\ 20$ is used in the frequency band $85\ kHz$. Coherent binary FSK modulation scheme

is implemented using a microcontroller, and phase-locked-loop (PLL) is used for demodulation. A custom hardware-software power amplifier is designed to maximize the power and efficiency. During reception the modem consumes $24\ mW$ and $120\ mW$ power is required to transmit data at the distance of $240\ m$ with $1000\ bps$ data-rate.

In [41], J. DelPreto et al. present a compact UW acoustic modem for remotely controlled UW operations. The modem transmitter consists of a low-cost hardware platform with Raspberry-Pi model B+ single board computer, Hi-Fi Berry DAC+, amplifier, and an audio output transformer. At the receiver side, an ARM Cortex-M3 processor and a microcontroller are used. The modem works from $30-36\ kHz$ signal bandwidth and uses FSK modulation scheme. The Aquarian hydrophone is used as an underwater acoustic transducer. The performance evaluation of the modem was carried out in a fish tank and a small pool by transmitting a pre-recorded wav file consisting of every possible data word. From the experiments, it was found that the modem can communicate at the data-rate of $20\ bps$ without error in the fish tank when the communication distance is $0.5\ m$. In a pool, error-free communication was up to the distance of $15\ m$, while at the distance of $20\ m$, the success rate was 97%.

A low-cost UW acoustic modem for shallow water communication is developed by G. Cario et al [67]. The architecture of SeaModem is based on a DSP $TMS320C5000$ and BeagleBone. The modem operates in the frequency range of $25-35\ kHz$ and uses MFSK modulation scheme due to its robustness and easy implementation. Selectable tones $2, 4$ and 8 are used to communicate at data-rates $750, 1500$ and 2250 respectively. A class-D amplifier that can deliver up to $40\ W$ is used to amplify signals before transmission. To communicate between host and the modem, a user interface is provided by UART serial port. The modem is capable of operating TCP-like and UDP-like protocols. The range measurement tests of the modem were conducted in a $100\ m$ long dock. The authors reported that a larger number of tones were not implemented due to the degradation of the stability of transmission. The power consumption and BER tests are currently in progress. The modem fulfills all typical research needs and is a useful solution for researchers working in the area of underwater acoustic communication.

In [84], N. Ahmed et al. present a low-cost underwater platform with the aim of easy-to-replicate in order to promote experiments in the area of underwater acoustic sensor networks. The hydrophone, which is one of the costly elements of an underwater acoustic modem, is designed by four piezo elements mounted at $90°$ with each other, to make the transducer omnidirectional. FSK modulation scheme is used in the frequency range of $15.5-17.5\ kHz$. Class-AB amplifier is used to deliver power up to $19\ W$ to drive the $4\ \Omega$ load. The GNU Radio based, software-defined modem uses the computer's sound card to transmit and receive data. The platform has been tested in a $10\ m$ long linear water channel, with the data rate of $100\ bps$. It was observed that the PRR was 90% at $3\ m$, but as the distance increased to $7\ m$, the PRR reduced to 20% due to echo. The authors foresee that the deployment of such testbeds will be helpful to the underwater protocol analysis in a real environment.

A low-cost underwater acoustic modem to be used in small-sized AUVs is presented by C. Renner et al. in [35]. The hybrid hardware-software solution is used in the modem. Signal amplification and filtration are handled by hardware, while software is responsible for demodulation. The selection of non-coherent binary frequency shift keying (BFSK) modulation scheme in the frequency band from

$14 - 30 \, kHz$ has been done due to easy implementation on less expensive hardware which is also suitable for moving objects. An ATMEL AVR32UC3 microcontroller is used for demodulation. Commercially available hydrophones from Aquarian Audio were used as transducers. The communication between the modem and host AUV is serial via packet-based protocols. The modular design of the modem can be easily modified by applying suitable changes in software for different applications. The modem has been tested in a pool environment at the distance of $9 \, m$ with the data-rate of $2000 \, bps$. The modem consumes $530 \, mW$ during the reception and $770 \, mW$ is used during data transmission. The authors faced several challenges during the process of modem design and they have planned to address them in future work e.g., testing of the modem in a lake or sea environments and to use single hydrophone both for transmission and reception to reduce the overall cost of modem.

A low-cost underwater acoustic modem prototype is designed by Benson et al. in [60]. The novelty of modem is its home-made underwater acoustic transducer made by a cheap piezo-ceramic material. This transducer is potted in a urethane compound for waterproofing and to match the acoustic coupling with water. The linear output response of the transducer has been observed up to $1000 \, V$ and $50 \, W$ with $35 \, kHz$ resonant frequency. The transmitter consists of a class-AB and class-D amplifier. The receiver consists of biquad band-pass filters to amplify signals around $35 \, kHz$. FPGA is used as a hardware platform for the modem for signal processing and control functions. Due to the robustness and easy implementation, FSK modulation scheme is used by the team. The power consumption by the analog transmitter can switch between output levels $2, 12, 24$ and $40 \, W$, while analog receiver consumes $0.75 \, W$. The modem has been tested underwater at a distance of $350 \, m$, with data rate up to $200 \, bps$ and BER 10^{-2}. We describe the proposed low-cost modem architecture in the following Section 3.3.

3.3. Low cost underwater acoustic modem architecture

As discussed in the above section, the main objective of the research is to design a low-cost underwater acoustic modem that can be used in economical projects. To make the design more flexible, a modular approach is followed that can be easily modified and upgraded as per the requirements. Figure 3.1 shows the low cost underwater acoustic modem architecture. The three main blocks of the modem include: (i) digital controller, used to control the functions of various blocks is based on a low-cost hardware platform and a microcontroller, (ii) analog module, responsible for modulation, demodulation and amplification, and (iii) transducers, for duplex communication of acoustic signal in water channel. The electronic circuitry in the two upper blocks is kept inside a waterproof chamber, while the transducers are submerged into the water channel for acoustic transmission and reception.

The functionality of the low-cost underwater modem as shown in Figure 3.1 is described using arrow directions to show the data flow. The modem works in both ways i.e., for data transmission and reception. A complete cycle starting from reception to transmission is explained for better understanding. The underwater RX transducer, submerged in a water channel, receives an acoustic signal from a similar kind of modem and passes it to the pre-amplifier that amplifies the signal and delivers it to the FSK demodulator. The signal is demodulated and converted into binary information and received by the microcontroller which is connected to the low-cost hardware platform Raspberry-Pi. A high level application running on the Raspberry-Pi is used to process the signal and return it to

the microcontroller in binary form. The signal is passed to the FSK modulator for modulation and then power amplifier for amplification before transmission using a TX transducer in the water channel. Details of each module are provided in the following subsections.
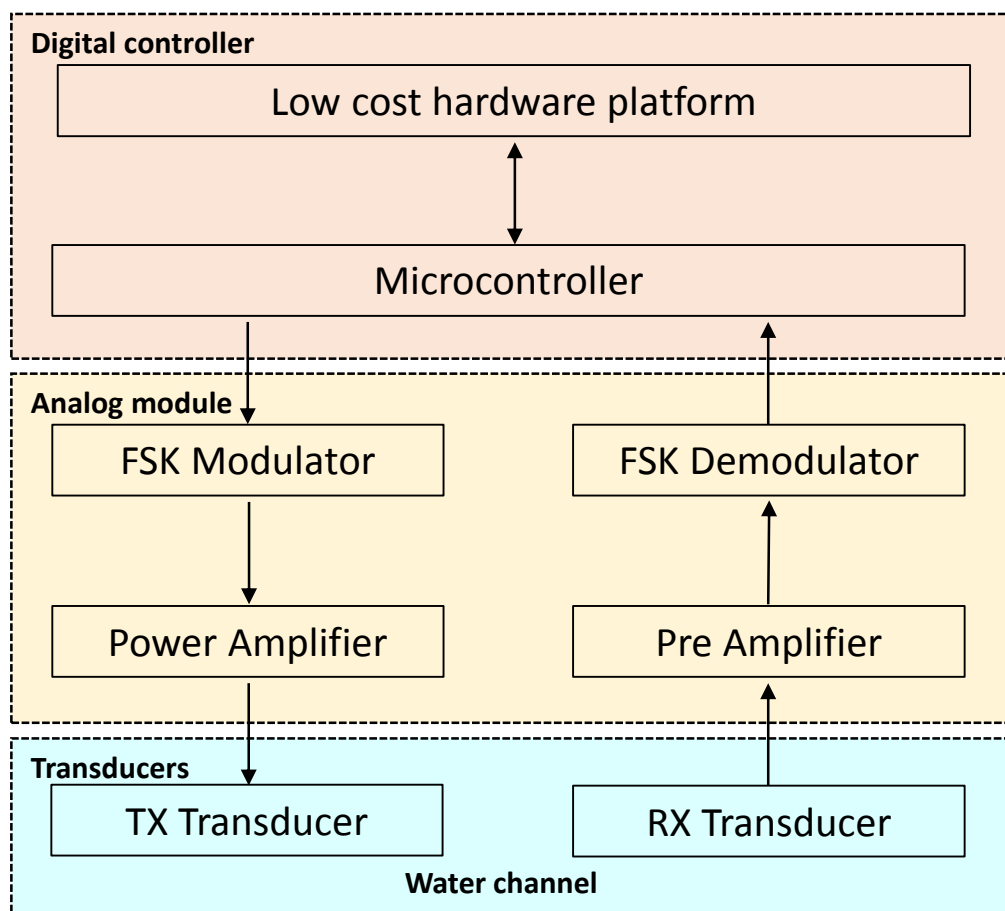

Figure 3.1. Low cost underwater acoustic modem architecture.

Section 3.3.1 describes the design process of underwater acoustic transducers. Section 3.3.2 explains analog module responsible for modulation, demodulation, and amplification (pre-amplifier and power amplifier). Section 3.3.3 presents a low cost platform Raspberry-Pi [81] and a microcontroller Atmega328P [82].

3.3.1. Underwater acoustic transducers

Acoustic transducer is a device that receives and converts sound signals into electrical signals and vice versa i.e., the electrical energy can be converted and transmitted in the form of acoustic energy in water medium. Piezoelectric ceramics are smart materials typically used to design an underwater acoustic transducer due to their low electric losses and high coupling coefficients [85]. Various manufacturers design acoustic transducers in different shapes, e.g., cylindrical, spherical; and radiation patterns, e.g., directional or omnidirectional etc., but these designs are expensive to be used in our research.

Since cost reduction is the primary goal of the research, to cut down the budget of our modem, we selected the piezo material $SM111$ to design our custom made underwater acoustic transducer. We selected the piezoelectric ceramic cylinder model $SMC3631T20111$ offers radial mode vibration with resonant frequency in the range $30 \pm 2\ kHz$ that is less attenuated in underwater environments [86].

There were several reasons to choose this particular model, especially the cost i.e. $USD 35$, which is much less compared to the commercial transducers [60], dimensions $(36 \times 31 \times 20)\ mm$ appropriate for the design. We tackled many challenges during the design of our custom made underwater acoustic transducer especially the frequency shift during the process of waterproofing.

A cylindrical shape raw piezo-ceramic material element is used to design the transducer as shown in Figure 3.2 (a). A shielded cable is soldered to the inner and outer sides of the cylinder to provide electrical connection and to reduce the impact of electromagnetic interference. We used a temperature controlled soldering iron to avoid overheating and lead-free soldering wire as recommended by the manufacturer [87]. The ends of the cable are insulated using a heat-shrink tube. The final step is to make the connections waterproof. In [60]. Urethane is used as a sealing compound to enclose the piezo ceramic element due to its acoustic transparent characteristics.

(a)   (b)

Figure 3.2. (a) Raw piezo-ceramic element (b) Water-proof underwater acoustic transducer.

We avoided it in our design due to its toxic properties, in addition it effectively assimilates the moisture. Some designs use mineral oil, which is a simple solution having similar impedance and density of water [40]. In both cases, the additional mass drifts the resonant frequency of the piezo ceramic element. We used varnish in our design to make the piezo ceramic element waterproof. We slightly heated the varnish in a small pot and placed the raw piezo-ceramic element inside for a while, then kept it in the air for a few hours to make it dry and waterproof as shown in Figure 3.2 (b).

3.3.2. Analog module

The analog module is responsible for all signal processing related tasks. It consists of a modulator, a demodulator, a pre-amplifier, and a power amplifier. Due to robustness, noise immunity and easy implementation, continuous phase FSK modulation scheme is used in the modem [5].

a) *Modulator.* The FSK modulator circuit is designed with a monolithic function generator [88]. The carrier frequency is set by the timing capacitor and resistors. The timing capacitor is connected to the terminals TC1 and TC2 of the voltage controlled oscillator (VCO), and timing resistors are connected to the terminals TR1 and TR2 of current switches to the ground. To obtain a desired

modulated frequency, a digital signal is applied to the input FSKI of the current switch and the modulated output is at the terminal denoted by "sine wave output". Block diagram of the FSK modulator IC [88] is shown in Figure 3.3 and the FSK modulator circuit prototype is shown in Figure 3.4.
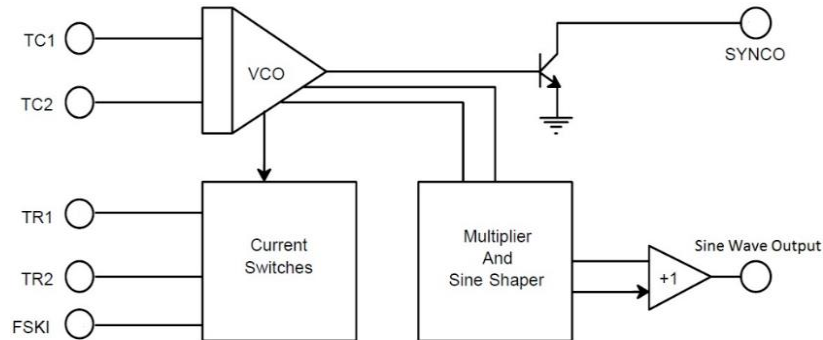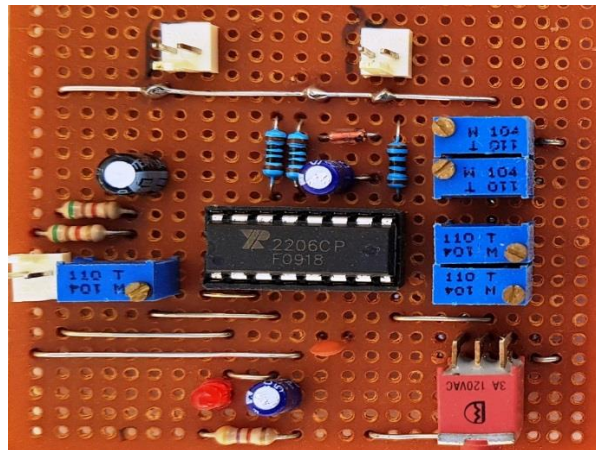

Figure 3.3. FSK modulator IC block diagram.

Figure 3.4. FSK modulator circuit prototype.

b) *Demodulator.* The FSK demodulator is designed around a tone decoder [89] that works in the range from $0.01 - 3\ V$, as shown in Figure 3.5. It can decode the frequency range from $0.01 - 300\ kHz$, which covers almost the complete range required by underwater acoustic communications. The operation of the FSK demodulator is adjusted by the timing resistor connected to the terminal TIM R, and timing capacitors connected on terminals TIM C1 and TIM C2. The analog signal is applied to the INP terminal and the decoded output is received at the terminal denoted by DO (digital output). The FSK demodulator circuit prototype is shown in Figure 3.6.
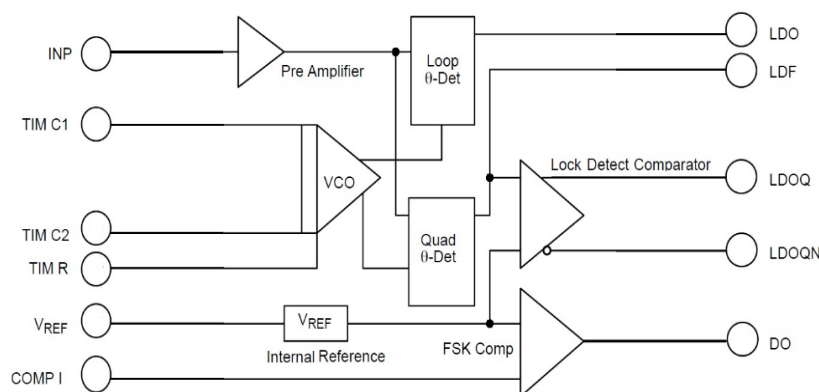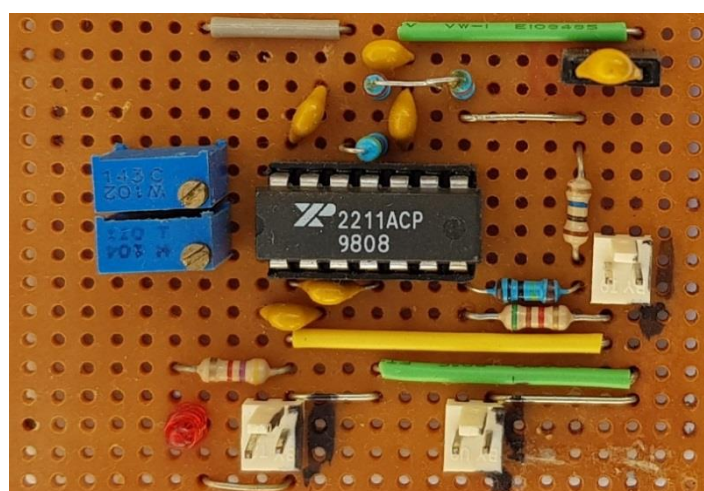
Figure 3.5. FSK demodulator IC block diagram.

Figure 3.6. FSK demodulator circuit prototype.

c) **Pre-amplifier.** A field effect transistor (FET) based preamplifier with the gain of 40 dB is used to amplify the signals coming from the acoustic RX transducer. The FET device is selected because of its less noise as compared to the BJT and integrated circuit-based preamplifier [90].

d) **Power amplifier.** The modulated signal is not strong enough to be transmitted at reasonable communication ranges in underwater environments due to absorption, therefore, amplification is required. Class-A amplifiers are simple to design, provide good linearity but, due to low-efficiency (in the vicinity of 35%), they are not a good choice to be used in such applications, as the modem is battery powered. In Class-B amplifiers, the efficiency is doubled (around 80%) but they amplify only the positive half cycle of the input signal, so they are also not recommended [91]. Class-AB amplifiers overcome the drawback of class-B amplifiers as both transistors conduct at the same time, hence they are good a choice in terms of efficiency and linearity. Class-C amplifiers also provide better efficiency, but they are not considered due to their linearity issue. Finally, Class-D amplifiers provide best power efficiency in low-cost, but they produce electromagnetic interference, and require an impedance matching network [92]. We decided to use class-AB amplifier in our design due to its linearity, low-cost and simplicity of the design.

3.3.3. Digital module

The digital controller consists of two processors, a Raspberry-Pi [81] and an Atmega328P microcontroller [82]. The Raspberry-Pi 2 Model B+ is a single board computer (SBC), equipped with a quad-core ARM Cortex processor operating at $900\ MHz$ with $1GB\ RAM$ as shown in Figure 3.7. The four USB ports, onboard $10/100\ Mbits/s$ Ethernet, 40 general purpose input-output (GPIO), support a of variety of Linux-based operating system and Windows 10 IoT Core, all features available in USD 35.00 is the strong reason to choose this platform for our modem design. All high level tasks are performed by the low-cost hardware platform, Raspberry-Pi. The Atmega328P is an $8-bit$ AVR RISC based microcontroller with $32\ kB$ Flash memory, $1\ kB$ EEPROM and $1-$UART port operating at $16\ MHz$, as shown in Figure 3.8 used to reduce the computational and peripheral load from Raspberry-Pi to make the modem design power efficient.
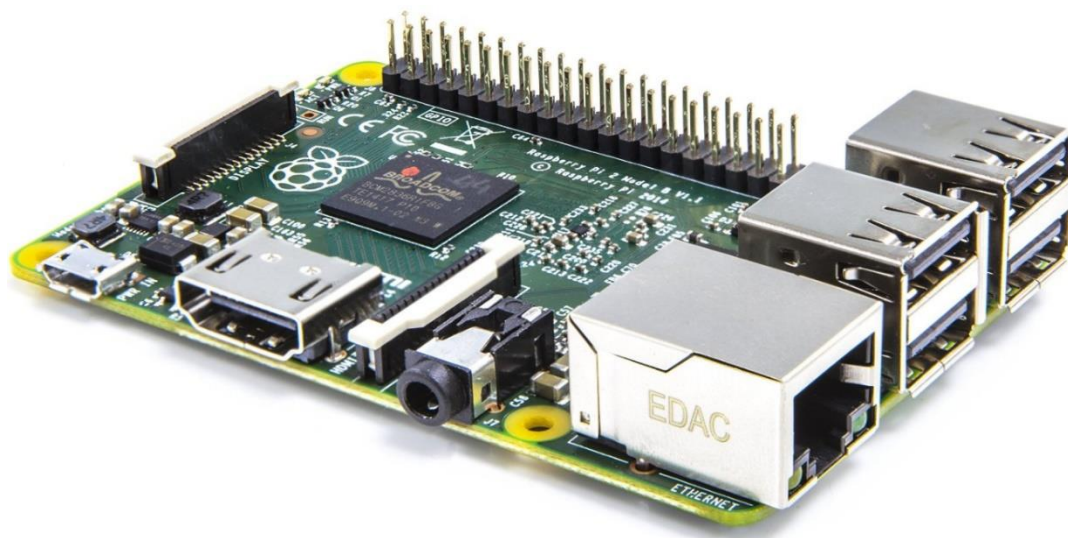
Figure 3.7. Raspberry-Pi 2 Model B+.
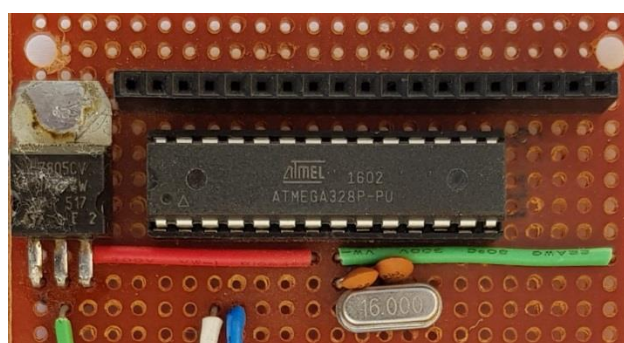
Figure 3.8. MCU Atmega328P.

3.4. Experimental results and discussion

To validate the functionality of the low-cost underwater acoustic modem, testing results for individual modules are first presented in Section 3.4.1 and Section 3.4.2. Subsequently, individual modules are connected to perform system level testing, as shown in Section 3.4.3. Finally, the results of system level testing and the associated discussion are presented in Section 3.4.4.

3.4.1. Underwater acoustic transducer

To obtain the frequency response of the underwater acoustic transducer, national instruments educational laboratory virtual instrumentation suite (NI ELVIS) II+ hardware has been used [93]. NI ELVIS II+ is a breadboard type modular workstation, consisting of 12 commonly used laboratory instruments, which can be connected to the PC via USB port. The test program is written in the laboratory virtual instrument engineering workbench (LabVIEW), which is a graphical programming language (GPL) from NI [94]. The LabVIEW programs are known as virtual instruments (VIs) consist of two major components, front panel, and block diagram. (i) The front panel provides a user interface with controls (inputs) and indicators (outputs). (ii) The block diagram contains the graphical source code. The benefits of using LabVIEW are reduced learning time, flexibility in designing, and better hardware-software support. Figure 3.9 shows the block diagram to test underwater acoustic transducer. It consists of inputs i.e., start and stop frequency ranges (left side), a "$for\ loop$" (in the middle), and the output, spreadsheet along with the filename (right side) of the figure. Inside the "$for\ loop$", the NI ELVISmx Impedance Analyzer, which is a stand-alone instrument, is used to measure the impedance of transducers. The test has been conducted in the frequency range from $20-40\ kHz$, with the increment of $0.5\ kHz$. The values were taken with $100\ ms$ delay, set by the wait function. Each output: magnitude, phase, reactance, and resistance has been recorded in a spreadsheet for further analysis.
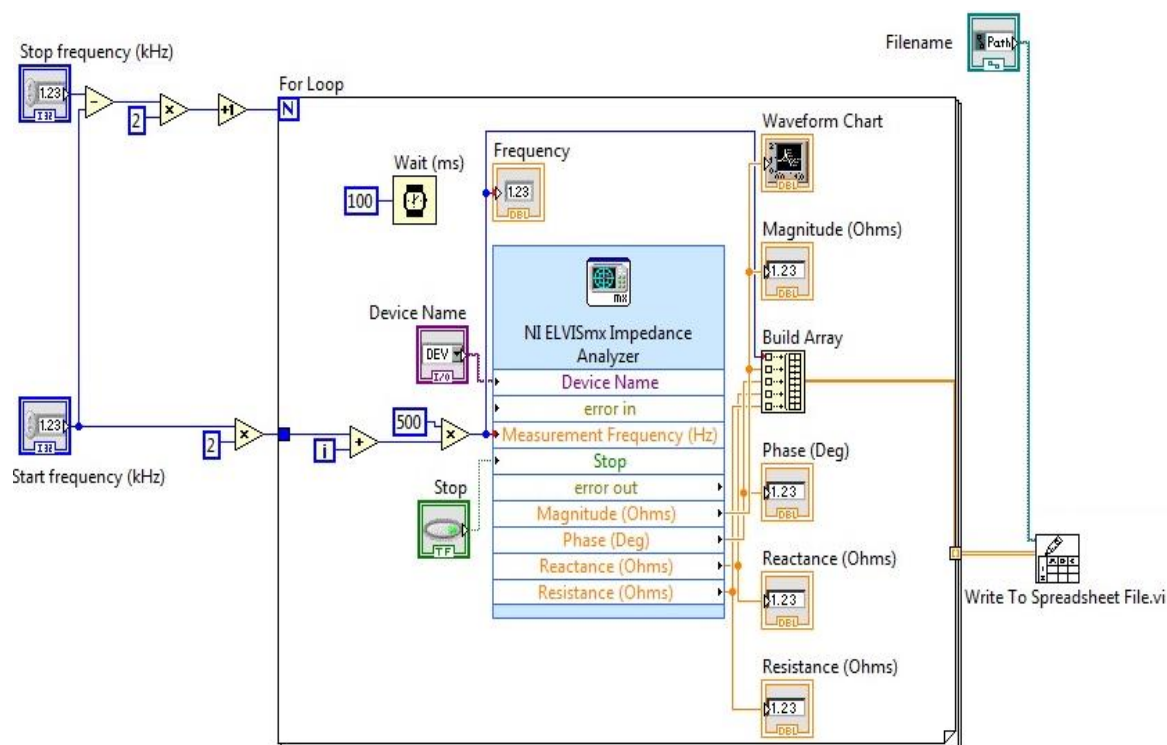

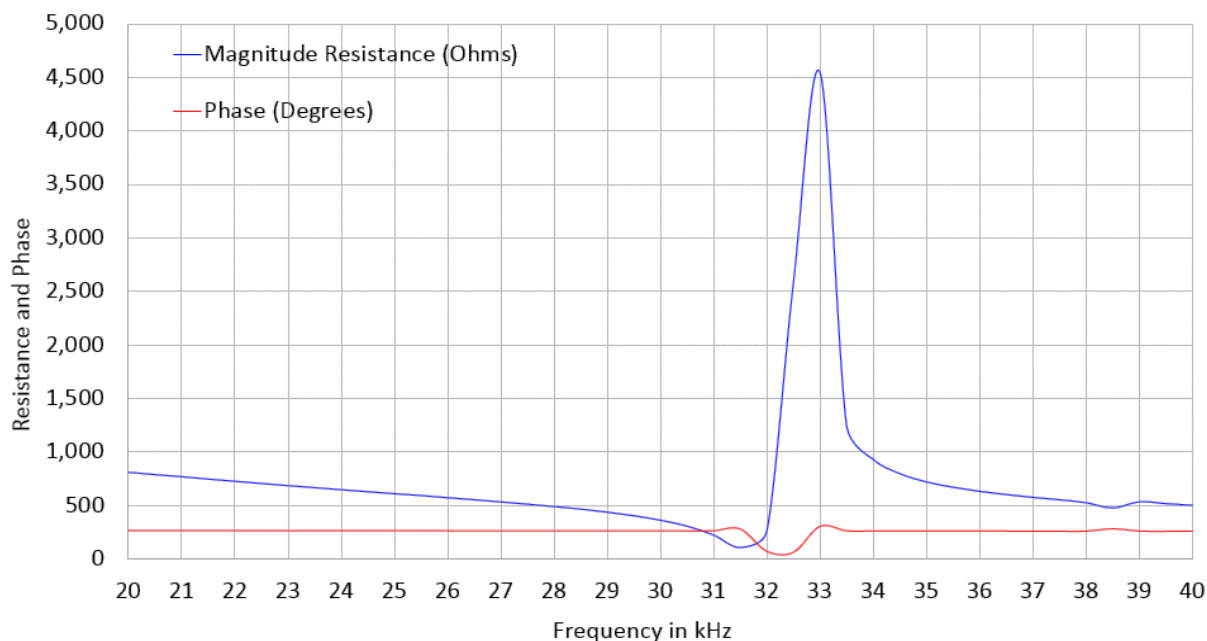Figure 3.9. Piezo-ceramic transducer testing in LabVIEW.

Figure 3.10. Piezo-ceramic transducer magnitude and phase responses.

3.4.2. Underwater analog module and digital controller

The analog module and the digital controller also have been tested using NI ELVIS II+ hardware [93] and LabVIEW [94] before final implementation. A fixed data stream stored in the Raspberry-Pi has been applied to the FSK modulator via microcontroller and the output is observed on the oscilloscope. On the other hand, FSK signal generated by NI ELVIS II+ and LabVIEW is applied to the FSK demodulator and the response is received on the oscilloscope. The functionality and gain of the amplifiers have also been tested by the similar setup.

3.4.3. System level testing

Preliminary indoor testing of the proposed modem has been performed in a water tank dimensions $(1.2 \times 0.5 \times 0.3)\ m$. The two transducers have been placed at a distance of $1\ m$ submerged in water, but not touching the bottom of the tank, while the electronic circuitry is placed beside the water tank. One of the transducers is used as a transmitter, while the other as receiver of the acoustic signals. A fixed data stream of $100\ bits$, (stored in the Raspberry-Pi), has been acoustically transmitted (after FSK modulation and amplification) by the TX transducer in the water channel. On the other side, the acoustic signal received by the RX transducer has been converted into electrical signal, amplified by pre-amplifier, demodulated, and stored into the memory of Raspberry-Pi for analysis. The experiment has been repeated several times using data rates $100, 300, 600$ and $1200\ bps$ in different time intervals to obtain consistent results.

3.4.4. Results for system level testing and discussion

Following section provides a qualitative comparison of our low-cost proposed modem design with the state-of-the-art low-cost modems of the same category as mentioned in Table 3.1. The authors in [40] and [84] designed a low-cost SDR modem based on laptop and personal computer, which are part of the design but their cost is not included in the modem cost. The modems are not standalone and operate

at a low data rate. The modems presented in [35] and [56], are low-cost designs but due to the use of a microcontroller, they have limited computational power. The [41] is built around Raspberry-Pi and ARM Cortex, and can communicate at low data rate as compared to the other designs. In [83] dual ARM Cortex M4 processors are used but the data rate is low i.e., $150\ bps$ with the PRR 40%. The center frequency of our modem i.e., $31.5\ kHz$ is closer to [60] and [67] but due to the cost of hardware platforms used in these designs i.e., FPGA and DSP, our UAM prototype is still low-cost design, with variable data rates. The range tests are in progress, however the initial tests were conducted at a distance of $1\ m$ in a water tank with different data rates from $100-1200\ bps$. Here we would like to mention that due to some technical reasons (e.g., the availability of larger aquatic environment with outside lab facility), the transducers of the modem were placed at a distance of $1\ m$, however the modem range can be extended by using an appropriate power amplifier if a suitable testing environment for larger distances is available. It implies that distance does not affect the proof of concept.

Table 3.1: Comparison of state-of-the-art underwater acoustic modems.

Reference	Hardware platforms	Center frequency (kHz)	Range (m)	Data rate (bps)	BER / PRR
[40]	Laptop (SDR)	15	24	100	80%
[84]	PC (SDR)	16.5	7	100	20%
[56]	Microcontroller	85	240	1000	-
[35]	Microcontroller	22	9	2000	-
[41]	Raspberry-Pi, ARM Cortex	33	15	20	97%
[83]	Dual ARM Cortex M4	21	140	150	40%
[60]	FPGA	35	350	20	10^{-2}
[67]	TI DSP & BeagleBone	30	100	750, 1500, 2250	-
Low-cost UAM	Raspberry-Pi & MCU	31.5	-	100, 300	100%, 100%
				600, 1200	95%, 70%

3.5. Conclusion

A low cost underwater acoustic modem has been designed using a modular approach to promote the research in underwater communication. Typically, state-of-the-art underwater modems are either DSP based (which increases their cost) or FPGA (that requires more energy). The proposed modem is designed using a low-cost single board computer (Raspberry-Pi) and a microcontroller. Other modules (modulator, demodulator, and amplifiers) are designed from discrete components and the transducers are made from piezo-ceramic elements to reduce the overall cost of the modem. Each module has been tested separately before integration.

FSK modulation scheme is used due to its robustness and easy implementation. We used ultrasonic frequency range $30.5-32.5\ kHz$ to reduce the noise and water absorption. Functionality testing of the modem has been performed in a $1.2\ m$ water tank in the range of $100-1200\ bps$. The data rates used for system level testing are $100, 300, 600$ and $1200\ bps$. The corresponding packet receiving rates for these data rates are $100, 100, 95$ and 70 percent respectively. The experiment is repeated several times for consistent results and it is observed that error-free communication is possible at lower data rates, while errors in receiving data increases with the increase of data rate which is due to echo from the walls of the water tank. Due to some technical difficulties the experiment could not be repeated in a

swimming pool or river, and the actual operating range could not be determined, however the modem can also communicate at a greater distance.

The main objective of the research is to design a low-cost underwater acoustic modem that has been achieved and validated by experiments, though the design can be used for further research. The modem has been designed using a modular approach, however the difficulties in testing hamper its overall adoption. Therefore, a low-cost testing is equally important to provide a complete low-cost solution. Next chapter addresses the issue of a low-cost testing platform.

Chapter 4: A Web-based Low Cost Underwater Communication Testing System [*]

Chapter 3 presents a low-cost underwater acoustic modem using modular approach and its basic functionality has been verified in an aquatic environment. During testing of the modem, we realized that in-field testing of underwater communication systems has several technical and operational challenges e.g., availability of laboratory facilities on a test site or to provide an aquatic environment inside an electronic laboratory. Either case is expensive as well as requires a lot of time and difficult to be implemented because of administrative and safety issues.

This chapter presents a web-based testbed to evaluate the performance of underwater wireless sensor network and its components. The motivation behind the research is to present a cost-effective emulator and easy to use simulator that can be used to investigate the functionality of underwater wireless sensor networks and its components including underwater modems, sensors and various modulation schemes in a controlled laboratory environment. The testing system also simulates underwater acoustic channel and propagation and mathematical models, protocols. Remote accessibility using a web-browser is the novelty of design.

This chapter is organized as follows: Section 4.1 provides the introduction to the underwater communication wireless sensor networks and their components. Section 4.2 describes the related work. Section 4.3 presents the underwater communication testing system architecture. Section 4.4 discusses experimental setup and results. Section 4.5 presents concluding remarks.

4.1. Introduction

To explore marine life, several UWSNs have been proposed [61]. Despite the efforts, research progress in UWSNs is slow due to the challenges posed by undersea communication medium as compared to the WSNs used in terrestrial communication [95, 96]. Testing of UWSNs and their components in a real environment is still a challenge owing to high deployment cost and time-consumption. Simulators offer an inexpensive solution; due to low setup time and cost but with the trade-off of low accuracy because they use a subset of environmental variables. Another technique is the emulator-based network, deployed using a combination of hardware and software. The test results of emulator-based networks are better as compared to simulator-based setup. However, in order to use emulator based networks, physical access is required [62].

Underwater modems are the backbone of emulator-based platforms. Commercial modems e.g., Evologics [19], LinkQuest [21] and Teledyne Benthos [26] and that are mainly designed for long distance reliable UW communication are being used in various testbeds. Research modems such as Sea modem [67] and WHOI Micro-modem [97] are economical to be used in the same setup with the tradeoff of BER. Some simulators are open source e.g., network simulator (NS-2), aqua-sim, etc.,[63], while there is another category of licensed software with additional features of simulation and emulation e.g., SUNSET [74], DESERT [75] etc. These simulators evaluate various UW network protocols such as medium access control (MAC) and multiple access with collision avoidance (MACA) [98]. They can be categorized at different levels, e.g., low-cost platforms are designed for small-scale UW scenarios, while medium to high-cost platforms are used for large-scale testing. To access the experimental facilities remotely, heterogeneous platforms are used which are costly and used for large-scale developments [99].

In this chapter, UW acoustic communication testbed and simulation platform is proposed, and its performance has been evaluated, both as an emulator and a simulator. In emulator mode, the initial testing has been done by using two low-cost UW acoustic modems [31] communicating in an aquatic environment inside a laboratory. The temperature in $°C$ and salinity in parts per thousand (PPT) is acquired using UW sensors and transmitted acoustically using UW modem in the water channel. Data is successfully received by another UW modem and graphically displayed. Similarly, various UW algorithms have been simulated using the proposed simulation platform. The parameters can be configured locally as well as remotely in the beginning or during simulation to get the desired results. Minimum development time and low-cost with remote monitoring facility is the novelty of proposed design. It can be easily modified to evaluate various kinds of UW communication systems and algorithms.

The proposed testbed software is designed in laboratory virtual instrument engineering workbench (LabVIEW) which is a graphical programming language [94]. LabVIEW, with built-in mathematical and analysis functions and graphical front-end controls and indicators, provides a platform that reduces the development time as compared to other software and applications. This helps in quickly creating the required graphical user interface (GUI). With the available instrument drivers, it is convenient to connect and acquire data from standard test equipment, sensors, and other test devices. LabVIEW uses icons instead of text-based coding. Its front panel is used to design GUI, while the code is written in a

block diagram using icons connected by wires. The file format used by LabVIEW is virtual instrument (VI). Web server is used to convert a VI into hypertext markup language (HTML) document and embed front panel images to be monitored and controlled using hyper-text-transfer-protocol (HTTP) in a web browser.

4.2.   Related work

Several testbed designs for UW acoustic communication systems have been proposed to evaluate various aspects of UWSNs including hardware, software, protocols, and mathematical models. These testbeds are available in different sizes e.g., small, medium, and large, and categorized as simulator, emulator or both and deployed in a controlled laboratory as well as in real-world environments. Some existing UW communication system testbeds are discussed in the following section.

An UW acoustic testbed is presented in [98] to examine the performance of cross-media networking by combining UW acoustic communication and wireless communication. The testbed consists of a UWA modem based on DSSS modulation and operates in the frequency band of $13 - 18 \, kHz$. A group of underwater sensor nodes is deployed in a lake to collect environmental data and pass it to a sink node which transmits the data to a terrestrial station. Field trials are conducted in a lake by using six nodes including three sensor nodes, a data generator node, a sink, and an offshore sink node. Two networking protocols, ALOHA and MACA, have been examined using the testbed. From the experiments, it has been found that the delay between the nodes is very short and some errors in data have been observed during wireless transmission. ALOHA, which does not have any collision avoidance system, works better than MACA in this setup because of simple network topology with minimum load.

X. Du et al., [100] have designed a UW acoustic testbed to investigate water quality of the Qinghai Lake. The testbed consists of a server and various sensor nodes deployed in water and equipped with an OFDM modem for UW communication. Micro-ANP software is running on each of the nodes to provide an interface between network transport layer and physical layer. The testbed has been used in UW protocol evaluation and aquatic environment monitoring of various parameters such as temperature, salinity, and conductivity. In protocol assessment, throughput of the proposed system becomes steady when payload exceeds $100 \, bytes$. Network performance of the testbed degrades with an increase in the time interval between two packets. Software design of the testbed facilitates researchers to use their own UW network protocols in real underwater environments.

The SUNSET framework, which is a customizable testbed for testing of UWSNs is presented by C. Petrioli et al., [74]. It is built using NS-2 for simulation, emulation, and in-field testing. The SUNSET core modules include (i) utilities unit that makes framework transparent to the client in simulation and emulation modes, (ii) timing unit to introduce delays and overheads usually ignored during simulation, (iii) debug unit to log and process debug information based on given precedence and (iv) statistics unit that provides a tool to gather readings to investigate protocol performance. Some of the features of SUNSET framework are, (a) it is capable of simulating various UW acoustic channel models, (b) the code can be reused after suitable modifications and (c) it supports five different types of commercial UW acoustic modems and uses different sensors for the measurement of temperature, pressure, salinity, and conductivity. The energy efficient SUNSET framework can run on small-size, low-priced hardware platforms such as ARM processors.

DESERT is a customizable platform that has been designed to perform experiments on UW network protocols to promote the experiments in UW networking [75]. Its modular architecture allows researchers to reuse their codes with slight modifications. This research targets the grasp on C language libraries to support UW networking protocols. It can be used as an emulator as well as a simulator. Evologics and WHOI Micro-modem have been tested in emulator configuration using the system running NS-2 Miracle. A similar scenario can be created using simulation. The performance of the system has been successfully tested during single and multiple hop configurations. The DESERT architecture is open source but resource hungry and consumes high energy.

WaterCom is a multi-function testbed designed to perform UW experiments at small, medium, and large scales [101]. The prototype supports UW acoustic and optical communications in three configurations; (i) small-scale UW experiments are performed in a water tank using two modems to test the UW transmission in a reflective environment, (ii) medium-scale experiments can be conducted in a dock with one mobile and two stationary nodes to test MAC and Network Protocols and (iii) in large-scale configuration, the testbed can be used to evaluate multi-hop UW communication and node movability in the aquatic environment. The testbed is fundamentally designed for small and medium level UW experiments, although, as mentioned above, it can be used in large scale configuration. Currently, point-to-point communication at small-scale configuration is implemented and test results are presented in the paper. The testbed can be accessed online for configuration and UW experiments.

The Porto University testbed has been designed by R. Martins et al., under SUNRISE project [73]. The main objectives of SUNRISE testbed are: UW protocol evaluation such as MAC and routing protocols, UW environment monitoring, ecological data collection, UW localization, and investigation of control algorithms with UW robots. The testbed include: AUVs equipped with UW acoustic modems, UW acoustic localization system, ASVs to be used as mobile UW gateways, ROVs for UW inspection, gateways to support UWSNs, buoys, sensors and shoreline control station. Neptus software toolchain provides complete command & control foundation for all operations. The testbed is compact and versatile with the web enabled clients able to control vehicles and resources through IP-suit.

A testbed for UW communication and networking is developed by J. Alves et al., [102] to evaluate hardware and software of UW communication systems near to conditions as in the real environment. Major blocks of the testbed include (i) the commercial UW acoustic modem placed at the seabed, (ii) an acoustic system to generate an arbitrary waveform, (iii) some instruments to collect oceanographic data, and (iv) a command system to provide an interface between other systems and to run experiments. Star topology is used in the test setup equipped with Evologics and WHOI Micro-modems using S2C and FSK modulations respectively. Some observations during the test include recording of sound speed at various time periods. Experimental results show a reduction in the transmitter sensitivity by $20\ dB$ due to biofouling. The testbed facility can be used by the scientists and is remotely accessible to the collaborating institutions.

A testbed for UWSN based on an ARM9 processor is developed by Kim, Y.-P., et al., [76]. The authors used ARM9 processor in UW applications because of its high speed, pipelining feature and energy efficiency. The experimental setup is built in a laboratory using a small water tank and six waterproof UW nodes, one each gateway and sink nodes and four sensor nodes. These are deployed at distances of $30-100\ cm$ to measure the temperature and salinity. Data is transmitted from testbed to

the PC using CDMA data transmission scheme. Authors highlighted several challenges during the experiments including power consumption due to long propagation delays, and packet re-transmission due to collision.

The UW network testbed Aqua-Lab designed in [103] is used to investigate UW algorithms and protocols in the actual aquatic environment as well as in lab facilities. It consists of (i) a low-power WHOI Micro-modem, (ii) water tank filled with around $2000\ liters$ water, (iii) hydrophone used to receive acoustic signals, (iv) UW speakers to transmit acoustic signals in water, (v) sound mixer that can combine various acoustic signals and ecological noises to mimic real marine environments, and (vi) a server to communicate and control the functionality of UW modem. Initial experiences of Aqua-Lab results are encouraging with some constraints including being unable to adjust SNR can be adjusted locally because the sound mixer cannot be accessed by a remote user. We describe the proposed underwater communication testing system architecture in the following Section 4.3.

4.3. Underwater communication testing system architecture

The underwater communication testing system architecture is presented in this section. The proposed testing system is a combination of hardware and software that uses state-of-the-art virtual instrumentation to test various types of modems. It is economical and easy-to-setup compared with existing systems [62]. The two major components of the proposed testing system are: (i) hardware interface that is used as an emulator to test the functionality of underwater communication systems, (ii) software module, that is graphical user interface based simulator, used to evaluate underwater equations, algorithms and simulations. Details of these modules are as under:

4.3.1. Hardware interface

The proposed underwater communication testing system is shown in Figure 4.1. It consists of a tank that has a capacity to store $400\ liters$ water to test the UW communication system. Low-cost UW acoustic modems operating in the range of $30.5 - 32.5\ kHz$ frequency band with FSK modulation are used in this testbed as a physical layer [31].

Each modem is equipped with UW transducers TX and RX for acoustic transmission and reception in the water channel. Temperature and salinity sensors are attached with the $Modem\ (A)$ to obtain the real-time data in controlled laboratory environment and transmit acoustically using TX transducer in UW channel. $Modem\ (B)$ receives the data from UW channel using RX transducer and passes it to the LabVIEW server running VI for further processing [94]. The LabVIEW server is connected to the local network / Internet to share information with clients.

The sensors connected with $Modem\ (A)$ measure the temperature and salinity of water. $Modem\ (A)$ transmits the values using acoustic transducer TX in the water channel. The values are received by the RX transducer attached with the $Modem\ (B)$ which is connected with the LabVIEW server via standard communication port. The LabVIEW server running the VI processes the data and presents it for monitoring and storing at local terminal as well as remote clients. This data is available on the local network / Internet clients via the web browser.
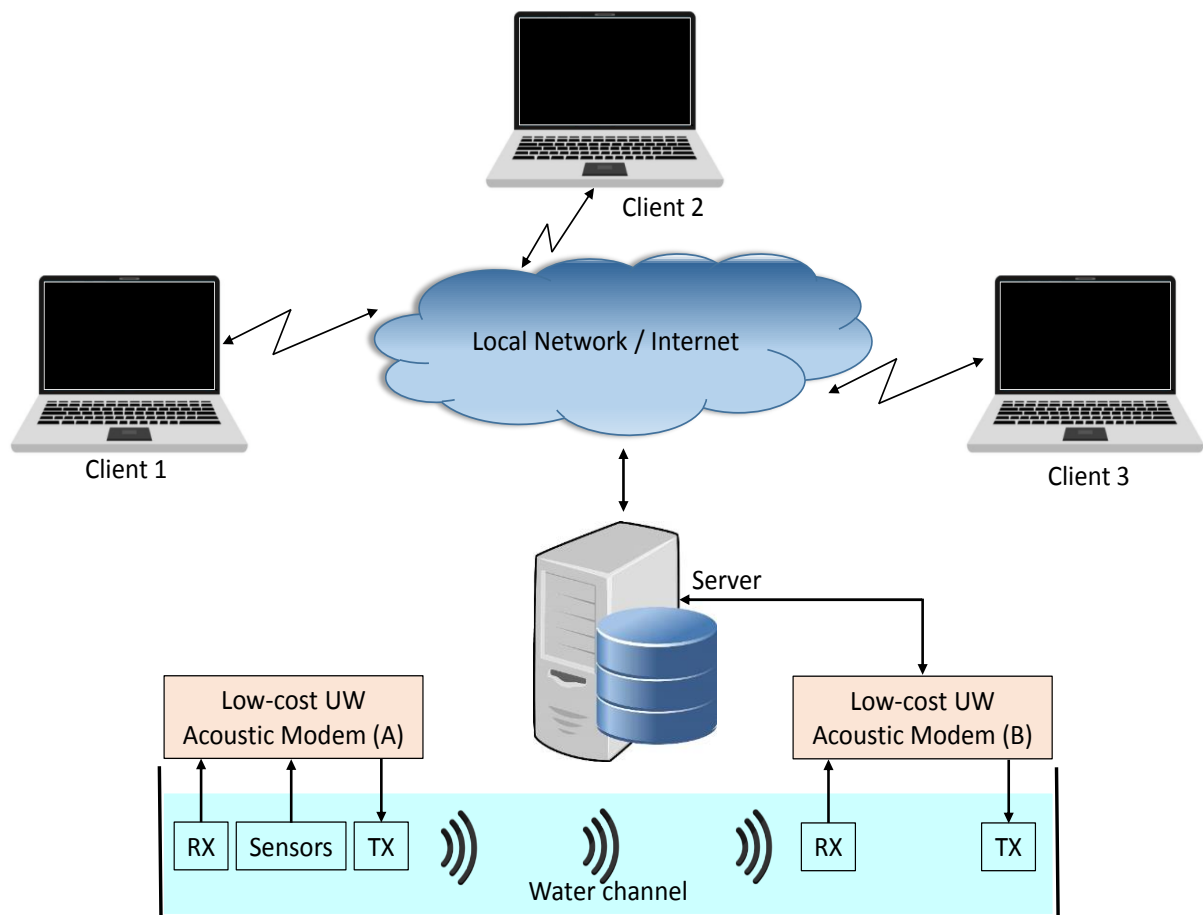
Figure 4.1. Proposed testbed architecture.

4.3.2. Software module

The testbed software is designed in LabVIEW which is a graphical programming language [94]. LabVIEW has built in functions for controlling instruments using general purpose interface bus (GPIB), universal serial bus (USB), serial, local area network (LAN), inter-integrated circuit (I2C), serial peripheral interface (SPI) and joint test action group (JTAG) etc., interfaces. The available mathematical, statistical and signal processing functions can be used for data and signal analysis. Acquired data can also be displayed using front panel and stored via MS Access and other databases.

LabVIEW also provides interface for various source code control applications, data validation systems and other management tools. Test results can also be generated using MS Office and hypertext markup language (HTML) templates and reports. The LabVIEW code can be deployed on target computers by creating standalone executables and installers. LabVIEW applications can also be controlled and monitored remotely.

LabVIEW applications can be created using three sets of programming objects which are tools palette, control palette and indicator, and functions palette. Tools palette is available on both front panel and diagram window while controls are available on front panel and indicator and functions palette are available on diagram window only. The functions and controls are connected to each other based on the datatype. There are debugging tools available in LabVIEW. The VI Analyzer tool help in improving and fault finding the VI's. Diagram window functions include loops, error handlers and other data

structures. Figure 4.2 shows the proposed testbed software designed in LabVIEW for sound speed, ambient noise and sound attenuation.
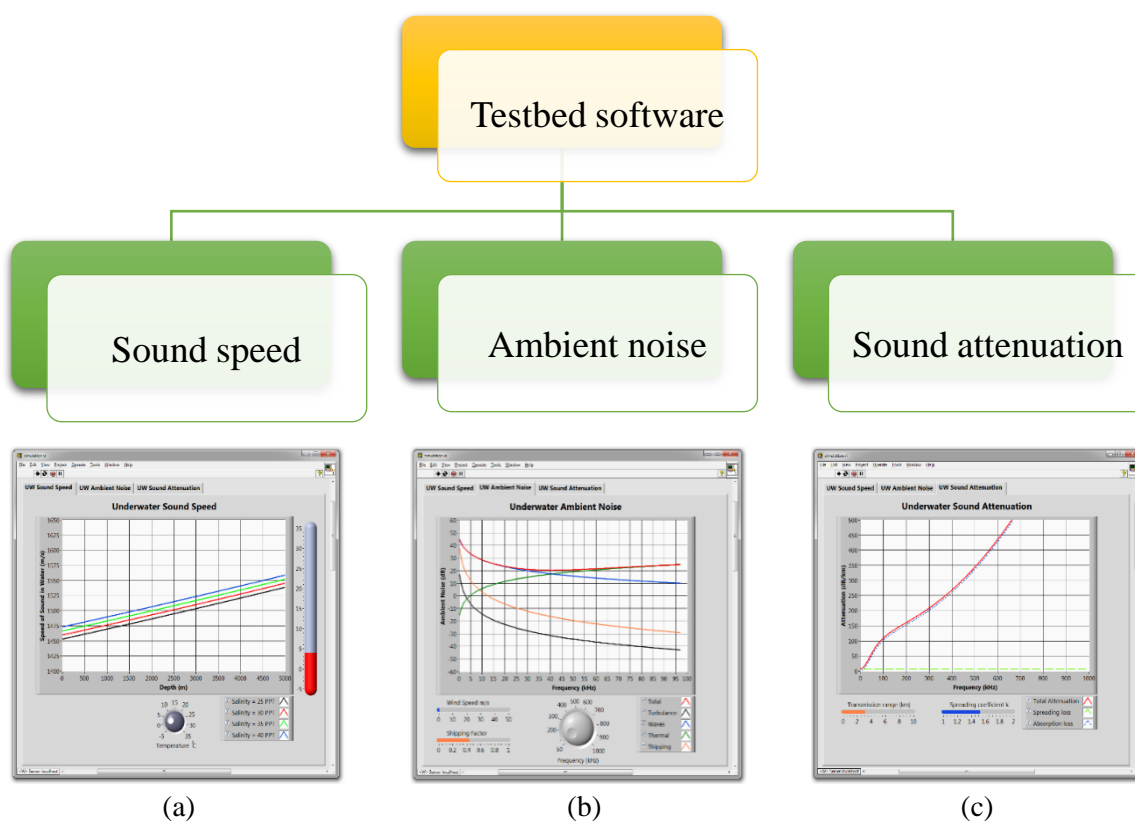

Figure 4.2. Proposed testbed software (a) sound speed (b) ambient noise (c) sound attenuation

4.4. Experimental results and discussion

The proposed underwater communication testing system operate in two modes. First, Section 4.4.1 presents the operation of the testbed as an emulator. Then, Section 4.4.2 describes the simulations of sound propagation, ambient noise and sound attenuation. A web interface is described in Section 4.4.3. Finally, Section 4.4.4 provides a discussion.

4.4.1. Testing system as an emulator

To demonstrate functionality of the proposed testbed as an emulator, we use two low-cost UW acoustic modems [31], as has been shown in Figure 4.1. The transducers, and temperature and salinity sensors are submerged in an aquatic environment. $Modem\ (A)$ collects ecological data using sensors and transmits this data by means of TX transducer in the water channel. $Modem\ (B)$ receives data using RX transducer from the aquatic environment and transfers it to the Personal Computer (PC) working as a LabVIEW server. Finally, the real-time temperature and salinity values are monitored on a GUI.

Figure 4.3 (a) shows the front panel indicators displaying instantaneous temperature and salinity values running on LabVIEW server. This is also called local monitoring. The temperature range on the scale is $-5\ to\ 30\ °C$ while the salinity range is between $20-40\ PPT$. On/off switch is used to start and stop the testing process.

Figure 4.3 (b) shows the front panel indicators displaying instantaneous temperature and salinity values published by LabVIEW web server and monitored by clients in a web browser. The temperature range on the scale is $-5\ to\ 35\ °C$, while the salinity range is between $20-40\ PPT$. A number of clients available on the same network can monitor the temperature and salinity values using the web address.
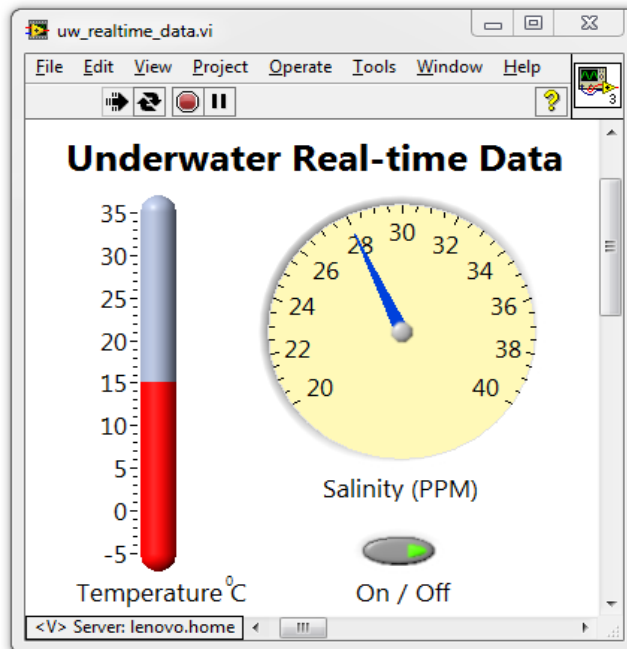
(a)
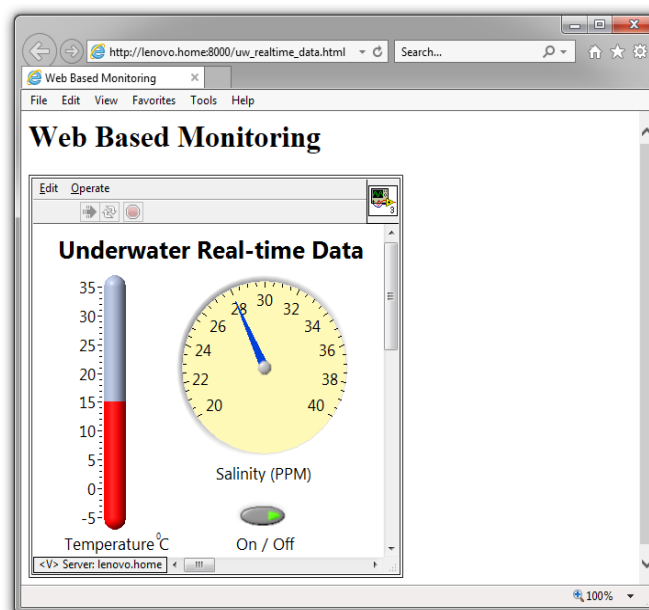
(b)

Figure 4.3. Underwater real-time data (a) local monitoring, (b) web-based monitoring.

Figure 4.4 is the LabVIEW front panel which shows the graphs plotted between temperature $(in\ °C)$ and salinity $(in\ PPT)$ vs time $(in\ minutes)$. The data is collected for a duration of 60 minutes interval. The initial value of temperature is recorded as $5\ °C$ that increases up to $17\ °C$ during $60\ minutes$. The salinity is recorded from $25-29\ PPT$ for the same duration of time.
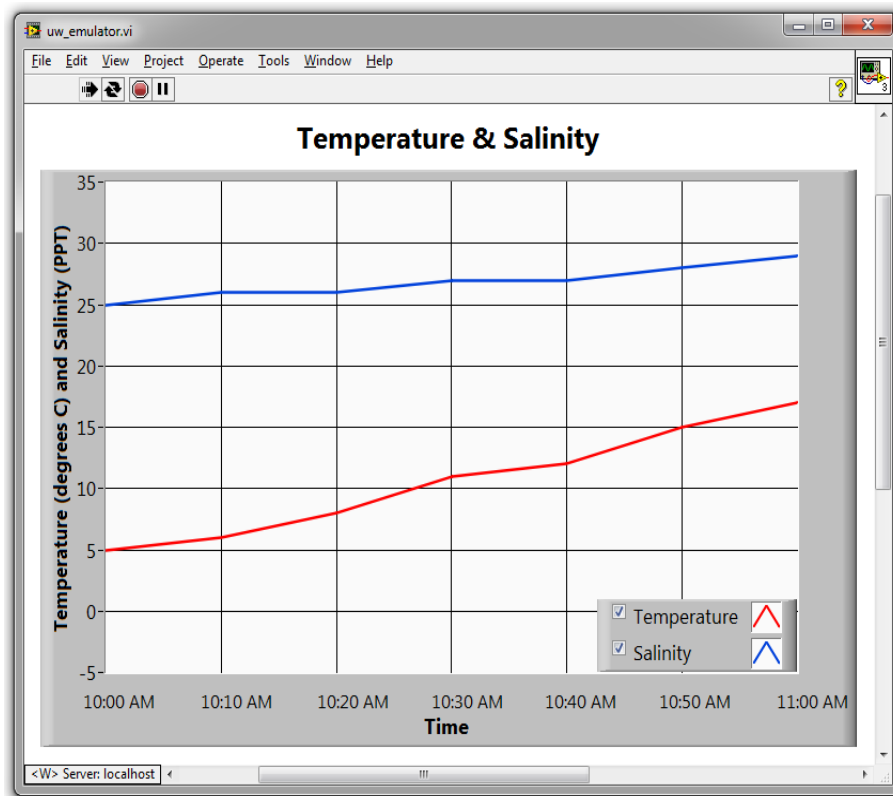
Figure 4.4. Underwater temperature and salinity measurements (Lab VIEW front panel).

4.4.2. Testing system as a simulator

The proposed UW acoustic simulation platform is based on a graphical development environment LabVIEW [94] commonly used by the scientific community. It is flexible, scalable and requires less programming skills as compared to state-of-the-art simulation platforms [62]. Researchers can easily design, implement, simulate, test and evaluate the performance of UW algorithms. System parameters can be configured in run-time to obtain the desired results. The graphical results of simulations can be monitored and controlled locally as well as remotely using web services. The proposed simulation platform has been tested to evaluate the following UW acoustic algorithms.

a) *Sound propagation.* To calculate the underwater sound propagation, several mathematical relationships have been formulated by real-world experiments as well as in controlled laboratory conditions. Mackenzie used following simple nine-term equation to determine the sound speed in UW environments with the typical error of $0.07 \, m/s$ [104, 105].

$$c = 1448.96 + 4.591T - 5.304 \times 10^{-2}T^2 + 2.374 \times 10^{-4}T^3 + \tag{4.1}$$
$$1.340(S - 35) + 1.630 \times 10^{-2}D + 1.675 \times 10^{-7}D^2$$

where c is speed of sound in m/s, T is temperature in degree Celsius from $-2 \leq T \leq 30 \, °C$, S is salinity in parts per thousand (PPT) in the range of $25 \leq S \leq 40$, and D is depth in meters from $1 \leq D \leq 8000 \, m$.

Speed of sound in UW is a function of temperature, salinity and depth. Figure 4.5 shows the relationship between UW speed of sound in m/s and depth in meters. The four graphs are plotted

for salinity values of $25, 30, 35,$ and $40\ PPT$ for a temperature of $4\ ^\circ C$ that can be seen on the thermometer. The temperature value can be adjusted any time before or during the simulation within the range of $-5\ to\ 30\ ^\circ C$ using the control knob available at bottom of the graph. The simulation allows to hide one or more graphs to improve visibility and the user may choose suitable values to get desired results.
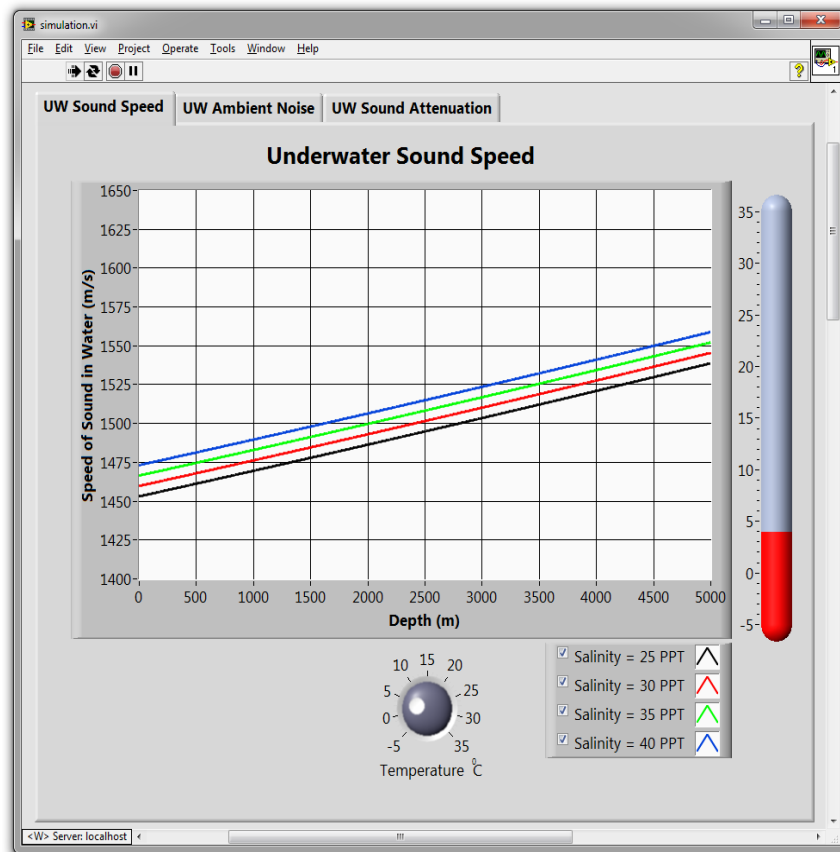

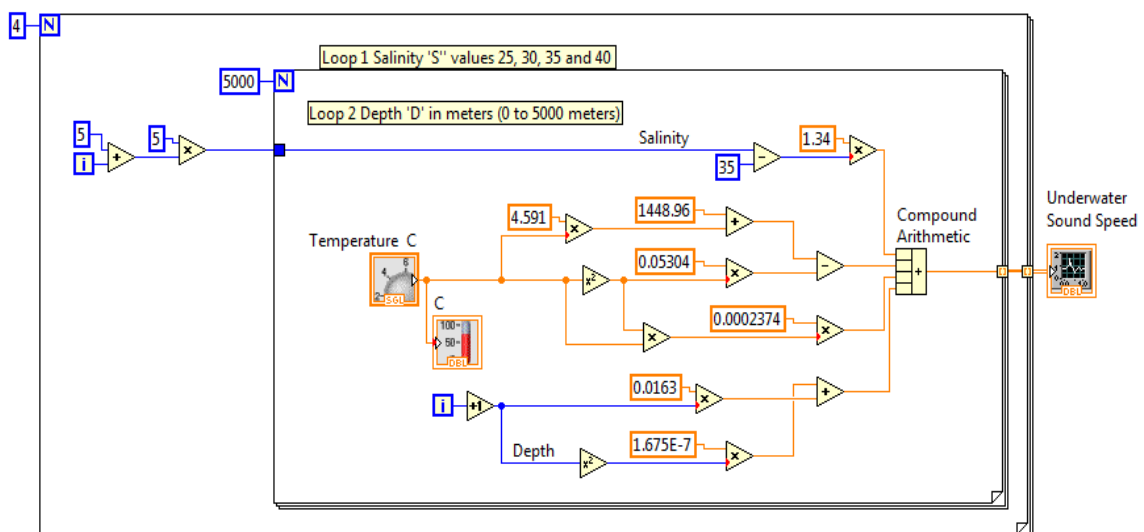Figure 4.5. Underwater sound speed vs depth (LabVIEW front panel).

Figure 4.6. Underwater sound speed vs depth (LabVIEW block diagram).

Figure 4.6 shows the diagram window of LabVIEW VI. This is implementation of the Equation used by Mackenzie [104]. The VI consists of two for loops. The outer loop is executed four times to generate salinity values that are offset by 5 to bring salinity values within the range of $25-40\ PPT$. The inner nested for loop runs 5000 times to generate depth values in meter. Each time the loop executes, the depth value is incremented by $1\ m$. The constant temperature value is used as an input inside the inner loop.

b) **Ambient noise.** Ambient noise is an undesirable sound in aquatic environment that causes interference during acoustic communication. To model the ambient noise in UW environment we use Equations (4.2)–(4.5) in the frequency range from few Hz to several kHz [105, 106].

$$10 \log N_t(f) = 17 - 30 \log f \tag{4.2}$$

$$10 \log N_s(f) = 40 + 20(s - 0.5) + 26 \log f - 60 log(f + 0.03) \tag{4.3}$$

$$10 \log N_w(f) = 50 + 7.5w^{0.5} + 20 log f - 40 \log(f + 0.4) \tag{4.4}$$

$$10 \log N_{th}(f) = -15 + 20 \log f \tag{4.5}$$

$$N(f) = N_t(f) + N_s(f) + N_w(f) + N_{th}(f) \tag{4.6}$$

Where N_t is the noise due to turbulence and is less than $10\ Hz$. N_s represents the noise generated by shipping activity. The range of shipping factor is from $0-1$, i.e., 0 for no shipping, 0.5 as moderate shipping, and 1.0 as high shipping activity from $10-100\ Hz$. Waves play a major role to the noise in the wide region of $100\ Hz-100\ kHz$. Finally, thermal noise is beyond $100\ kHz$. The overall effect is presented in Equation (4.6). The relationship between UW ambient noises in dB vs frequencies in kHz is shown in Figure 4.7. The four graphs show the behavior of turbulence, waves, shipping and thermal noise as a function of frequency. The total ambient noise is obtained by adding all the four types of noise. For simulation, the frequency range can be selected from the control using LabVIEW. The shipping factor can also be set between $0-1$. Similarly, the wind speed can be set in the range of $0 - 50\ m/s$.

Figure 4.8 represents the diagram window designed in LabVIEW. This is basically the implementation of the four noise Equations (4.2)–(4.5) and their combined effect (4.6), mentioned above. The code is inside a *"for loop"* which generates the frequency values selected by the knob. The loop is incremented by $1\ kHz$ within the range of $50-1000\ kHz$. The four noise values are plotted individually as a function of frequency. All the four noise values are also combined to plot the fifth graph which is the ambient noise in dB. The number of times the *"for loop"* is executed is based on the frequency knob setting. While generating the Waves noise the value of the Wind speed is taken into account and similarly shipping factor value is used for shipping noise. The values of frequency, wind speed and shipping factor can be set before or during the simulation.
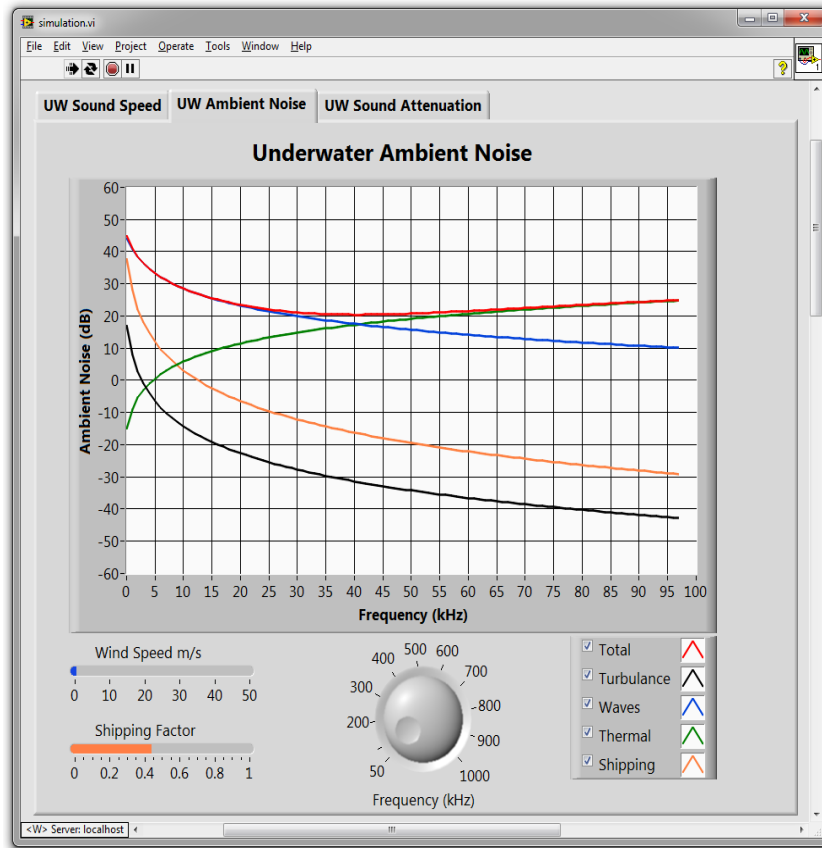
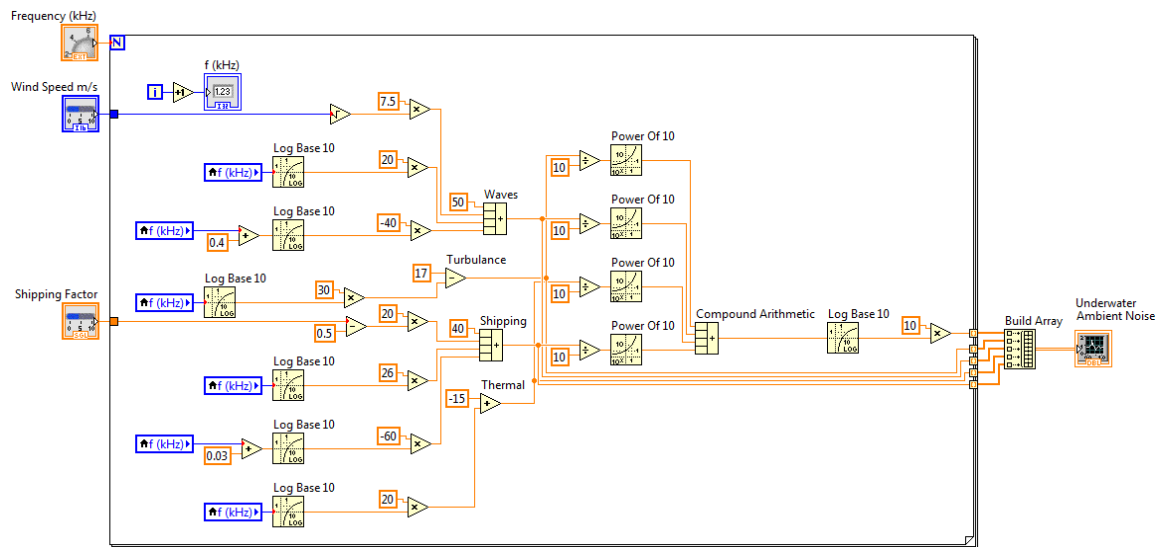Figure 4.7. Underwater ambient noise vs frequency (LabVIEW front panel).

Figure 4.8. Underwater ambient noise vs frequency (LabVIEW block diagram).

c) ***Sound attenuation.*** The attenuation in underwater acoustic channel is a function of distance "l" for a signal of frequency "f" and is given by Equation (4.7). The first term is spreading loss and second term is absorption loss.

$$10 \log A\,(l, f) = k.\,10 \log l + l.\,10 \log a(f) \tag{4.7}$$

Where the spreading factor k depicts the propagation geometry. For spherical spreading, the value of $k = 1$, for cylindrical spreading $k = 2$, while $k = 1.5$ for practical spreading [105, 107]. The absorption coefficient $\alpha(f)$ can be calculated by Thorp's formula given below.

$$10 \log \alpha\,(f) = 0.11 \frac{f^2}{1+f^2} + 44 \frac{f^2}{4100+f} + 2.75 \times 10^{-4} f^2 + 0.003 \tag{4.8}$$

The UW sound attenuation based on spreading loss and absorption loss is illustrated in Figure 4.9 using Equations (4.7) and (4.8). The total attenuation in dB/km is plotted against a frequency range of $0-1000\ kHz$ shown using red color, while the individual losses i.e., spreading loss and absorption loss are shown by green and dotted blue colors respectively. The transmission range can be controlled from $0-10\ km$ while the spreading coefficient k can be adjusted in the range of $1-2$.
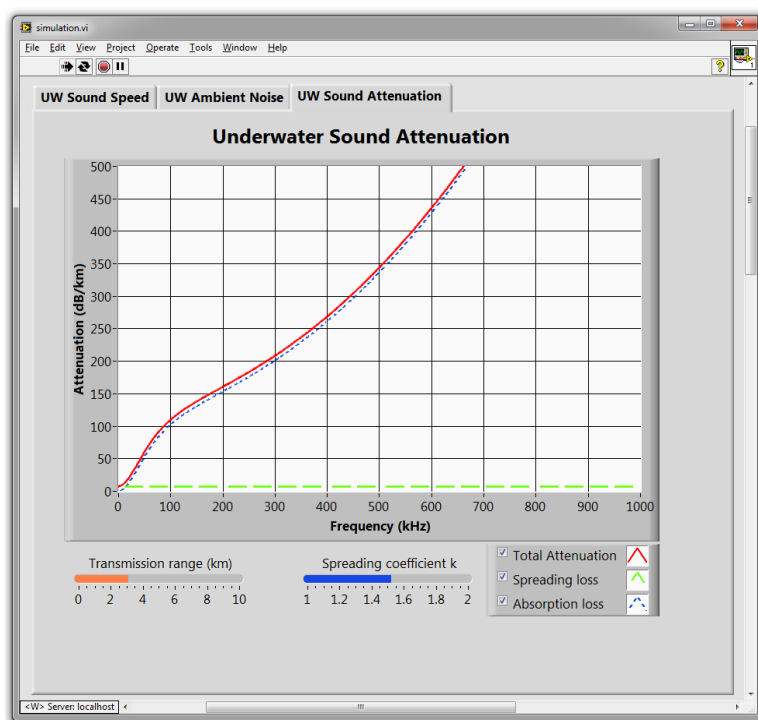
Figure 4.9. Underwater sound attenuation vs frequency (LabVIEW front panel).

The diagram window of UW sound attenuation designed in LabVIEW is shown in Figure 4.10. This is the implementation of Equations 3(a) and 3(b) using for loop running in the frequency range of $0-1000\ kHz$, with the increment of $1\ kHz$. The individual values of spreading loss, absorption loss and their combined effect is calculated inside the loop. The array function outside the loop is used to display all values on the same graph. Transmission range in km and spreading coefficient k in the range of $0-2$ can be adjusted before or during the simulation to get the desired graph.
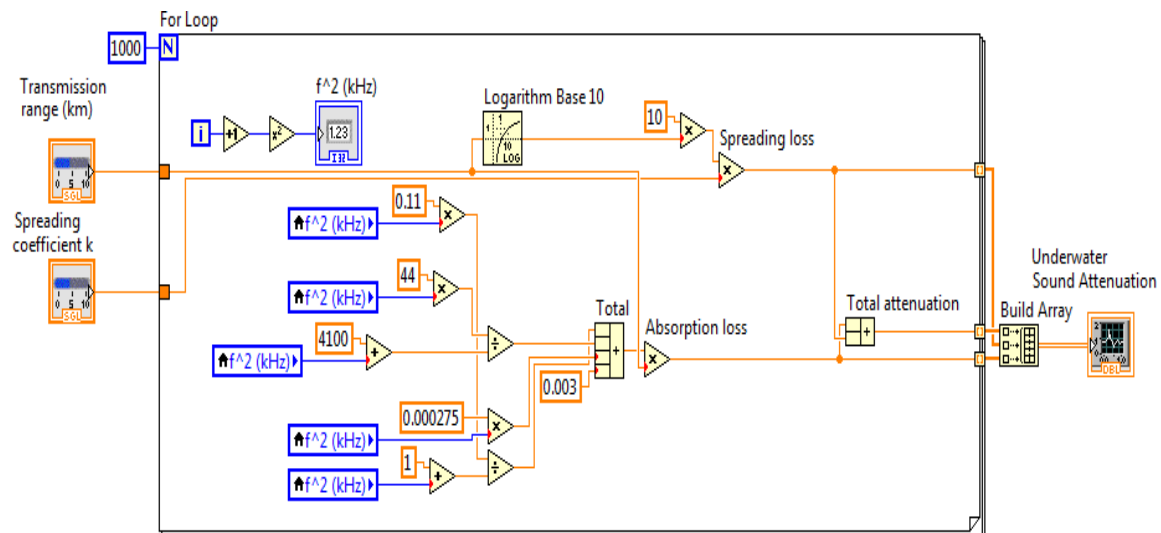
Figure 4.10. Underwater sound attenuation vs frequency (LabVIEW block diagram).

4.4.3. Web interface

LabVIEW is used as the platform to implement web interface. Web publishing tool enables the LabVIEW VI's to be controlled and monitored using a webpage. The remote client can change parameters to generate required results. Multiple clients can monitor the simulation at the same time. If control is required, then a client can request control of the VI to change parameters. To monitor or control data, the client first establishes a connection with the web server through webpage. In monitor mode, the webpage is refreshed automatically when the VI is updated. The LabVIEW web server generates a URL for the VI to control or monitor remotely, an example is given below.

$$http://\{IP\_address\ or\ name\}:\{port\ number\}/\{VI\_name.html\} \qquad (4.9)$$

Remote user can access the VI through webpage by either using the server name or IP address. Depending on the requirement, a secure connection (https) can be established instead of normal (http) protocol. Server name or IP address is followed by a unique port number which is used by LabVIEW web server. Port number can be changed if it is engaged by another application. Different port number can also be used if the port is not available or busy with another application.

a) ***Web based monitoring of underwater sound speed.*** Web based monitoring of UW sound speed Web based monitoring of UW sound speed simulation is shown in Figure 4.11. The four graphs are plotted for salinity values of $25, 30, 35,$ and $40\ PPT$ for the temperature $4\ °C$ to obtain sound speed in m/s vs depth in meters. The temperature value can be adjusted any time before or during the simulation within the range of $-5\ to\ 30\ °C$ using the control knob available at bottom of the graph. The temperature can be varied from LabVIEW server and the response can be observed on clients accessing the VI in their browser using URL:

$$http://\ 192.168.1.7:8000\ /\ simulation.html \qquad (4.10)$$

b) *Web based controlling of ambient noise.* Web based controlling of UW ambient noise simulation in client browser is shown in Figure 4.12. The four graphs show the relationship between turbulence, waves, shipping and thermal noise responses in dB vs frequencies in kHz. The total ambient noise graph combines the effect of each factor and displays on the same graph. A remote client can change the frequency range, wind speed from $0-50\ m/s$ and shipping factor in the range of $0-1$ in real-time to obtain desired results. The parameters can be adjusted by the client and the VI can be observed and controlled by the client in its browser using URL.

$$\text{http://lenovo.home:8000/simulation.html} \qquad (4.11)$$

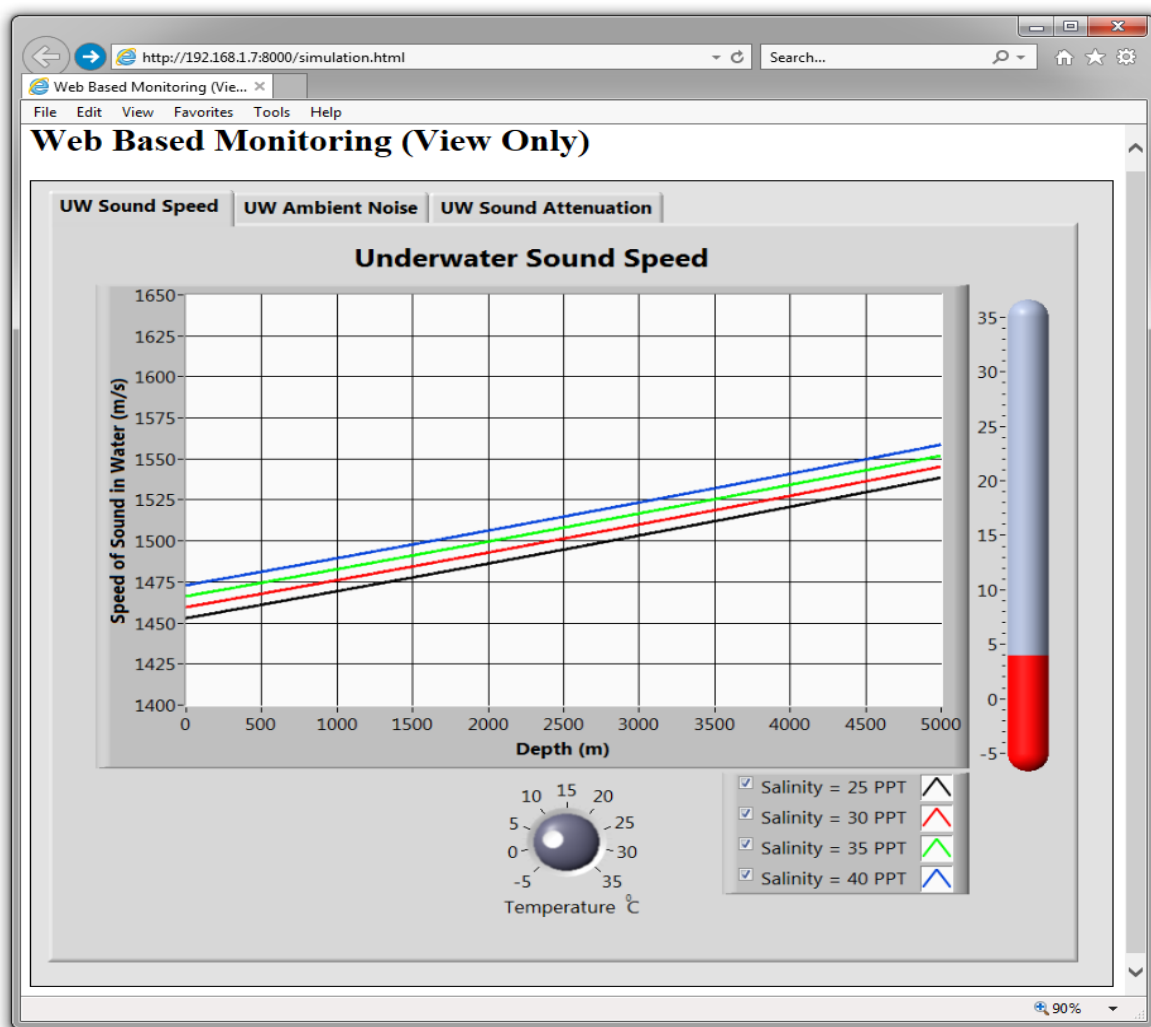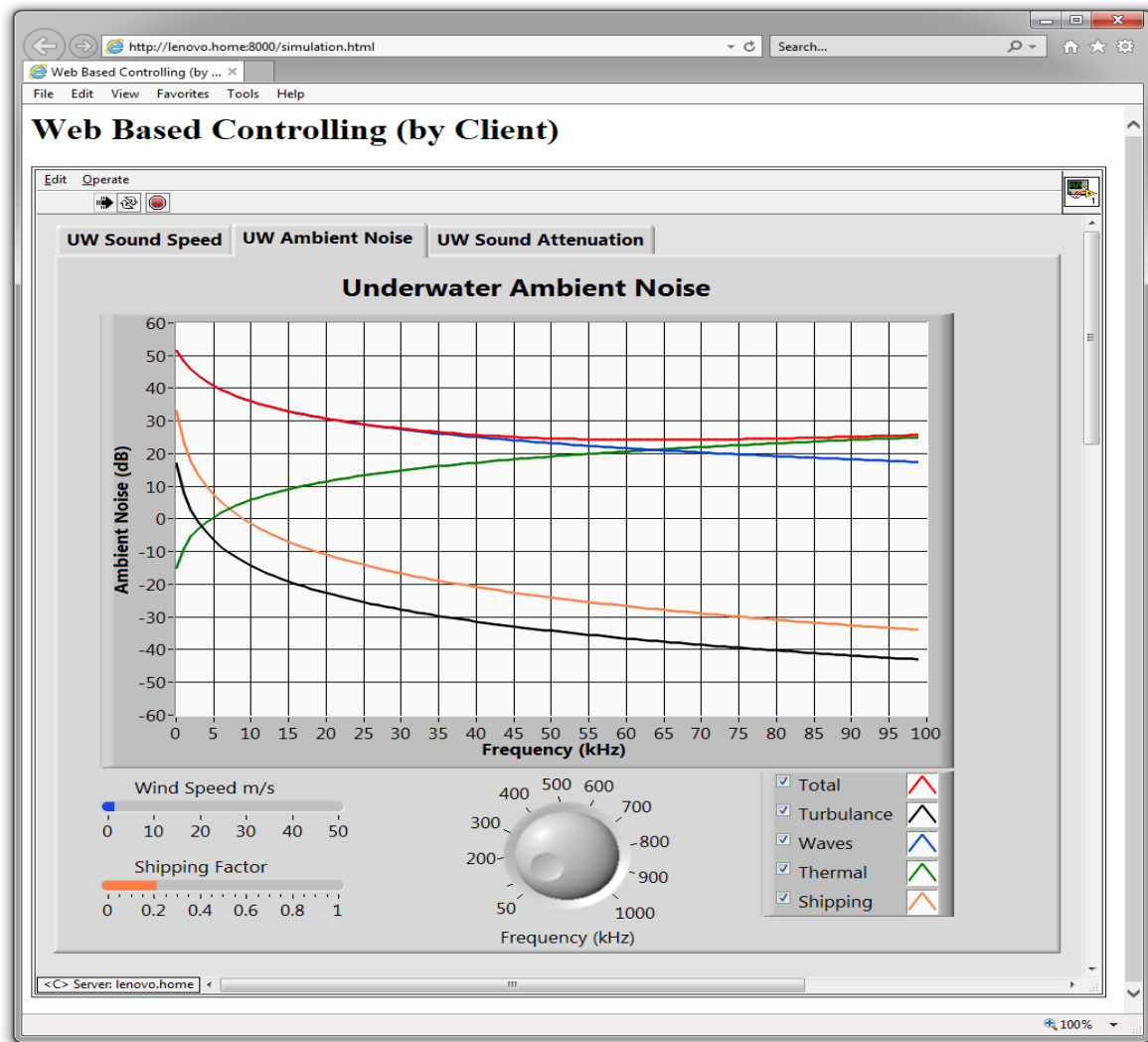Figure 4.11. Underwater sound speed vs depth (web based monitoring)

Figure 4.12. Underwater sound speed vs depth (web based controlling)

4.4.4. Discussion

A qualitative comparison of proposed design and state-of-the-art UW communication testbeds is presented in Table 4.1. From the scalability point of view, the testbeds are divided into three groups and arranged according to the testing environment and scalability. The first group includes two large-scale testbeds, i.e., SUNRISE project [73] and SUNSET framework [74]. Both are deployed and evaluated in a real aquatic environment, however, they can also be used in laboratory testing and have simulation facilities. The second medium-scale group comprises of three UW communication testbeds i.e., cross-media network [98], ecological monitoring [100] and UW communication and networking [102]. These are also tested in real aquatic environment i.e., a Lake and a harbor, but as compared to the above two they have limited features. The third group of four testbeds DESERT [75], UW-ASN [76], Aqua-Lab [103], and WaterCom [101] are listed along with the proposed testbed, classified as small-scale. Details of the testing environment i.e., real-aquatic environment or laboratory testing and simulation facilities of each group are described below. The Table 4.1 provides information related to commercial and research UW modems used as part of these testbeds. Finally, the remote accessibility feature of the testbeds for monitoring and controlling is compared.

Table 4.1: Comparison of UW communication testbeds

Ref.	Testbed name	Testing environment	Modems used/tested	Simulation facility	Remote accessibility
[73]	SUNRISE	In field & laboratory	Evologics, Micro-modem	Yes	Monitoring & controlling
[74]	SUNSET	In field & laboratory	Micro-modem, Evologics, Kongsberg, Teledyne Benthos	Yes	Monitoring & controlling
[98]	Cross-media networking	Lake	DSSS modem	N/A	N/A
[100]	Ecological monitoring	Lake	OFDM modem	N/A	Monitoring
[102]	UW Comm. & Networking	Harbor	Evologics, Micro-modem	Yes	Monitoring & controlling
[75]	DESERT	Laboratory	Evologics, Micro-modem	Yes	N/A
[76]	UW-ASN	Laboratory	UW modem based on ARM9 Processor	N/A	N/A
[103]	Aqua-Lab	Laboratory	Micro-modem	N/A	Monitoring
[101]	WaterCom	Laboratory	AquaSeNT OFDM modem	N/A	Monitoring & controlling
This work	Proposed testbed	Laboratory	Low-cost UW acoustic modem	Yes	Monitoring & controlling

The first group consists of two testbeds, SUNRISE project [73] and SUNSET framework [74] used in large-scale scenarios. Both testbeds are deployed in a real-aquatic environment to collect ecological data, and testing of UW networking protocols such as MAC, routing, and cross-layer protocols. The testbed hardware supports commercial modems e.g., Evologics using S2C modulation, and research modem such as Micro-modem with FSK and PSK modulations for UW acoustic communication. The SUNSET framework also supports other commercial modems e.g., Kongsberg and Teledyne Benthos. Laboratory testing in a controlled environment i.e., emulation and simulation of UW acoustic channel model and other empirical formulae are the common features of SUNRISE project, SUNSET framework, and the proposed testbed. The performance of the proposed testbed has been successfully evaluated during environmental data collection e.g., temperature and salinity as an emulator in a laboratory environment using two low-cost UW acoustic modems [31].

We used inexpensive modems that we designed ourselves, but other types of modems can also be interfaced with the proposed testbed via standard communication ports. SUNRISE project [73] and SUNSET framework [74] provide a number of features and consists of AUVs, ASVs, ROVs, Buoys, sensor, commercial and research modems and coastal control station, almost a complete solution, available at huge cost. In contrast, our proposed solution which is a subset of above-mentioned facilities is an inexpensive and reliable tool for the research community. Our design is based on LabVIEW which can be used to test UWSNs components, communication systems and UW acoustic modems in a laboratory environment. However, it can be used in a real environment with suitable modifications. Simulation of UW empirical formulae and remote accessibility for monitoring and controlling are common features of above-mentioned testbeds and our proposed design.

The second medium-scale group has three testbeds. i.e., cross-media network [98], ecological monitoring [100] and UW communication and networking [102]. The UW acoustic network testbed [98] is used to evaluate cross-media networking and to examine UW networking protocols ALOHA and MACA using DSSS UW acoustic modem. The testbed in [100] collects ecological data such as

temperature, salinity, and electrical conductivity using sensors. An OFDM acoustic modem is used for UW communication. Remote access feature is used to present online results. The UW communication and networking testbed [102] is used to evaluate the hardware and software of UW communication systems in conditions similar to a real aquatic environment. Evologics modem using S2C modulation and an FSK version of Micro-modem are used in the testbed for UW communication. It has a simulation facility and can be accessed remotely for monitoring and controlling from the collaborating institutions. Performance of the first two testbeds has been evaluated in a Lake, while the third one has been tested in a harbor.

Compared with these testbeds, performance of the proposed testbed has been examined by obtaining UW ecological parameters i.e., temperature and salinity using two low-cost UW acoustic modems [31] in a controlled laboratory environment. The aforesaid testbeds have been used in field testing and no details are available in the research work to use them in a controlled laboratory environment. The proposed testbed has an additional feature of simulation of UW algorithms and empirical formulae which is not available in these medium scale testbeds excluding the UW communication and networking [102]. Another extra feature of our design is its remote accessibility that enables several clients to monitor, and selected clients to control the emulation and simulation in real-time. Only the UW communication and networking testbed has similar features [102]. However, the testbed used for ecological monitoring [100] offers clients to monitor the work and in cross-media network [98] remote accessibility is unavailable.

Finally, the third group of four UW testbeds DESERT [75], UW-ASN [76], Aqua-Lab [103] and WaterCom [101] are classified as small-scale scenarios. The common feature in all designs is the testing procedure using a small water tank inside a laboratory. Among the four testbeds, DESERT [75] uses Evologics and Micro-modem for UW communication, while our testbed uses low-cost UW acoustic modem [31] to obtain the UW ecological data. Another common feature of DESERT and the proposed testbed is simulation of UW algorithms. However, the additional feature of remote accessibility during monitoring and controlling as an emulator and a simulator makes our design superior to DESERT. Another design UW-ASN [76] uses ARM9 processor-based sensor nodes to deploy UWSN testbed in a water tank along with temperature and salinity sensors. Our testbed setup and testing procedures are similar to UW-ASN except for the number of nodes, which are more in UW-ASN, while we use two low-cost UW acoustic modems [31].

Our design is superior due to two features namely, simulation and remote accessibility. None of these is present in UW-ASN architecture. In the end, Aqua-Lab [103] uses Micro-modem and WaterCom [101] uses AquaSeNT OFDM modem for UW communication. Similar to our case, the performance of both testbeds has been evaluated in a laboratory environment using a water tank. WaterCom is designed to operate at different levels, but preliminary results are provided using a small-scale configuration. Again our proposed UW acoustic communication testbed offers an edge over the two designs due to the simulation facility which is not available in these testbeds. WaterCom offers the remote accessibility similar to our design for both monitoring and controlling but this is restricted in case of Aqua-Lab in which only monitoring is allowed, and no control is available. In addition, development of software-defined networking (SDN) based experimental testbed [107] and simulation software [108] are at their preliminary stages for evaluating the performance of UWSN.

4.5. Conclusion

A web-based underwater acoustic communication testbed is designed and implemented at small-scale with simulation and emulation features and remote connectivity. As compared to state-of-the-art UW acoustic communication testbeds that are usually implemented using high level programming languages, the proposed testbed uses GUI designed in LabVIEW. The main features include: less development time, low-cost and remote monitoring facility. The proposed UW communication testbed is not only economical but requires low setup and learning time for test setup. The remote monitoring and controlling facility using a web browser is an additional characteristic of the testbed to access the facility without physical access.

The testbed has been used to evaluate the functionality of two low-cost modems (equipped with temperature and salinity sensors) however other types of modems can be tested using the same facility in a controlled laboratory setup in an aquatic environment. The remote users can monitor and evaluate the performance of the low-cost UW acoustic modems in real-time using the LabVIEW server based testbed. The simulator is designed in LabVIEW requires low learning and setup time and has been used to simulate UW sound propagation model, ambient noise, and sound attenuation. The same technique can be used to analyze various types of UW communication systems and algorithms. The real-time data and results can be published locally as well as remotely using a web browser. The simulation parameters can also be adjusted both locally as well as remotely by authorized users for a given period of time. While the simulation platform is useful in evaluating the overall system performance along with its limitations, the emulation alternative provides a real hardware-software test facility in a controlled laboratory environment.

The motivation behind the research is to present a cost-effective emulator and simulator that can be used to investigate the functionality of underwater wireless sensor networks and its components including underwater modems, sensors and various modulation schemes in a controlled laboratory environment. The proposed system also simulates underwater acoustic channel and propagation and mathematical models, protocols. Remote accessibility using a web-browser is the novelty of design. In addition to the cost, the energy consumption also plays an important role in UW communication systems as they are battery operated. Next chapter addresses the issue of energy consumption.

Chapter 5: Integration of a Digital Modulator and a Class-D Amplifier[*]

A low-cost modem prototype for short-range underwater acoustic communications is presented in Chapter 3. The modem is designed using a modular approach that can be modified to be used in different kinds of applications. A web-based testbed is proposed in Chapter 4 to evaluate the performance of underwater wireless sensor networks and their components in a controlled environment in addition to simulating the underwater channel and sound propagation models. The motivation behind the research is to provide a cost-effective solution in the domain of underwater communications.

While a low-cost design and verification was the main objective in previous two chapters, this chapter is targeting the energy efficiency. It presents an integration of a digital modulator and a class-D amplifier to improve the energy efficiency of the system. The proposed integrated system provides amplification as well as phase shift keying modulated signal in real-time. The simulation has been done using MATLAB and a model designed and tested in Simulink. Finally, a prototype circuit is built and tested using Multisim. Experimental results show that the proposed system is an energy-efficient and cost-effective solution compared to the existing designs.

This chapter is organized as follows: Section 5.1 provides the introduction to the integration of a digital modulator and a class-D amplifier. Section 5.2 discusses necessary background to understand the contents of the subsequent sections. Section 5.3 describes the related work. Section 5.4 presents the proposed system architecture. Section 5.5 presents the experimental setup, results and discussion. Section 5.6 concludes the chapter.

5.1. Introduction

Energy consumption is always a key feature in devices powered by electric accumulators. With the increasing demand for mobility, more devices incorporating digital wireless communication systems are being operated by electric accumulators (batteries), e.g., human surveillance to crops monitoring, and aerial drones to autonomous underwater vehicles (AUVs). Preserving an accumulator's energy is of paramount importance in difficult-to-access areas, which is also the case in underwater communication systems.

Power amplifier is the most energy-demanding module in mobile devices, portable appliances, static transceivers, and even nodes used in UW acoustic networks. These devices incorporate a modulator, typically a pulse-width modulation (PWM) and a class-D power amplifier, for higher efficiency [109]. Designers have conceived different technologies for power amplification, which are denominated into classes and denoted by capital letters: Class $A, B, AB,$ and D. Class-D amplifiers are the most efficient in terms of power, with values on the order of 90% in practical designs [109], and are preferred in applications where autonomy is essential.

A traditional class-D amplifier consists of an analog modulator of a digital carrier followed by a switch circuit that drives the current from a DC power supply. This current passes to the load through a filter that retrieves the baseband signal. Due to their complexity, class-D amplifiers are not appropriate for small signals, but in power applications, they are the best choice because of their low losses. Obviously, the power delivered to the load is sensitive to the voltage of the DC source, and the switch must be able to drive high current. In many of their applications, class-D amplifiers are used at high fidelity ($hi-fi, 20\,Hz-20\,kHz$) frequencies and the retrieving filter is a low-pass filter (LPF). If the amplifier is intended to be at the output stage of an ultrasonic communication system, a band-pass filter (BPF) is incorporated.

Usually, a PW-modulator is available at the input stage of a class-D amplifier. The frequency of the digital carrier of the PW-modulator must be greater than the highest frequency of the analog input signal, typically ten times. However, again, if the amplifier is part of a digital communication system, the analog input signal to the amplifier will be the output signal of a digital modulator that could be a phase-shift keying (PSK) or a frequency-shift keying (FSK) modulator. That is, the digital signal at the input of the communication transmitter will modulate an analog carrier, modulate again a digital carrier at a much higher frequency, and finally be restored to the digital modulated signal.

We propose a technique to integrate the modulator of a transmitter and PW-modulator of a class-D amplifier to improve the overall efficiency of the system. This integrated set operates as an up-converter, phase modulator (PM), and binary phase-shift keying (BPSK) modulator under certain conditions. In our proposed design, integration of a PW-modulator of a class-D amplifier and BPF provides (i) signal amplification, (ii) filtering and (iii) generation of a PSK-modulated output. The digital signal applied at the input of the class-D amplifier directly drives the power switch. This novelty in the design prevents the need of modulation before amplification, which makes the proposed design energy efficient as well as inexpensive. Finally, a BPF is used instead of a LPF at the output of the class-D amplifier to obtain an amplified PSK-modulated signal. This complex modulation is performed on a real-time basis using the ability of the class-D amplifier to provide high-efficiency in order to prolong battery life [110].

The theoretical concept is verified using MATLAB and a model is designed and simulated in Simulink. For validation purposes, an electronic circuit is built and tested using Multisim. The results obtained by simulations and circuit implementation show that the proposed integrated system is an energy-efficient and cost-effective solution compared to conventional techniques.

5.2. Background

PW−modulations can be classified according to several criteria. The first is pulse values, which can be symmetric or asymmetric. The former means $V_L = 0\ V$ and the later means $V_L = -V_H$, where V_L and V_H are, respectively, the low and high levels of the output voltage. The symmetric case is slightly more complex to generate from the circuit point of view, and its frequency spectrum has a much lower DC component and larger fundamental and harmonic components. However, other than that, it has little influence on the frequency spectrum of the modulated signal.

A second criterion is related to the fact that the input is a continuous signal but the output signal is a train of pulses, which means that the input signal has been somehow sampled at certain instants. The way sampling is performed also has an impact on the frequency spectrum. There are two options, the so-called uniform sampling, when it is synchronous with the system clock, or the natural sampling, which happens when simple circuits are used to modulate the pulses, i.e., when sampling is achieved by a simple comparator circuit and is not synchronous with the system clock. The basic block diagram of a PW-modulator is shown in Figure 5.1 [111]. Of course, the average sampling frequency over a long period of time is the frequency of the system clock.
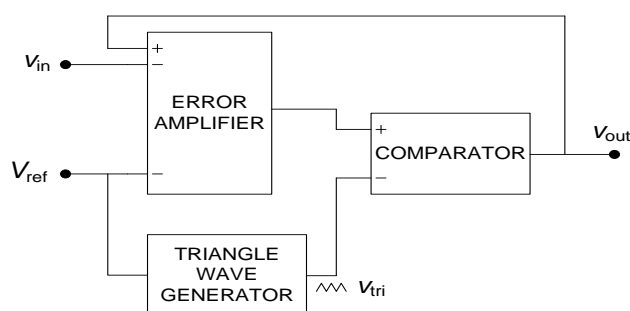

Figure 5.1 Basic block diagram of a PW-Modulator.

The third criterion is related to how the sample modulates the output pulses. The samples can determine the positions of either the leading edges, the trailing edges, or both. In the double-edge case, the position of both edges can be symmetrically determined by a single sample or each of them can be determined by two consecutive samples.

Song and Sarwate determined the frequency spectra of different possible PW-modulations [112]. A brief summary of their work is presented here, for the sake of completeness. Let us assume the following conditions: (i) Symmetric pulse amplitudes are -1 and $1\ V$. (ii) The input signal $x(t)$ is frequency-limited, the module of its maximum amplitude is $1\ V$, and it has no DC component. (iii) The modulation index is 100% and the duty cycle is 50%. (iv) The pulse repetition frequency f_c (better than sampling frequency in natural sampling) is at least π times the maximum frequency of the input signal. Under these conditions, the Fourier expansions of the natural sampling of the PW-modulated signals are [112]:

$$p_{\text{TE}}(t) = x(t) + \sum_{k=1}^{\infty} \frac{2}{k\pi} \left[\sin(2\pi k f_c t) - (-1)^k \sin(2\pi k f_c t - k\pi x(t)) \right] \qquad (5.1)$$

$$p_{\text{LE}}(t) = x(t) + \sum_{k=1}^{\infty} \frac{2}{k\pi} \left[(-1)^k \sin(2\pi k f_c t + k\pi x(t)) - \sin(2\pi k f_c t) \right] \qquad (5.2)$$

$$p_{\text{DE}}(t) = x(t) + \sum_{k=1}^{\infty} \frac{2(-1)^k}{k\pi} \left[\sin\left(2\pi k f_c t + k\pi \frac{x(t)+1}{2} \right) - \sin\left(2\pi k f_c t - k\pi \frac{x(t)+1}{2} \right) \right] \qquad (5.3)$$

where the subscripts, TE, LE and DE stand, respectively, for trailing-edge, leading-edge and double-edge (asymmetric version). If the trigonometric identities.

$$\sin\alpha \pm \sin\beta = 2\sin\frac{1}{2}(\alpha \pm \beta)\cos\frac{1}{2}(\alpha \mp \beta) \qquad (5.4)$$

$$\sin(\alpha + \beta) = \sin\alpha\cos\beta + \cos\alpha\sin\beta \qquad (5.5)$$

are used, every term in the summations of (1)-(3) becomes

TE, k odd: $\qquad \frac{4}{k\pi} \cos\left(\frac{k\pi x(t)}{2}\right) \cos\left(2\pi f_c kt - \frac{k\pi x(t)}{2} + \frac{\pi}{2}\right) \qquad (5.6)$

TE, k even: $\qquad \frac{4}{k\pi} \sin\left(\frac{k\pi x(t)}{2}\right) \cos\left(2\pi f_c kt - \frac{k\pi x(t)}{2}\right) \qquad (5.7)$

LE, k odd: $\qquad \frac{4}{k\pi} \cos\left(\frac{k\pi x(t)}{2}\right) \cos\left(2\pi f_c kt + \frac{k\pi x(t)}{2} - \frac{\pi}{2}\right) \qquad (5.8)$

LE, k even: $\qquad \frac{4}{k\pi} \sin\left(\frac{k\pi x(t)}{2}\right) \cos\left(2\pi f_c kt + \frac{k\pi x(t)}{2}\right) \qquad (5.9)$

DE, k odd: $\qquad \frac{-4}{k\pi} \sin\left(\frac{k\pi}{2}\right) \cos\left(\frac{k\pi x(t)}{2}\right) \cos(2\pi f_c kt) \qquad (5.10)$

DE, k even: $\qquad \frac{4}{k\pi} \cos\left(\frac{k\pi}{2}\right) \sin\left(\frac{k\pi x(t)}{2}\right) \cos(2\pi f_c kt) \qquad (5.11)$

When the six terms in (6)–(11) are observed, it is clear that all three PWM versions will include the frequency spectrum of $x(t)$ in their base band, and, as a consequence, all of them can be used in class-D amplifiers. However, we want to now bring attention to the harmonic contents. Double-edge-modulated signals have harmonic components that are amplitude-modulated by $x(t)$, while single-edge modulations have harmonic components modulated both in amplitude and phase. This remark leads to the idea of using a harmonic component to generate a simple modulation of $x(t)$.

5.3. Related work

In the past few years, several class-D amplifier designs and modulation schemes have been presented, and some of them are briefly discussed in the following paragraphs of this section.

The class-D amplifier [113] is based on a digital pulse-width modulator. It receives digital input data and uses a digital loop filter to reduce distortion and mitigate the need of an analog-to-digital converter (ADC). The system is designed for low output power up to $1.2\ W$, and to keep away from the necessities of additional filtering, a sigma-delta modulator is used. The proposed system is designed using complementary metal–oxide–semiconductor (CMOS) technology and has been tested to drive a load of an $8\ \Omega$ speaker with a signal-to-noise ratio (SNR) of $99.9\ dB$ with 91% efficiency.

A class-D amplifier based on the delta-sigma modulator with uniform pulse-width modulation is presented in [114]. The major design blocks are an interpolation filter, digital delta-sigma modulator, uniform pulse-width modulator, driver circuitry, and power stage. A $1-bit$, sixth order noise shaping modulator with a uniform pulse-width modulator quantizer is used along with the pole moving technique to balance the modulator and make the noise transfer function more determined. The system has been simulated with a $1\ kHz$ sine wave, and a $120\ dB$ SNR has been achieved.

In [115], a high-power pulse-width modulation model based on the class-D amplifier is discussed. To eliminate the effect of third and fifth harmonics, the proposed triple-pulse model is designed by adding two narrow pulses with an equivalent comparative to the original single pulse. Initially, the model is verified by simulations, and then a platform is designed with underwater acoustic transducers submerged in a water tank to test the functionality of the system. From the experiments, it was found that the proposed amplifier consumes low power, which reduces 41% of the third and fifth harmonic energy [115].

A class-D amplifier using pulse-width modulation is designed in [116]. The system consists of modulation, power and filter stages. In this research, two modulation techniques: (i) Pulse-width modulation and (ii) pulse density modulation, are used. The system has been verified by PSpice simulations to test the total harmonic distortion using both modulation techniques with a $1\ kHz$ test tone and switching frequency in the range of $300 - 800\ kHz$. From the simulations, it is found that the total harmonic distortion of the pulse density modulation is less at higher frequencies.

A low-voltage class-D amplifier design is presented in [117]. The objective of the research is to propose a class-D amplifier for audio applications with minimum distortion. The analysis is performed using a pulse density modulation (PDM) technique for different test tone frequency ranges from $0.7 - 5\ kHz$ with three amplitudes $(0.5, 0.8, and\ 1.0)\ V$, using the carrier frequency range of $500 - 2000\ kHz$. From the results, it is found that the total harmonic distortion is a function of both amplitude and frequency of the test tone. For the highest switching frequency, i.e., $2000\ kHz$, and at the smallest amplitude of the input signal, the lowest value of total harmonic distortion is achieved at less than 1%.

5.4. Proposed system architecture

The robust modulation schemes used in underwater communication (e.g., FSK and PSK), suitable to be used in our proposed design are discussed in Section 5.4.1. Subsequently, the block diagram of a half-bridge class-D amplifier, the PSK modulator that drives a class-D power amplifier, architecture of coder and PW-modulator and integrated PSK modulator/amplifier are described in Section 5.4.2.

5.4.1. Preferred modulation scheme

Angular modulation schemes such as FSK and PSK are more robust than linear techniques such as ASK or OOK [118] while maintaining simplicity. Quadrature amplitude modulation (QAM) modulation has an increased spectral efficiency, but transceivers are more complicated and more power needs to be transmitted to achieve a similar bit-error rate [119]. Among its resources, the software-defined radio (SDR) includes direct digital synthesis (DDS), which provides sinusoidal signals with arbitrary frequency or phase [120-122]. This makes PSK a good choice for wireless links where power is a limited resource. A switching-circuit phase modulator is shown in Figure 5.2 [118]. Actually, the signal

at the output of the comparator block of figure is the rising edge PWM of v_{in}, with a carrier frequency of $2f_c$. The flip-flop circuit divides the number of pulses between the two.
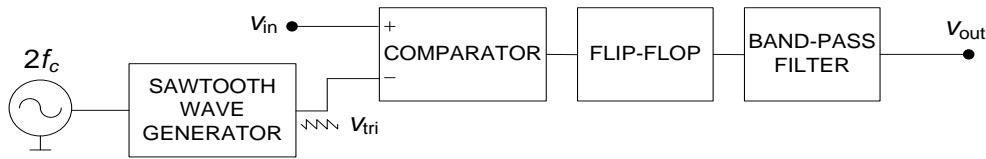

Figure 5.2. Switching-circuit phase modulator.

5.4.2. Integrated system

The block diagram of the class-D amplifier is shown in Figure 5.3. The first block in the diagram is a PW-modulator. The switching block consists of two metal-oxide semiconductor field-effect transistor (MOSFET) and the corresponding gate drivers. If the three diagrams in Figures (5.1–5.3) are compared, we realize that if the low-pass filter is replaced by a band-pass filter, the high-power output signal will be the carrier modulated in phase by v_{in}. To improve power efficiency of the wireless communication system, a question arises: As the class-D amplifier already contains a modulator, is it possible to directly drive the PW-modulator with a signal that, when band-pass filtered, becomes the PSK modulation of the digital input? The idea is shown schematically in Figure 5.4 [123]. Obviously, the coder blocks in the upper and lower parts of Figure 5.4 will have to be different.
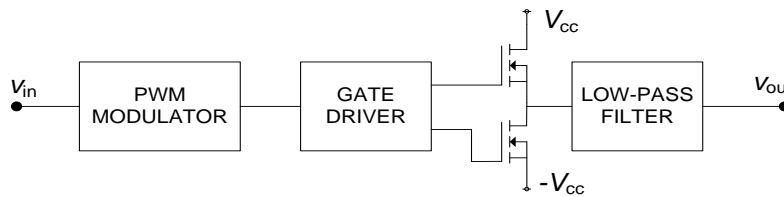

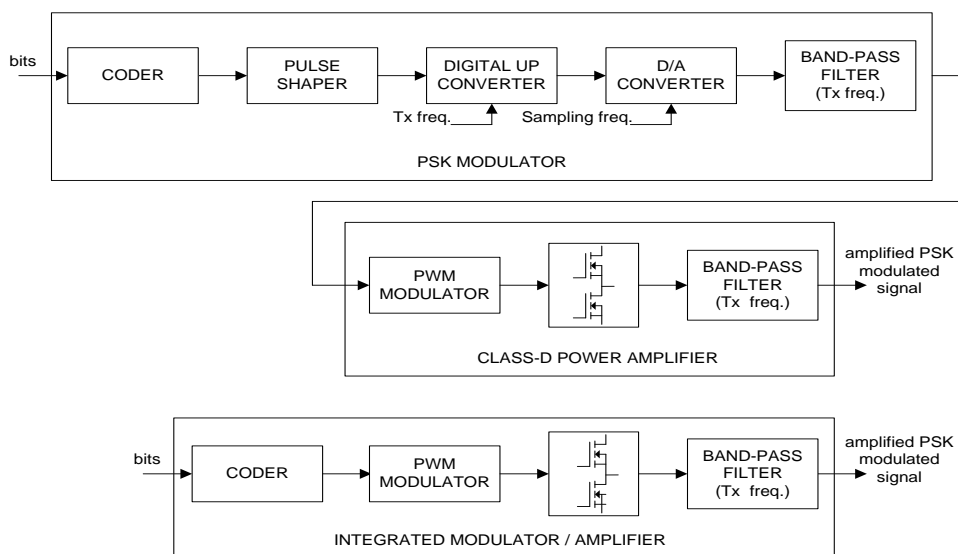Figure 5.3. Block diagram of a half-bridge class-D power amplifier.

Figure 5.4. Block diagram of a PSK modulator that drives a class-D power amplifier.

The coder and the PW-modulator blocks of the lower part of Figure 5.4 have already been developed [124]. They can be implemented either with a microcontroller or a DSP unit with the architecture of Figure 5.5. The frequency of the clock input is N-times larger than the sampling frequency. Additionally in [125], it has been used to directly feed the switching circuit of the class-D power amplifier in audio applications. The question now is how to obtain the FSK-modulated signal. At this point, we realize that by using a rectangular carrier, we can easily obtain a PSK output instead of an FSK.
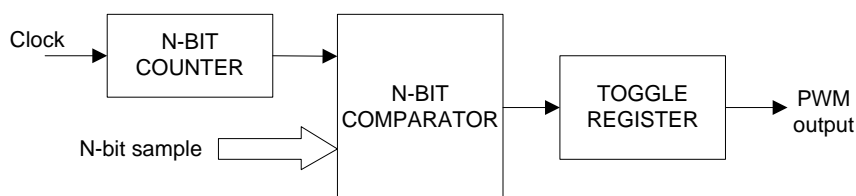
Figure 5.5. Architecture of coder and PW-Modulator blocks.

The proposed integrated PSK modulator is sketched in Figure 5.6. The input data bits are converted to a bipolar voltage signal that eventually multiplies a square bipolar carrier, changing its phase according to the input bit. The square signal then drives the power bridge of the class-D amplifier, whose output goes through a band-pass filter centered at the frequency of the bipolar carrier, to obtain a PSK-modulated signal.
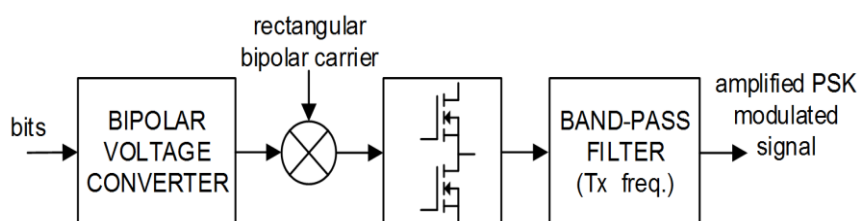
Figure 5.6. Integrated PSK modulator/amplifier (functional diagram).

5.5. Experimental setup and results

The simulation results of the proposed design using MATLAB and Simulink model are presented in Section 5.5.1. An electronic circuit is built and tested in Multisim to validate the results and presented in Section 5.5.2. A qualitative comparison with the related work along with the discussion is provided in Section 5.5.3.

5.5.1. Simulations

The PSK modulator using the PWM and a band-pass filter, as shown in the lower part of Figure 5.4, has been simulated with the help of MATLAB. The coder simply converts bits into a symmetrical normalized voltage signal $(\pm 1\,V)$. The output band-pass filter is tuned to the carrier frequency of the PW-modulator. Figure 5.7 shows the input signal, the carrier, and the modulated PSK signal at the filter output. Figure 5.8 shows the power spectrum at the input of the band-pass filter.
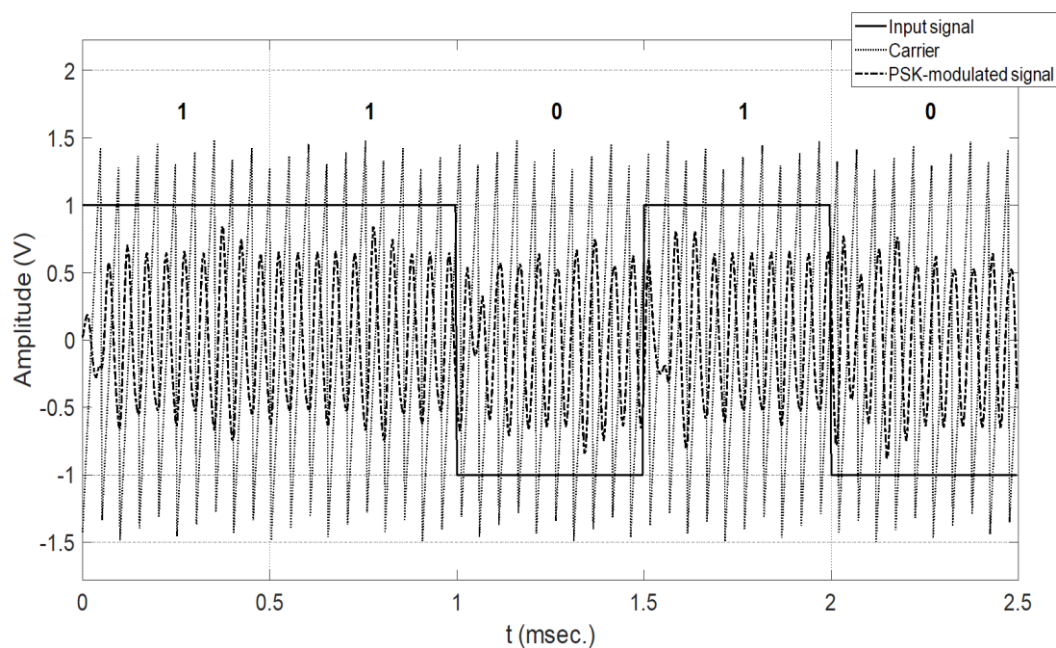
Figure 5.7. Input signal, carrier, and modulated PSK signal at the filter output.

For the simulations, the following numbers have been used: $(\pm 1.5\ V)$ sawtooth carrier signal $f_c = 19.8$ kHz; bit duration time $T_s = 0.5$ ms. The length of the simulation was 1000 bits, randomly generated. Only five bits are shown below, for the sake of clarity, but the whole simulation provided correct results. Figure 5.8 shows the normalized spectrum of the modulated signal at the output of the band-pass filter of the lower part of Figure 5.4. A MATLAB built-in PSK demodulator "$pmdemod$"has been used to verify that the modulation process was correct. Figure 5.9 shows the same five bits shown in Figures (5.7 and 5.8) after using "$pmdemod$".

Figure 5.8. Normalized spectrum of the modulated signal at the filter output.

Figure 5.9. Demodulated signal, to verify the whole process.

To be doubly sure of the validity of the concept, the circuit in the lower part of Figure 5.4 has been modeled and simulated in Simulink, as shown in Figure 5.10. A binary input signal with the bit dur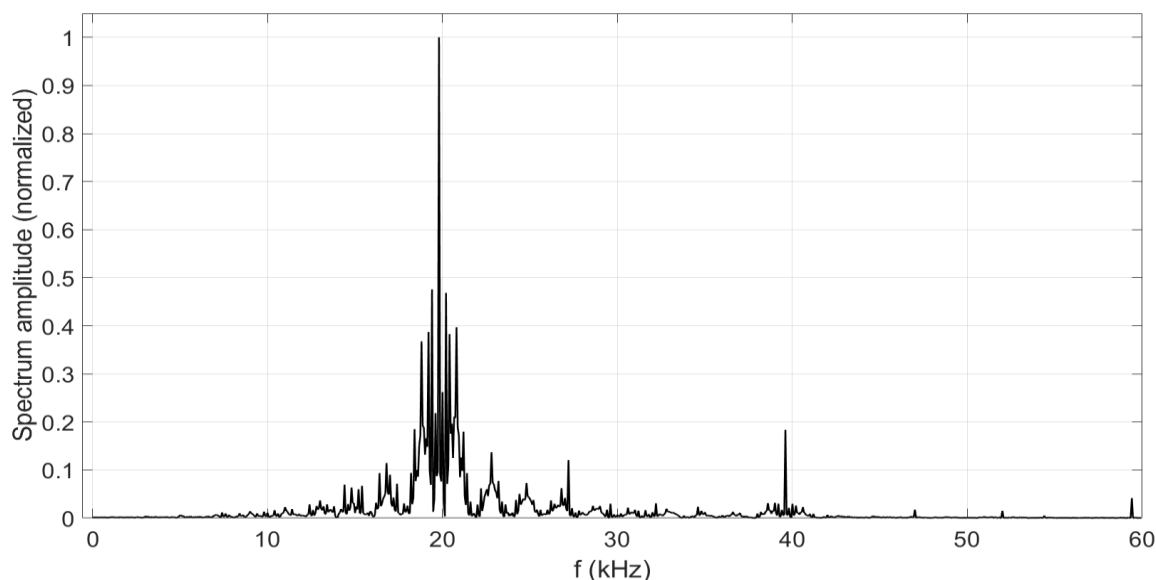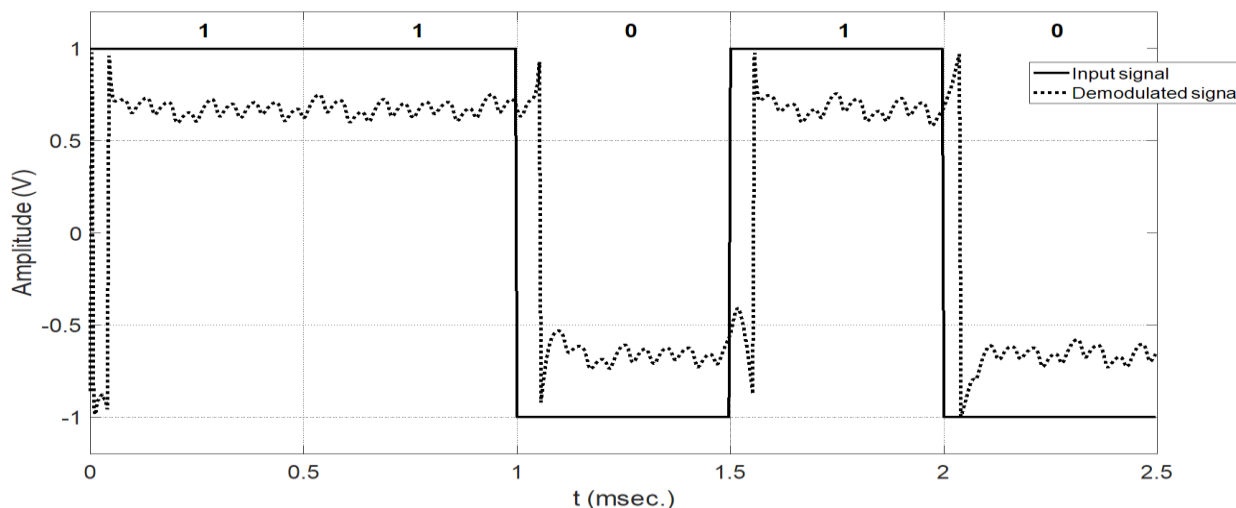ation time $T_s = 0.5$ ms is applied to the input of the unipolar-to-bipolar block that converts it into a symmetrical normalized voltage signal ($\pm 1\,V$). This signal is compared to the sawtooth carrier frequency $f_c = 19.8$ kHz to obtain a PW-modulated signal. The signal is then converted into bipolar and a gain of 30 is provided to represent the amplification through the power stage as per the functionality of the class-D amplifier. The band-pass filter tuned to the carrier frequency of the PW-modulator output blocks undesired frequency components and provides a PSK-modulated output. A scope and spectrum analyzer are used to measure the output in time and frequency domains.
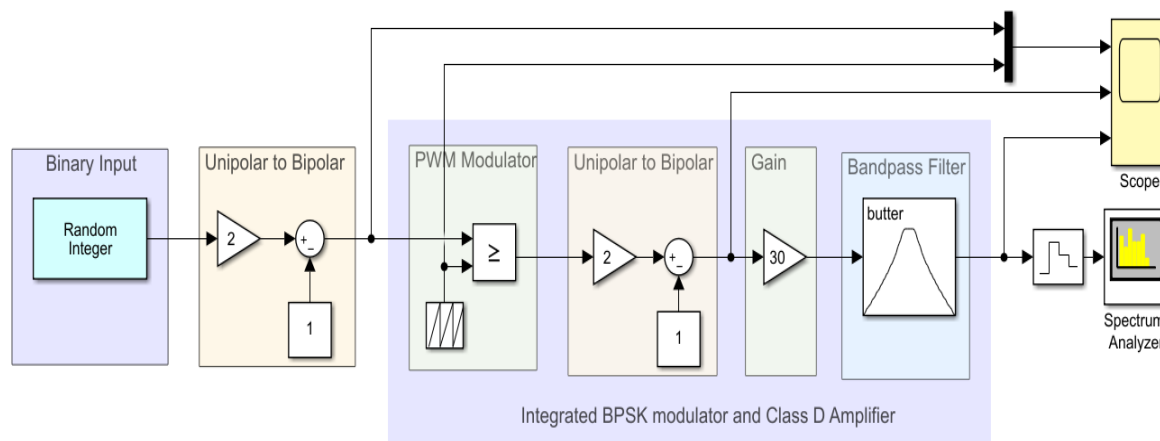
Figure 5.10. Proposed Simulink model.

Figure 5.11 shows the results obtained from the Simulink model in the time domain using the scope. In this figure, the binary input signal has been shown with a red color in the top part of the figure. In the same figure, the sawtooth waveform that acts as a carrier signal has been shown with a green color. The middle part of the figure is the PW-modulated signal that has been converted to a bipolar signal and is shown in blue color. Finally, the amplified and filtered PSK-modulated output received from the band-pass filter has been shown with a purple color in the bottom part of the figure.
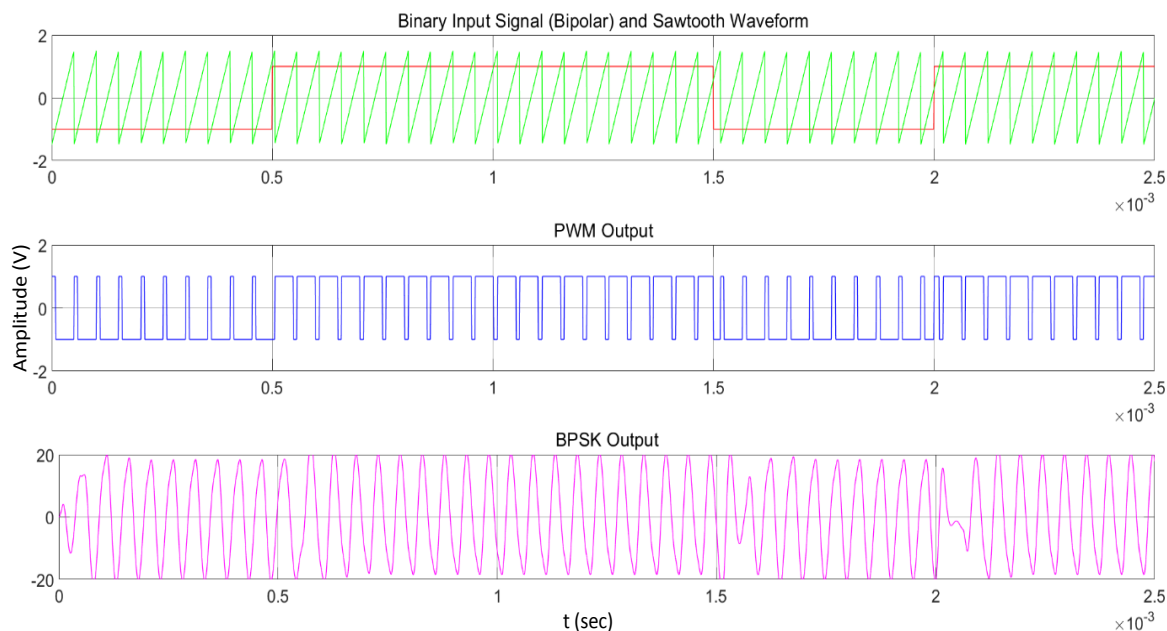
Figure 5.11. Simulation results of proposed model.

Figure 5.12 shows the overall power spectrum of the proposed model. As is evident, the fundamental frequency component of the system will have maximum amplitude; it can be observed that at $19.8\ kHz$, the third and fifth harmonics are visible at around 59 and $99\ kHz$, respectively. A band-pass filter tuned at the carrier frequency has been used to eliminate unwanted frequency components and to obtain a binary phase-shift keying (BPSK)-modulated output.
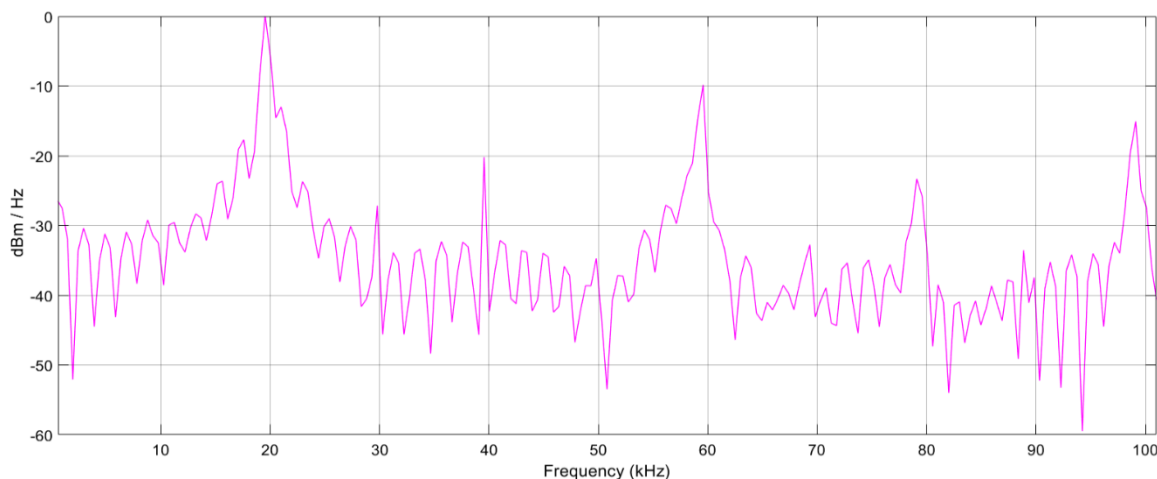
Figure 5.12. Power spectrum of proposed model.

5.5.2. Prototype

To fully demonstrate the concept, a circuit has been designed in interactive software Multisim [126] that not only provides powerful simulation and analysis, but is also used for the printed circuit board (PCB) design. A schematic of the proposed circuit prototype is shown in Figure 5.13. The circuit can be divided into five major blocks for better comprehension. On the left side, the 555 timer IC generates a sawtooth waveform of $f_c = 19.8$ kHz to be used as a carrier, and the OPAMP $LM358$ shown at the bottom adjusts the gain and offset of the waveform. The second block is the comparator where a binary

input signal is applied to the $+ve$ input of the IC $LM393$, while the carrier is connected to the $-ve$ input. The output of the comparator is a pulse width-modulated (PWM) signal. The third block is the driver circuitry and works as a buffer and designed using IC $LM358$ to prevent the loading effect and to drive the fourth block, i.e., $IRLZ44N$ Power MOSFET transistors. The amplified signal is fed into the fifth block, i.e., the second-order band-pass passive LC filter circuit removes unwanted signal components and provides an amplified PSK-modulated signal at the output.

Figure 5.13. Circuit diagram of proposed design.

Figure 5.14 shows the waveform acquired from testing the prototype circuit, which is similar to the waveform as obtained in Figure 5.11 from the simulation. The horizontal axis represents the time in seconds, while the amplitude is shown on the vertical axis in volts.

Figure 5.14. Waveform of the proposed circuit.

The sawtooth waveform shown in green represents the carrier, i.e., the $-ve$ input of the comparator IC LM393, while the binary input signal is shown in red applied to the $+ve$ input of the comparator.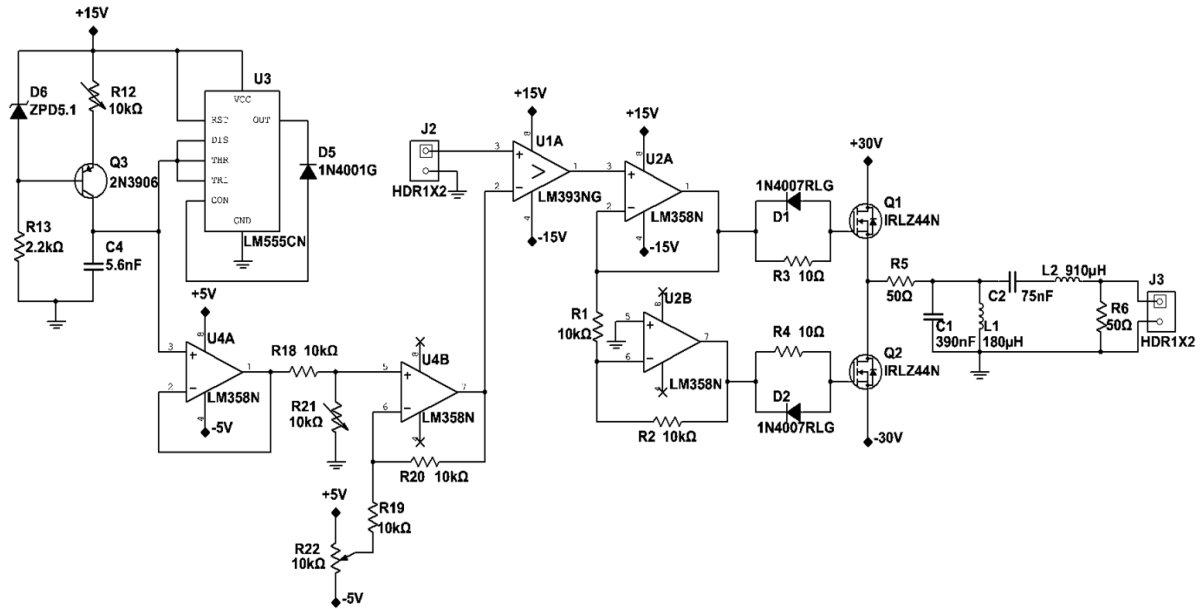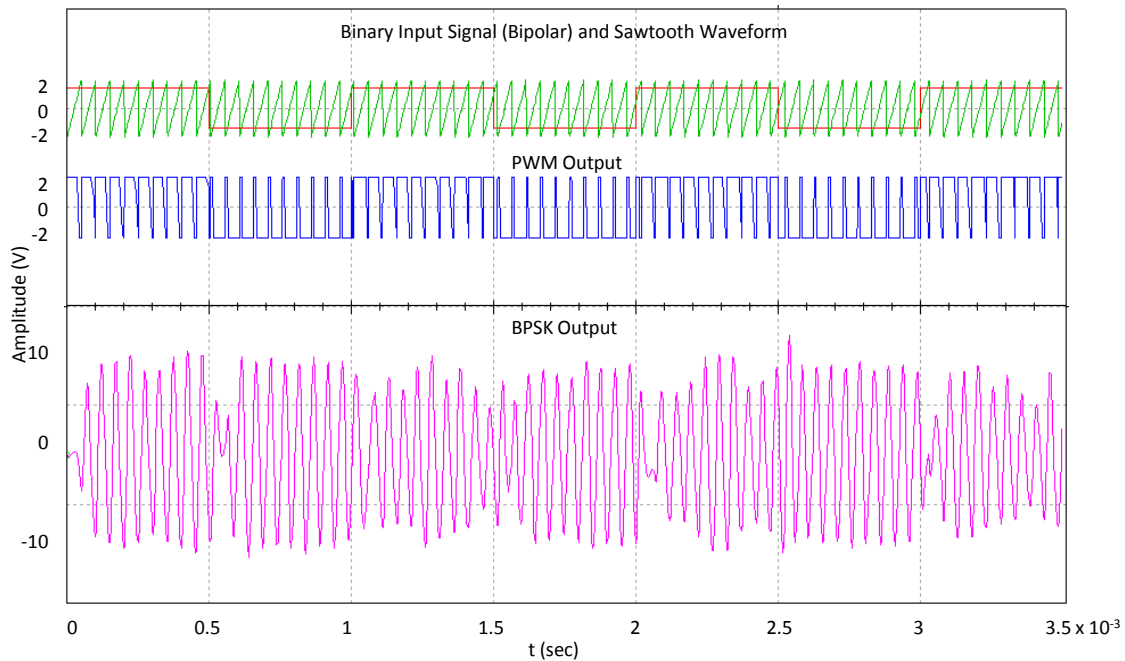 The PWM output of the comparator is shown in blue and passes to the buffers to drive the power MOSFET transistors. Finally, the filter output, i.e., amplified PSK-modulated signal, is shown in purple.

5.5.3. Discussion

A qualitative comparison with the related work is presented in Table 5.1. The input signal type in most of the designs is analog, while our proposed amplifier design accepts a digital signal of 1 V. We have tested our design on a 2 kHz input frequency range compared to 1 kHz in many cases and 5 kHz in [116]. The switching frequency used in the related work is in the range of $200 - 2000$ kHz, while in our case, it is much lower, i.e., $f_c = 19.8$ kHz, which is a plus point. Mostly, PWM or, in some cases, PDM is used inside the class-D amplifier followed by an LPF. We used BPF that not only filters but provides PSK modulation without using any modulator block. This unique feature is the novelty of our design that reduces the cost as we did not use any modulator, as well as increases the power efficiency of the overall system. The proposed design can deliver up to 6 W under a controlled environment at room temperature.

Table 5.1: Comparison with related work.

Parameter	[113]	[114]	[115]	[116]	[117]	This Work
Input signal type	Digital	Analog	Analog	Analog	Analog	Digital
Input signal voltage (V)	-	-	-	1	1	1
Input signal frequency (kHz)	-	1	-	1, 5	1	2
Switching frequency (kHz)	390	384	200	300–800	500–2000	19.8
Class-D amplifier modulation	PWM	UPWM	PWM	PWM	PDM	PWM
Filter type	Digital	-	LPF	LPF	LPF	BPF
Output type	Amplified	Amplified	Amplified	Amplified	Amplified	Amplified-PSK
Output power (W)	1.2	-	-	-	-	6

5.6. Conclusion

In this research, an integration of the modulator of a transmitter and PW-modulator of a class-D amplifier is presented to improve the energy efficiency of the system. The concept stems from the idea of the class-D amplifier where a power switching block is driven by a digital carrier modulated by the signal of interest. A band-pass filter is used to obtain an amplified PSK output. The concept can be of vital importance in the ultrasound band used in applications related to underwater acoustic communications. We use several steps to verify the concept. Initially, the hypothesis is verified using MATLAB, and then a model is designed and simulated in Simulink. Finally, an electronic circuit is built and experimentally tested to validate the feasibility of the concept. The results obtained by simulations and circuit implementation show that the proposed integrated system is an energy-efficient and cost-effective solution compared to existing solutions.

Chapter 6: Conclusions and Future Work

This chapter summarizes the work presented in this dissertation and indicates some interesting directions in which this work can be extended.

6.1. Conclusions

The primary topic of this thesis is to propose some cost-effective and energy-efficient hardware /software physical layer techniques for budget limited and long-life underwater acoustic communication modems.

First, a comprehensive survey is performed to find state-of-the-art commercial and research underwater acoustic modems. Various performance attributes e.g., (operating range, data-rates, center frequency, bandwidth, power consumption, modulation schemes and bit-error-rate) of commercial and research modems have been statistically analyzed/compared and results are graphically presented. The analysis shows that the operating range, data rate and reliability of commercial modems is much better than research modems. To achieve industrial grade performance, commercial modems use proprietary modulation schemes and hardware platforms make them better as well as expensive and less energy-efficient to be used in an economical project. In addition, their replication is difficult because the design information is not available due to trade secret. Hence there is a need for an economical and energy-efficient underwater acoustic modem and a testbed with known parameters that can be configured/ modified to be used in economical projects.

Furthermore, a low-cost acoustic modem using a modular approach has been designed for short-range underwater communications. The design can be configured/modified to be used in low-budget applications. The proposed modem is built around a single board computer Raspberry-Pi and a microcontroller. In order to reduce the overall design cost, the modules e.g., modulator, demodulator and amplifiers are designed with discrete components. Piezo ceramic material is used to design the acoustic transducers to further reduce the cost of the design. Initially, the module level testing is performed in the laboratory, then the system level testing is conducted in a controlled aquatic environment. Results show that the proposed modem can communicate from $300 - 1200\ bps$, however the packet receiving rate is 100% up to $600\ bps$ that gradually decreases with the increase of

data-rate and becomes 70% at 1200 *bps*. The transducers are placed at the distance of one meter throughout the experiment.

It is important to note that we have faced several technical challenges during the testing of our low-cost modem. It has compelled us to design a low-cost testbed. It means that in addition to the design cost, the verification cost is equally important. Therefore, a web based underwater acoustic communication testbed, along with a simulation platform, has been designed. The proposed system (testbed) works as an emulator to test the hardware/software of UWSN and their components and simulates underwater acoustic channels and mathematical models. Although the proposed testbed has been used to validate the performance of our low-cost modems using temperature and salinity sensors. However, the similar setup is equally useful for other types of modems. In addition, the simulations of underwater acoustic channel and sound propagation models have been done using LabVIEW. The proposed simulator requires less setup time to simulate mathematical models. The emulator, simulator and remote accessibility in a single framework is a major significance of the proposed testing platform.

Another important factor besides the cost-effectiveness is the energy efficiency of an underwater acoustic modem. The modems are battery operated which cannot be easily recharged. Therefore, an efficient energy mechanism is required to maintain the battery power for a long duration of time. In UW modems the power amplifier consumes much energy due to this reason a class-D amplifier is the best choice to be used as a power amplifier due to its higher efficiency. In the proposed energy efficient design, the integration of a digital modulator and a class-D amplifier provides much better efficiency as it reduces the double modulation and utilizes fewer number of components. The system has been mathematically proved using MATLAB simulations. Subsequently, the Simulink model is validated. Finally, the circuit level implementation has been performed in Multisim. The proposed system provides a PSK modulated and amplified signal without using a dedicated modulator block which ensures an overall reduction in energy requirements.

Ultimately, we believe that the cost-effective and energy-efficient physical layer techniques presented in this thesis can contribute to the advancement of UW acoustic communication modem. It is further hoped that the modular design approach of hardware and easy-to-learn software systems could be helpful for the community to promote research in underwater communication.

6.2.   Future work

The proposed low-cost underwater acoustic modem using modular approach presented in Chapter 3 which can be modified to be used in different kinds of applications. Similarly, a web-based economical underwater communications testbed proposed in Chapter 4, has been used at small scale configuration and can be extended to test large scale communication systems. An energy efficient integration of digital modulator and a class-D amplifier is presented in Chapter 5 and can be used in a UAM for a better energy efficiency. Hence this work opens various directions of research in underwater acoustic communications. Some other directions are discussed below.

a) ***Bandwidth efficiency vs power efficiency.*** In general, there is a fundamental trade-off between bandwidth and power efficiencies. Typically, the techniques, such as error control coding or m-ary modulation schemes, leading to an improvement in one of them are linked to a reduction in the other. In underwater acoustic communications, energy and bandwidth resources are equally scarce,

the former due to the limited battery lifetime, the latter due to the allocable frequencies of acoustic waves [37, 45]. Both need to be carefully considered. Therefore, adaptive techniques such as power control or adaptive modulation are in the sight of communications engineers and no general priority can be set for one of the two efficiencies. Only a close analysis of the communication requirements will help to determine which particular techniques or schemes are most suitable for a particular application.

b) *Multi-hop network.* A typical underwater sensor network consists of many sensor nodes. These nodes are densely deployed in the extreme underwater environment. Creating a high speed and energy efficient design is still an unsolved issue. Some strategies aim to locate all nodes within the same broadcast domain [127]. However, this solution largely constraints the reach of the network. More suitable strategies analyze the possibility of dynamic routing, with both proactive and reactive mechanisms [128-131]. Building upon these mechanisms, some authors suggest splitting the network in clusters, with only a handful of nodes, the heads of such clusters, participating in the backbone communications. The hybrid approaches offer a performance which is based upon geographical proximity, without so much energy expenditure in the update of routing paths [132].

Anyway, optimal solutions are still much dependent on the specific scenarios under consideration. When designing the route update protocols, care must be taken not to overload the network capacity with control information. In densely populated networks, reactive strategies such as [133] provide good performance, as a neighbor is easily found when transmissions occur. Authors have suggested broadcast strategies with back-off pruning in order to minimize the signaling overhead and find a nearly optimal path in nearly all transmissions without overloading the network. However, in scenarios such as river mouth monitoring, where string linear topologies are used [134], being the reachable distance one design criteria, the number of nodes is small, usually only one or two within reach, and static routing with time-to-time updates offers a better overhead vs capacity ratio. Multi-hop networks thus present the problems of determining the appropriate transmission range, which means a mechanism for adaptive power control is required, using efficient routing protocols, and avoiding wasting transmission capacity because of guard times and collisions.

c) *Standardization of UW communication.* The underwater acoustic modems designed and developed by the research community as well as the commercial modems available in the market have different characteristics. Each device has its acoustic communication interface, with varying data rate, modulation schemes and channel coding. Currently, companies interested in deploying an UW network have to rely on the products from one manufacturer, due to the lack of flexibility. Even products designed for similar transmission ranges use different modulation schemes and protection codes, thus rendering them incompatible.

The military sector has developed the Janus standard, whose Edition A, Version-1 has been published in March 2016 [135]. This standard describes the physical and link layer design for underwater acoustic modems in the band $9440 - 13,600\ Hz$, but the data rate is very low, around $110\ bauds$ for a $700\ m$ distance. Commercial modems achieve much higher data rates. And this

is the goal of the subsea wireless group (SWiG) [136, 137], which intends to take the JANUS standard as the base for a new community standard for the offshore energy industry.

Bibliography

[1]   S. Jiang and S. Georgakopoulos, "Electromagnetic wave propagation into fresh water," *Journal of Electromagnetic Analysis and Applications,* vol. 3, p. 261, 2011.

[2]   N. Farr, A. Bowen, J. Ware, C. Pontbriand, and M. Tivey, "An integrated, underwater optical/acoustic communications system," in *OCEANS'10 IEEE SYDNEY*, 2010, pp. 1-6.

[3]   Z. Ghassemlooy, S. Arnon, M. Uysal, Z. Xu, and J. Cheng, "Emerging optical wireless communications-advances and challenges," *IEEE journal on selected areas in communications,* vol. 33, pp. 1738-1749, 2015.

[4]   M. Murad, A. A. Sheikh, M. A. Manzoor, E. Felemban, and S. Qaisar, "A survey on current underwater acoustic sensor network applications," *International Journal of Computer Theory and Engineering,* vol. 7, p. 51, 2015.

[5]   R. Manjula and S. S. Manvi, "Issues in underwater acoustic sensor networks," *International Journal of Computer and Electrical Engineering,* vol. 3, p. 101, 2011.

[6]   I. F. Akyildiz, D. Pompili, and T. Melodia, "Challenges for efficient communication in underwater acoustic sensor networks," *ACM Sigbed Review,* vol. 1, pp. 3-8, 2004.

[7]   Y. Luo, L. Pu, M. Zuba, Z. Peng, and J.-H. Cui, "Challenges and opportunities of underwater cognitive acoustic networks," *IEEE Transactions on Emerging Topics in Computing,* vol. 2, pp. 198-211, 2014.

[8]   M. Chitre, S. Shahabudeen, and M. Stojanovic, "Underwater acoustic communications and networking: Recent advances and future challenges," *Marine technology society journal,* vol. 42, pp. 103-116, 2008.

[9]   M. Y. I. Zia, A. M. Khan, P. Otero, and J. Poncela, "Investigation of underwater acoustic modems: Architecture, test environment & performance," in *3rd International Conference on Computing for Sustainable Global Development (INDIACom)*, 2016, pp. 2031-2036.

[10]   S. Sendra, J. Lloret, J. M. Jimenez, and L. Parra, "Underwater acoustic modems," *IEEE Sensors Journal,* vol. 16, pp. 4063-4071, 2015.

[11]   *AppliCon: Underwater Acoustic SeaModem*. Available at: http://www.applicon.it (Last seen on 26 September, 2020)

[12]   *AquaSeNT: Underwater Acoustic Modems*. Available at: http://www.aquasent.com (Last seen on 26 September, 2020)

[13]   *Aquatec: Underwater Acoustic AQUAmodems*. Available at: http://www.aquatecgroup.com (Last seen on 26 September, 2020)

[14]   *Blueprint Subsea: SeaTrac Underwater Acoustic Modems*. Available at: https://www.blueprintsubsea.com (Last seen on 26 September, 2020)

[15]   *Desert Star: SAM-1 Underwater Acoustic Modem*. Available at: http://www.desertstar.com (Last seen on 26 September, 2020)

[16]   *Develogic: Hydro Acoustic Modem*. Available at: http://www.develogic.de (Last seen on 26 September, 2020)

[17]   *DiveNET: Acoustic Modems*. Available at: https://www.divenetgps.com (Last seen on 26 September, 2020)

Bibliography

[18] *DSPComm: Aquacomm Underwater Wireless Modems*. Available at: https://www. dspcomm.com (Last seen on 26 September, 2020)

[19] *EvoLogics: S2C Underwater Acoustic Modems*. Available at: https://www.evologics.de/ (Last seen on 26 September, 2020)

[20] *Kongsberg: cNODE Underwater Acoustic Modems*. Available at: https://www.km.kongsberg.com (Last seen on 26 September, 2020)

[21] *LinkQuest: SoundLink Underwater Acoustic Modems*. Available at: http://www.link-quest.com (Last seen on 26 September, 2020)

[22] *Oceania: GPM 300 Underwater Acoustic Modem*. Available at: https://www2.l3t.com/oceania (Last seen on 26 September, 2020)

[23] *Sercel: MATS 3G Underwater Acoustic Modems*. Available at: http://www.sercel.com (Last seen on 26 September, 2020)

[24] *Sonardyne: Modem 6 Underwater Acoustic Modems*. Available at: https://www.sonardyne.com (Last seen on 26 September, 2020)

[25] *Subnero: Software Defined Underwater Acoustic Modem*. Available at: https://subnero.com (Last seen on 26 September, 2020)

[26] *Teledynemarine: Teledyne Benthos ATM-9xx Underwater Acoustic Modems*. Available at: http://www.teledynemarine.com (Last seen on 26 September, 2020)

[27] *Tritech: Micron Data Modem*. Available at: https://www.tritech.co.uk (Last seen on 26 September, 2020)

[28] E. Demirors, G. Sklivanitis, G. E. Santagati, T. Melodia, and S. N. Batalama, "A high-rate software-defined underwater acoustic modem with real-time adaptation capabilities," *IEEE Access,* vol. 6, pp. 18602-18615, 2018.

[29] Q. Dong, Y. Wang, and X. Guan, "The Design and Implementation of an Underwater Multimode Acoustic Modem for Autonomous Underwater Vehicles," in *37th Chinese Control Conference (CCC)*, 2018, pp. 4201-4205.

[30] S. Indriyanto and I. Y. M. Edward, "Ultrasonic Underwater Acoustic Modem Using Frequency Shift Keying (FSK) Modulation," in *4th International Conference on Wireless and Telematics (ICWT)*, 2018, pp. 1-4.

[31] M. Y. I. Zia, P. Otero, and J. Poncela, "Design of a Low-Cost Modem for Short-Range Underwater Acoustic Communications," *Wireless Personal Communications,* vol. 101, pp. 375-390, 2018.

[32] M. Sadeghi, M. Elamassie, and M. Uysal, "Adaptive OFDM-based acoustic underwater transmission: system design and experimental verification," in *2017 IEEE International Black Sea Conference on Communications and Networking (BlackSeaCom)*, 2017, pp. 1-5.

[33] A. A. Sheikh, E. Felemban, and A. Ashraf, "Coralcon: An open source low-cost modem for underwater IoT applications," in *2017 13th IEEE International Conference on Intelligent Computer Communication and Processing (ICCP)*, 2017, pp. 503-508.

[34] B. Peng and H. Dong, "DSP based real-time single carrier underwater acoustic communications using frequency domain turbo equalization," *Physical Communication,* vol. 18, pp. 40-48, 2016.

[35]   C. Renner, A. Gabrecht, B. Meyer, C. Osterloh, and E. Maehle, "Low-power low-cost acoustic underwater modem," in *Quantitative Monitoring of the Underwater Environment: Results of the International Marine Science and Technology Event MOQESM´14 in Brest, France*, ed: Springer, Cham, 2016, pp. 59-65.

[36]   A. S. Vershinin, "Experimental testing of hydroacoustic modem layout," in *2016 17th International Conference of Young Specialists on Micro/Nanotechnologies and Electron Devices (EDM)*, 2016, pp. 75-77.

[37]   H. Zhang, S. Xiong, Z. Yue, and Z. Wang, "Sea trials of an underwater acoustic network in the east china sea 2015," in *2016 IEEE/OES China Ocean Acoustics (COA)*, 2016, pp. 1-5.

[38]   R. Zhao, H. Mei, X. Shen, W. Fang, and H. Wang, "Underwater acoustic network node design and anechoic pool network experimentation with five nodes," in *2016 IEEE/OES China Ocean Acoustics (COA)*, 2016, pp. 1-5.

[39]   C. C. Naidu and E. Stalin, "Establishment of underwater wireless acoustic MODEM using C-OFDM," in *2016 International Conference on Microelectronics, Computing and Communications (MicroCom)*, 2016, pp. 1-6.

[40]   W. bin Abbas, N. Ahmed, C. Usama, and A. A. Syed, "Design and evaluation of a low-cost, DIY-inspired, underwater platform to promote experimental research in UWSN," *Ad Hoc Networks,* vol. 34, pp. 239-251, 2015.

[41]   J. DelPreto, R. Katzschmann, R. MacCurdy, and D. Rus, "A compact acoustic communication module for remote control underwater," in *Proceedings of the 10th International Conference on Underwater Networks & Systems*, 2015, p. 13.

[42]   M. S. Martins, J. Cabral, G. Lopes, and F. Ribeiro, "Underwater acoustic modem with streaming video capabilities," in *OCEANS 2015-Genova*, 2015, pp. 1-7.

[43]   D. Torres, J. Friedman, T. Schmid, M. B. Srivastava, Y. Noh, and M. Gerla, "Software-defined underwater acoustic networking platform and its applications," *Ad Hoc Networks,* vol. 34, pp. 252-264, 2015.

[44]   W. A. van Kleunen, N. A. Moseley, P. J. Havinga, and N. Meratnia, "Proteus II: Design and evaluation of an integrated power-efficient underwater sensor node," *International journal of distributed sensor networks,* vol. 11, p. 791046, 2015.

[45]   J. Younce, A. Singer, T. Riedl, B. Landry, A. Bean, and T. Arikan, "Experimental results with HF underwater acoustic modem for high bandwidth applications," in *2015 49th Asilomar Conference on Signals, Systems and Computers*, 2015, pp. 248-252.

[46]   W. Lee, J.-H. Jeon, and S.-J. Park, "Micro-modem for short-range underwater communication systems," in *2014 Oceans-St. John's*, 2014, pp. 1-4.

[47]   L. Ma, G. Qiao, and S. Liu, "Heu OFDM-modem for underwater acoustic communication and networking," in *Proceedings of the International Conference on Underwater Networks & Systems*, 2014, p. 14.

[48]   C. Wang, Q. Zhang, Z. Yan, J. Han, K. Lei, and L. Zhang, "Implementation of underwater acoustic modem based on the OMAP-L138 processor," in *2014 IEEE International Conference on Signal Processing, Communications and Computing (ICSPCC)*, 2014, pp. 800-805.

[49]   L. Xu and S. Yan, "Design of Underwater Acoustic Modems Through High Performance DSPs," in *Proceedings of the International Conference on Underwater Networks & Systems*, 2014, p. 32.

[50]   A. Bourré, S. Lmai, C. Laot, and S. Houcke, "A robust OFDM modem for underwater acoustic communications," in *2013 MTS/IEEE OCEANS-Bergen*, 2013, pp. 1-5.

[51]   G. Qiao, S. Liu, Z. Sun, and F. Zhou, "Full-duplex, multi-user and parameter reconfigurable underwater acoustic communication modem," in *2013 OCEANS-San Diego*, 2013, pp. 1-8.

[52]   Z. Shaolong, F. Dong, L. Xun, L. Yu, and H. Haining, "Modularized real-time communication modem design based on software defined radio of underwater acoustic network," in *Proceedings of the 2012 International Conference on Communication, Electronics and Automation Engineering*, 2013, pp. 1197-1204.

[53]   M. Chitre, I. Topor, and T.-B. Koay, "The UNET-2 modem—An extensible tool for underwater networking research," in *2012 Oceans-Yeosu*, 2012, pp. 1-7.

[54]   J.-H. Jeon, S.-H. Hwangbo, H. Peyvandi, and S.-J. Park, "Design and implementation of a bidirectional acoustic micro-modem for underwater communication systems," in *2012 Oceans*, 2012, pp. 1-4.

[55]   W. Lei, D. Wang, Y. Xie, B. Chen, X. Hu, and H. Chen, "Implementation of a high reliable chirp underwater acoustic modem," in *2012 Oceans-Yeosu*, 2012, pp. 1-5.

[56]   A. Sánchez, S. Blanc, P. Yuste, A. Perles, and J. J. Serrano, "An ultra-low power and flexible acoustic modem design to develop energy-efficient underwater sensor networks," *Sensors,* vol. 12, pp. 6837-6856, 2012.

[57]   T.-H. Won and S.-J. Park, "Design and implementation of an omni-directional underwater acoustic micro-modem based on a low-power micro-controller unit," *Sensors,* vol. 12, pp. 2309-2323, 2012.

[58]   H. Yan, L. Wan, S. Zhou, Z. Shi, J.-H. Cui, J. Huang, *et al.*, "DSP based receiver implementation for OFDM acoustic modems," *Physical Communication,* vol. 5, pp. 22-32, 2012.

[59]   H. Nam and S. An, "Low-power based coherent acoustic modem for emerging underwater acoustic sensor networks," *Wireless Personal Communications,* vol. 57, pp. 291-309, 2011.

[60]   B. Benson, Y. Li, B. Faunce, K. Domond, D. Kimball, C. Schurgers, *et al.*, "Design of a low-cost underwater acoustic modem," *IEEE Embedded Systems Letters,* vol. 2, pp. 58-61, 2010.

[61]   E. Felemban, F. K. Shaikh, U. M. Qureshi, A. A. Sheikh, and S. B. Qaisar, "Underwater sensor network applications: A comprehensive survey," *International Journal of Distributed Sensor Networks,* vol. 11, p. 896832, 2015.

[62]   H. Luo, K. Wu, R. Ruby, F. Hong, Z. Guo, and L. M. Ni, "Simulation and experimentation platforms for underwater acoustic sensor networks: Advancements and challenges," *ACM Computing Surveys (CSUR),* vol. 50, p. 28, 2017.

[63]   A. P. Das and S. M. Thampi, "Simulation tools for underwater sensor networks: a survey," *Network protocols and Algorithms,* vol. 8, 2016.

[64]   L. Wu, X. Cui, and D. Yu, "Design and implementation of a BPSK acoustic modem for underwater communication," 2012.

[65]   *Introduction to orthogonal frequency division_multiplexing.* Available at: https://www.csd.uoc.gr/~hy439/reading/list_2010/introduction_orthogonal_frequency_division_multiplex.pdf (Last seen on 26 September, 2020)

[66]   J.-H. Jeon, H. An, and S.-J. Park, "Design and implementation of bidirectional OFDM modem prototype for high-speed underwater acoustic communication systems," in *OCEANS 2016-Shanghai*, 2016, pp. 1-4.

[67]   G. Cario, A. Casavola, M. Lupia, and C. Rosace, "SeaModem: A low-cost underwater acoustic modem for shallow water communication," in *OCEANS 2015-Genova*, 2015, pp. 1-6.

[68]   E. Gaalaas. *Class D audio amplifiers [Online]*. Available at: https://www.analog.com/media/en/analog-dialogue/volume-40/number-2/articles/class-d-audio-amplifiers.pdf (Last seen on 26 September, 2020)

[69]   M. Y. I. Zia, P. Otero, A. Siddiqui, and J. Poncela, "Design of a Web Based Underwater Acoustic Communication Testbed and Simulation Platform," *Wireless Personal Communications,* pp. 1-23, 2020.

[70]   C. Özgen, "Design of a multi-frequency underwater transducer using cylindrical piezoelectric elements," Citeseer, 2011.

[71]   D. Ponnamma, M. M. Chamakh, K. Deshmukh, M. B. Ahamed, A. Erturk, P. Sharma*, et al.*, "Ceramic-based polymer nanocomposites as piezoelectric materials," in *Smart Polymer Nanocomposites*, ed: Springer, 2017, pp. 77-93.

[72]   *Basics-of-underwater-acoustic-transducer.* Available at: https://www.piezohannas.com/Basics-of-underwater-acoustic-transducer-id3112465.html (Last seen on 26 September, 2020)

[73]   R. Martins, J. B. de Sousa, R. Caldas, C. Petrioli, and J. Potter, "SUNRISE project: Porto university testbed," in *2014 Underwater Communications and Networking (UComms)*, 2014, pp. 1-5.

[74]   C. Petrioli, R. Petroccia, J. R. Potter, and D. Spaccini, "The SUNSET framework for simulation, emulation and at-sea testing of underwater wireless sensor networks," *Ad Hoc Networks,* vol. 34, pp. 224-238, 2015.

[75]   R. Masiero, S. Azad, F. Favaro, M. Petrani, G. Toso, F. Guerra*, et al.*, "DESERT Underwater: an NS-Miracle-based framework to DEsign, Simulate, Emulate and Realize Test-beds for Underwater network protocols," in *2012 Oceans-Yeosu*, 2012, pp. 1-10.

[76]   Y.-P. Kim, J.-I. Namgung, N.-Y. Yun, H.-J. Cho, I. A. Khan, and S.-H. Park, "Design and implementation of the test-bed for underwater acoustic sensor network based on arm9 processor," in *2010 IEEE/IFIP International Conference on Embedded and Ubiquitous Computing*, 2010, pp. 302-306.

[77]   M. Y. I. Zia, J. Poncela, and P. Otero, "State-of-the-Art Underwater Acoustic Communication Modems: Classifications, Analyses and Design Challenges," *Wireless Personal Communications,* 2020.

[78]   M. Y. I. Zia, R. Tierno, M.-Á. Luque-Nieto, and P. Otero, "An Energy-Efficient Integration of a Digital Modulator and a Class-D Amplifier," *Electronics,* vol. 9, p. 1319, 2020.

[79]   J. Sather, "Battery technologies for IoT," in *Enabling the Internet of Things*, ed: Springer, Cham, 2017, pp. 409-440.

[80] D.-S. Lee, S.-H. Hwangbo, J.-H. Jeon, and S.-J. Park, "Cortex-M3 and TMS320C6416 Based Acoustic Modem Implementation for Underwater Wireless Communication," in *2012 IEEE 15th International Conference on Computational Science and Engineering*, 2012, pp. 679-682.

[81] *Raspberry Pi*. Available at: https://www.raspberrypi.org/ (Last seen on 26 September, 2020)

[82] *Microcontroller Atmega328P*. Available at: http://www.microchip.com/wwwproducts/en/ATmega328P (Last seen on 26 September, 2020)

[83] W. A. van Kleunen, N. A. Moseley, P. J. Havinga, and N. Meratnia, "Proteus II: design and evaluation of an integrated power-efficient underwater sensor node," *International journal of distributed sensor networks,* vol. 2015, p. 1, 2015.

[84] N. Ahmed, W. b. Abbas, and A. A. Syed, "A low-cost and flexible underwater platform to promote experiments in UWSN research," in *Proceedings of the seventh ACM international conference on underwater networks and systems*, 2012, pp. 1-8.

[85] H. Li, Z. D. Deng, and T. J. Carlson, "Piezoelectric materials used in underwater acoustic transducers," *Sensor Letters,* vol. 10, pp. 679-697, 2012.

[86] *STEMINC - Piezo Ceramic Cylinder*. Available at: https://www.steminc.com/PZT/en/piezo-ceramic-cylinder-36x31x20mm-30-khz (Last seen on 26 September, 2020)

[87] *Lead Free No-Clean Flux Core Silver Solder*. Available at: https://www.steminc.com/PZT/en/lead-free-no-clean-flux-core-silver-solder (Last seen on 26 September, 2020)

[88] *Monolithic Function Generator*. Available at: https://www.sparkfun.com/datasheets/Kits/XR2206_104_020808.pdf (Last seen on 26 September, 2020)

[89] *FSK Demodulator / Tone Decoder*. Available at: https://www.exar.com/ds/xr2211av104.pdf (Last seen on 26 September, 2020)

[90] *JFET Amplifier*. Available at: http://www.electronics-tutorials.ws/amplifier/amp_3.html (Last seen on 26 September, 2020)

[91] *Amplifier Classes*. Available at: http://www.electronics-tutorials.ws/amplifier/amplifier-classes.html (Last seen on 26 September, 2020)

[92] A. Sánchez, S. Blanc, P. Yuste, and J. Serrano, "A low cost and high efficient acoustic modem for underwater sensor networks," in *OCEANS 2011 IEEE-Spain*, 2011, pp. 1-10.

[93] *NI ELVIS Engineering Lab Workstation*. Available at: http://www.ni.com/en-lb/shop/select/ni-elvis-engineering-lab-workstation (Last seen on 26 September, 2020)

[94] *LabVIEW*. Available at: http://www.ni.com/download/labview-development-system-2018/7406/en/ (Last seen on 26 September, 2020)

[95] R. Bansal, S. Maheshwari, and P. Awwal, "Challenges and Issues in Implementation of Underwater Wireless Sensor Networks," in *Optical and Wireless Technologies*, ed: Springer, 2018, pp. 507-514.

[96] J. Poncela, M. Aguayo, and P. Otero, "Wireless underwater communications," *Wireless Personal Communications,* vol. 64, pp. 547-560, 2012.

[97] *WHOI Micromodem*. Available at: https://acomms.whoi.edu/micro-modem/ (Last seen on 26 September, 2020)

[98] S. Zheng, X. Wang, W. Jiang, and F. Tong, "Lake trial of an underwater acoustic cross-media network testbed," in *2017 IEEE International Conference on Signal Processing, Communications and Computing (ICSPCC)*, 2017, pp. 1-4.

[99]   C. Raj and R. Sukumaran, "Modeling UWSN simulators–a taxonomy," *World Acad Sci Eng Technol Int J Comput Electr Autom Control Inf Eng,* vol. 9, pp. 585-592, 2015.

[100]   X. Du, X. Liu, and Y. Su, "Underwater acoustic networks testbed for ecological monitoring of Qinghai Lake," in *OCEANS 2016-Shanghai*, 2016, pp. 1-4.

[101]   C. M. Goldrick, M. Matney, E. Segura, Y. Noh, and M. Gerla, "Watercom: A multilevel, multipurpose underwater communications test platform," in *Proceedings of the 10th International Conference on Underwater Networks & Systems*, 2015, p. 14.

[102]   J. Alves, J. Potter, G. Zappa, P. Guerrini, and R. Been, "A testbed for collaborative development of underwater communications and networking," in *MILCOM 2012-2012 IEEE Military Communications Conference*, 2012, pp. 1-8.

[103]   Z. Peng, J.-H. Cui, B. Wang, K. Ball, and L. Freitag, "An underwater network testbed: design, implementation and measurement," in *Proceedings of the second workshop on Underwater networks*, 2007, pp. 65-72.

[104]   L. Bjørnø, *Applied Underwater Acoustics*: Elsevier, 2017.

[105]   A. F. Harris III and M. Zorzi, "Modeling the underwater acoustic channel in ns2," in *Proceedings of the 2nd international conference on Performance evaluation methodologies and tools*, 2007, p. 18.

[106]   R. F. Coates, *Underwater acoustic systems*: Macmillan International Higher Education, 1990.

[107]   H. Luo, C. Liu, and Y. Liang, "A SDN-based Testbed for Underwater Sensor Networks," 2019.

[108]   L. Wei, Y. Tang, Y. Cao, Z. Wang, and M. Gerla, "Exploring simulation of software-defined underwater wireless networks," in *Proceedings of the International Conference on Underwater Networks & Systems*, 2017, p. 21.

[109]   J. Honda and J. Adams. *Class D Audio Amplifier Basics, Application Note AN-1071, International Rectifier (USA), Feb. 2005.* Available at: https://www.infineon.com/dgdl/an-1071.pdf (Last seen on 26 September, 2020)

[110]   D. Xu, G. Zhou, R. Huang, X. Liu, and F. Liu, "High Efficiency Half Bridge Class-D Audio Amplifier System with Front-end Symmetric Bipolar Outputs LLC Converter," *IEEE Transactions on Industrial Electronics,* 2020.

[111]   J. Caldwell. *Analog pulse width modulation, TI precision Designs: Verified Design (Texas Instruments application recommendations), June 2013*. Available at: http://www.ti.com/lit/ug/slau508/slau508.pdf (Last seen on 26 September, 2020)

[112]   Z. Song and D. V. Sarwate, "The frequency spectrum of pulse width modulated signals," *Signal Processing,* vol. 83, pp. 2227-2258, 2003.

[113]   M. Auer and T. Karaca, "A Class-D Amplifier with Digital PWM and Digital Loop-Filter using a Mixed-Signal Feedback Loop," in *ESSCIRC 2019-IEEE 45th European Solid State Circuits Conference (ESSCIRC)*, 2019, pp. 153-156.

[114]   C.-H. Kuo and Y.-J. Liou, "A Delta-Sigma Modulator with UPWM Quantizer for Digital Audio Class-D Amplifier," in *2019 MIXDES-26th International Conference" Mixed Design of Integrated Circuits and Systems"*, 2019, pp. 293-297.

[115]   Y. Li, F. Duan, J. Jiang, and X. Wang, "High-efficiency and low-consumption underwater sonar transmitter with improved triple-pulse HP-PWM signal model based on class D amplifier," *EURASIP Journal on Wireless Communications and Networking,* 2016.

[116]   J. Galić, T. Pešić-Brdjanin, and L. Iriškić, "Class-D Audio Amplifier using Pulse Width Modulation," in *6th Small Systems Simulation Symposium*, 2016, pp. 133-136.

[117]   S. Kovačević, T. Pešić-Brdjanin, and J. Galić, "Class D Audio Amplifier with Reduced Distortion," in *2018 International Symposium on Industrial Electronics (INDEL)*, 2018, pp. 1-4.

[118]   P. B. Crilly and A. B. Carlson, *Communication Systems*, 5th ed.: McGraw-Hill Education, 2009.

[119]   J. G. Proakis, M. Salehi, and G. Bauch, *Contemporary communication systems using MATLAB*: Nelson Education, 2012.

[120]   J. Mitola, *Software Radio: Object-oriented Approaches to Wireless Systems Engineering*: J. Wiley & Sons, 2000.

[121]   E. Grayver, *Implementing software defined radio*: Springer Science & Business Media, 2012.

[122]   *Texas Instruments Mixed-Signal Products, "FSK Modulation and Demodulation With the MSP430 Microcontroller," 1998. ", Application Report SLAA037, Texas Instruments*. Available at: http://www.ti.com/lit/an/slaa037/slaa037.pdf (Last seen on 26 September, 2020)

[123]   C. Pascual, Z. Song, P. T. Krein, D. V. Sarwate, P. Midya, and W. J. Roeckner, "High-fidelity PWM inverter for digital audio amplification: Spectral analysis, real-time DSP implementation, and results," *IEEE Transactions on Power Electronics,* vol. 18, pp. 473-485, 2003.

[124]   E. Koutroulis, A. Dollas, and K. Kalaitzakis, "High-frequency pulse width modulation implementation using FPGA and CPLD ICs," *Journal of systems architecture,* vol. 52, pp. 332-344, 2006.

[125]   K. C. Nguyen and D. V. Sarwate, "Up-sampling and natural sample value computation for digital pulse width modulators," in *2006 40th Annual Conference on Information Sciences and Systems*, 2006, pp. 1096-1101.

[126]   *National Instruments Multisim*. Available at: https://www.ni.com/en-lb/support /downloads/ software-products/download.multisim.html#312060 (Last seen on 26 September, 2020)

[127]   P.-H. Huang, Y. Chen, B. Krishnamachari, and A. Kumar, "Link scheduling in a single broadcast domain underwater networks," in *2010 IEEE International Conference on Sensor Networks, Ubiquitous, and Trustworthy Computing*, 2010, pp. 205-212.

[128]   D. Pompili, T. Melodia, and I. F. Akyildiz, "Distributed routing algorithms for underwater acoustic sensor networks," *IEEE transactions on Wireless Communications,* vol. 9, pp. 2934-2944, 2010.

[129]   G. G. Xie and J. H. Gibson, "A network layer protocol for UANs to address propagation delay induced performance limitations," in *MTS/IEEE Oceans 2001. An Ocean Odyssey. Conference Proceedings (IEEE Cat. No. 01CH37295)*, 2001, pp. 2087-2094.

[130]   M. Barbeau, S. Blouin, G. Cervera, J. Garcia-Alfaro, and E. Kranakis, "Location-free link state routing for underwater acoustic sensor networks," in *2015 IEEE 28th Canadian Conference on Electrical and Computer Engineering (CCECE)*, 2015, pp. 1544-1549.

[131]   J. Shen, J. Wang, J. Wang, J. Zhang, and S. Wang, "Location-Aware Routing Protocol for Underwater Sensor Networks," in *Advanced Technologies, Embedded and Multimedia for Human-centric Computing*, ed: Springer, Dordrecht, 2014, pp. 609-617.

[132]   J. Jiang, G. Han, H. Guo, L. Shu, and J. J. Rodrigues, "Geographic multipath routing based on geospatial division in duty-cycled underwater wireless sensor networks," *Journal of Network and Computer Applications,* vol. 59, pp. 4-13, 2016.

[133]   S. M. Ghoreyshi, A. Shahrabi, and T. Boutaleb, "An opportunistic void avoidance routing protocol for underwater sensor networks," in *2016 IEEE 30th International Conference on Advanced Information Networking and Applications (AINA)*, 2016, pp. 316-323.

[134]   W. Zhang, M. Stojanovic, and U. Mitra, "Analysis of a linear multihop underwater acoustic network," *IEEE Journal of Oceanic Engineering,* vol. 35, pp. 961-970, 2010.

[135]   *JANUS: An   Open   Source   Underwater   Signaling   Protocol*.   Available   at: http://www.januswiki.com/tiki-index.php (Last seen on 26 September, 2020)

[136]   A. Smerdon, F. Bustamante, and M. Baker, "The SWIG acoustic standard: an acoustic communication standard for the offshore energy community," in *2016 IEEE Third Underwater Communications and Networking Conference (UComms)*, 2016, pp. 1-4.

[137]   *Subsea Wireless Group (SWiG)*. Available at: https://subseawirelessgroup.com/ (Last seen on 26 September, 2020)

Appendix A

Curriculum vitae

Experience

Faculty member, Computer Engineering Department	2011−date
Umm Al Qura University, Makkah Al Mukarammah, Saudi Arabia	
Faculty member, Electrical Engineering Department	2005−2011
National University of Computer & Emerging Sciences − FAST, Karachi, Pakistan	
Faculty member, Electronic Engineering Department	2001−2005
Sir Syed University of Engineering & Technology, Karachi, Pakistan	
Electronic Engineer, Research & Development Department	1999−2000
Advance Electronics International, Karachi, Pakistan	

Education

Doctor of Philosophy in Telecommunication Engineering (dissertation accepted)	2015−2020
University of Malaga, Málaga, Spain	
Master in Computer Engineering	2000−2002
NED University of Engineering & Technology, Karachi, Pakistan	
Bachelor in Electronic Engineering	1995−1998
Sir Syed University of Engineering & Technology, Karachi, Pakistan	

Training / certifications

NI Software Radio Peripherals (USRP) Software Defined Radio, Saudi Arabia	2019
NI LabVIEW Communications, Saudi Arabia	2019
NI LabVIEW Core-II, Saudi Arabia	2011
NI LabVIEW Core-I, Saudi Arabia	2011
NI Control Design & Robotics Hands-on training, Lebanon	2011
NI LabVIEW Hands-on training, Lebanon	2011
NI Multisim & ELVIS Hands-on training, Lebanon	2011
NI FPGA Hands-on training, Lebanon	2011
NI Veristand Hands-on training, Lebanon	2011
NI DIAdem Hands-on training, Lebanon	2011
Fundamentals of Project Management, USA	2009
Workshop on Biometrics: Recent Advances, Future Prospects & Applications, Pakistan	2007

Workshop on Cellular Wireless Comm. based on CDMA2000 3G standards, Pakistan	2007
Linux Red-Hat Training, Pakistan Software Export Board, Pakistan	2005
Workshop on Remote Sensing & GIS organized by the United Nations, Pakistan	2004
Radio Telegraph Operator's Certificate, Second Class, PMG-II	1998
Radio Telegraph Operator's Certificate, Special Class	1998
Radio Telegraph Operator's Certificate, RRT	1998
Radio Telegraph Operator's Certificate, RT	1995

Publications [9, 31, 69, 77, 78]

[9]   M. Y. I. Zia, A. M. Khan, P. Otero, and J. Poncela, "Investigation of underwater acoustic modems: Architecture, test environment & performance," in 3rd International Conference on Computing for Sustainable Global Development (INDIACom), 2016, pp. 2031-2036.

[31]   M. Y. I. Zia, P. Otero, and J. Poncela, "Design of a Low-Cost Modem for Short-Range Underwater Acoustic Communications," Wireless Personal Communications, vol. 101, pp. 375-390, 2018, doi: 10.1007/s11277-018-5694-5.

[69]   M. Y. I. Zia, P. Otero, A. Siddiqui, and J. Poncela, "Design of a Web Based Underwater Acoustic Communication Testbed and Simulation Platform," Wireless Personal Communications, pp. 1-23, 2020, doi: 10.1007/s11277-020-07203-7.

[77]   M. Y. I. Zia, J. Poncela, and P. Otero, "State-of-the-Art Underwater Acoustic Communication Modems: Classifications, Analyses and Design Challenges," Wireless Personal Communications, 2020, doi: 10.1007/s11277-020-07431-x.

[78]   M. Y. I. Zia, R. Tierno, M.-Á. Luque-Nieto, and P. Otero, "An Energy-Efficient Integration of a Digital Modulator and a Class-D Amplifier," Electronics, vol. 9, p. 1319, 2020, doi:10.3390/electronics9081319.

Professional memberships

Project Management Institute (PMI) Membership no. 1373583	2009−date
International Association of Engineers − IAENG, Membership No. 62370	2006−date
Pakistan Engineering Council, Life time member ELECTRO/5229	1999−date
Canadian Council of Professional Engineers, CCPE Assessment no. 05002375	2005−date